Raman spectroscopy of crystalline and vitreous borates

RAMAN SPECTROSCOPY OF CRYSTALLINE AND VITREOUS BORATES

T. W. BRIL

RAMAN SPECTROSCOPY OF CRYSTALLINE AND VITREOUS BORATES

PROEFSCHRIFT

TER VERKRIJGING VAN DE GRAAD VAN DOCTOR IN DE TECHNISCHE WETENSCHAPPEN AAN DE TECHNISCHE HOGESCHOOL EINDHOVEN, OP GEZAG VAN DE RECTOR MAGNIFICUS, PROF. DR. IR. G. VOSSERS, VOOR EEN COMMISSIE AANGEWEZEN DOOR HET COLLEGE VAN DEKANEN, IN HET OPENBAAR TE VERDEDIGEN OP VRIJDAG 14 MEI 1976 TE 16.00 UUR

DOOR

THIJS WILLEM BRIL

GEBOREN TE EINDHOVEN

PROMOTOR: PROF. DR. J. M. STEVELS
CO-PROMOTOR: PROF. DR. G. C. A. SCHUIT
CO-REFERENT: DR. D. L. VOGEL

aan Letty
aan mijn ouders

Dankbetuiging

Dit proefschrift is tot stand gekomen met de hulp en medewerking van velen. Vooral de goede samenwerking binnen de groep silikaatchemie van de sectie Anorganische Chemie van de Technische Hogeschool Eindhoven heeft de introduktie van de Ramanspectroscopie bij het struktuuronderzoek aan glazen een grote impuls gegeven.

In het bijzonder ben ik dank verschuldigd aan Dr. D. L. Vogel voor de nauwe samenwerking gedurende het onderzoek, waardoor met veel optimisme de niet eenvoudige problemen van de computerberekeningen aan grote moleculen en kristallen tot een goed einde konden worden gebracht.

Ir. E. Strijks dank ik voor het uitvoeren van de vele, vaak gecompliceerde Ramanmetingen en vooral omdat hij mij liet zien dat er muziek in de Ramanspectroscopie zat.

Ook dank ik Ir. J. P. Bronswijk voor zijn medewerking aan het onderzoek, speciaal voor de vervaardiging van een groot aantal preparaten.

Mej. C. M. A. M. v. Grotel dank ik voor het maken van de röntgenopnamen en het uitvoeren van de chemische analyses.

Dr. Ir. W. L. Konijnendijk ben ik dank verschuldigd voor de vele discussies die geleid hebben tot een beter begrip van de Ramanspectroscopie in relatie tot glasachtige systemen.

Voor het kritisch doorlezen van het manuscript ben ik dank verschuldigd aan Ing. H. v.d. Boom, Ir. A. P. Konijnendijk, Ir. H. Verwey en G. E. Luton, die ook heeft zorg gedragen voor een deel van de vertaling in het engels.

De directie van het Natuurkundig Laboratorium van de N.V. Philips' Gloeilampenfabrieken ben ik erkentelijk voor de medewerking bij de publikatie van dit proefschrift.

CONTENTS

1. INTRODUCTION 1
References 4

2. RING-TYPE METABORATES 6
2.1. Introduction 6
2.2. Structure considerations 7
2.2.1. Description of the structure 7
2.2.2. Factor group analysis 9
2.2.3. Site group analysis 11
2.2.4. Correlation D_{3h}–D_3–D_{3d} 13
2.2.5. Vibrations of the 'free' ion $B_3O_6^{3-}$ 14
2.2.6. Displacement configurations 15
2.2.7. Vibration-intensity relations between ring and crystal . . 19
2.2.8. Single crystals 22
2.3. Experiments 28
2.3.1. Preparation of the samples 28
2.3.2. Raman and infrared measurements 28
2.4. Assignment of the spectra 34
2.4.1. Introduction 34
2.4.2. Isotope effects 34
2.4.3. Infrared and Raman spectra 36
2.4.4. Single-crystal Raman spectra 37
2.4.5. Out-of-plane vibrations A_{2u} (A''_2) and E_g (E'') 37
2.4.6. Species E_g (E') and E_u (E') 43
References 43

3. NORMAL COORDINATE ANALYSIS 45
3.1. Introduction 45
3.2. *G-F* matrix method and the Schachtschneider programs 45
3.3. GMOP, the subroutine SPC and *GZ* conversion 51
3.3.1. GMOP 51
3.3.2. Sun–Parr–Crawford method 55
3.3.2.1. Introduction 55
3.3.2.2. Calculation 56
3.4. Calculations on $B_3O_6^{3-}$ 61
3.4.1. GMOPSECONDVERSION 61
3.4.2. *F* matrix (*Z* matrix) 63
3.4.3. *GZ* CONVERSION 66
3.4.4. Out-of-plane vibrations 67
3.4.5. In-plane vibrations 68

3.4.6. Application of the isotope product rule 73
3.4.7. Potential energy distribution and the displacements of the atoms during the normal vibrations 74
3.5. Calculations on $Na_3B_3O_6$ 75
References 77

4. RAMAN SPECTRA OF SOME BORATE GLASSES 79
4.1. Introduction 79
4.2. Vibration spectra of glasses 79
4.3. Alkali borate glasses 80
References 90

Appendix 1. Numerical data for $B_3O_6^{3-}$ 91
Appendix 2. Results of program FLEPO 98
Appendix 3. A. Potential energy distribution 103
B. Amplitudes 104
Appendix 4. Crystalline $Na_3B_3O_6$ 107

Summary 115

Samenvatting 116

Levensbericht 118

1. INTRODUCTION

This thesis describes an investigation of some structural aspects of crystalline sodium metaborate and vitreous alkali borates. An investigation of the structural properties of glasses is of interest for the purpose of explaining and predicting their physical and chemical behaviour.

We chose the vitreous alkali borates for several reasons. One of them was their low melting point, which makes them easy to handle. From the scientific point of view these glasses are very interesting because of the different ways in which the boron atom may be surrounded by the oxygen atoms. This property is responsible for extremes in some physical properties as a function of composition. The occurrence of these extremes is often called the boron oxide anomaly. Generally it is assumed that with increasing alkali oxide percentage the amount of four-membered boron atoms (with four bridging oxygen atoms *)) increases and the amount of three-membered boron atoms (with three bridging oxygen atoms) decreases. At a definite percentage of alkali oxide the number of four-membered boron atoms reaches a maximum. Opinions about the percentage differ, since three-membered boron atoms with one non-bridging oxygen atom also arise (see for instance Beekenkamp [1-1]), Bray and O'Keefe [1-2])). The differences in the attraction forces of these three different units within the network explain the non-linear properties (the boron oxide anomaly). The three smallest structural units observed in borate glasses and compounds will be indicated with an *a* for the BO_3 triangle with three bridging oxygens, with a *b* for the BO_3 triangle with one non-bridging oxygen and with a *c* for the BO_4 tetrahedra with four bridging oxygens.

The vitreous borates are probably built up from much larger groups than these units. These larger groups are similar to those found in crystalline borates. Some of them are shown in fig. 1.1. In chapter 4 we shall demonstrate that these groups occur in the alkali borate glasses. The nomenclature of the groups will follow Krogh-Moe [1-3]) and Konijnendijk [1-4]). Between brackets we will always give the smallest units from which the group is made. Konijnendijk [1-4]) gives a review of the occurrence of the various groups in crystalline borates found by X-ray diffraction.

Two points of interest are the glass-forming region and the area of phase separation. The glass-forming region of the sodium borates goes up to a composition of about 40% Na_2O. This figure cannot be given exactly, because the glass-forming is a function of the cooling rate. We found for instance that it is possible to vitrify a sample of composition 50% Na_2O.50% B_2O_3. The glass-forming regions of the other alkali borates extend to a limit which is approximately equal to that for sodium borate. According to Shaw and Uhlmann [1-5])

*) A bridging oxygen is an oxygen that is bound to the glass network with two covalent bonds. A non-bridging oxygen has only one covalent bond to the network.

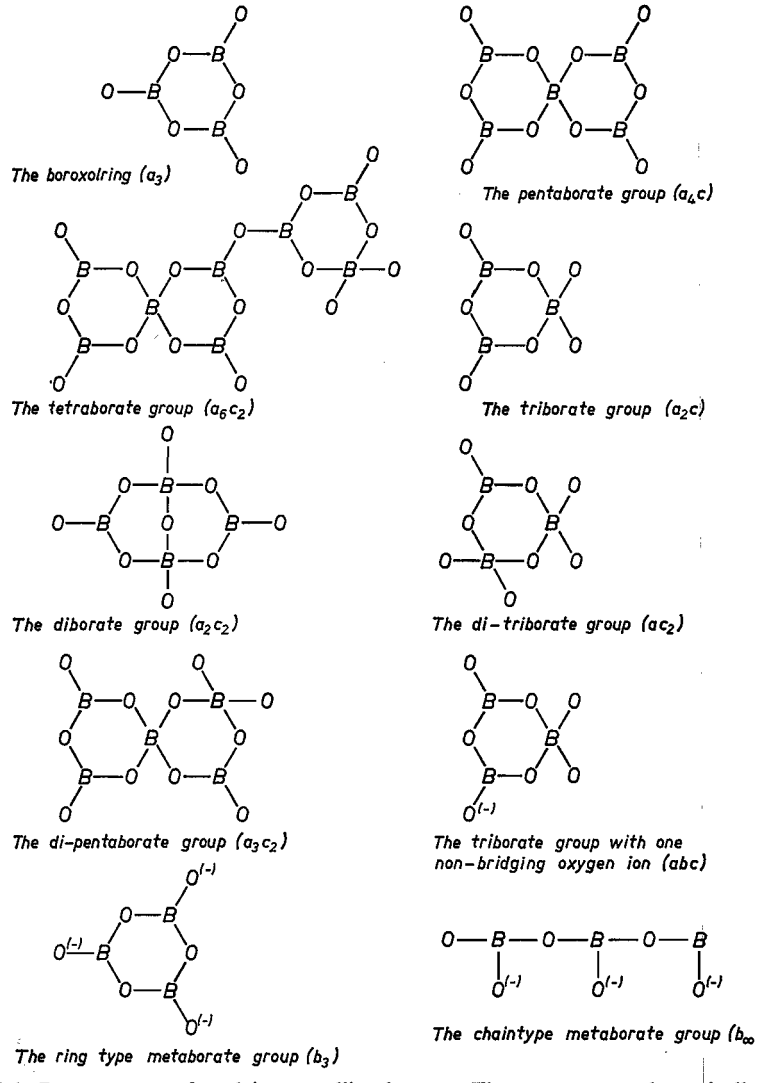

Fig. 1.1. Borate groups found in crystalline borates. The groups are schematically drawn. The configurations in space will usually be different.

and Vogel [1–6]) the area of phase separation in the sodium borates is between 8 % and 25 % Na_2O. These authors also give the areas for the other alkali borates.

The chosen experimental method in this thesis for obtaining new information about the structure of the vitreous borates is Raman spectroscopy. Although Kujumzelis [1–7]) made some Raman spectra of glasses only a few years after the discovery of the effect (1923–1928), the method first became a valuable tool of research with the introduction of the ion-gas lasers. The first articles on laser Raman spectroscopy of glasses appeared in 1970–1971: notable publications

include those by Etchepare [1-8]), White [1-9]) and Tobin [1-10]). The spectra appeared to have some marked properties:

(1) They possessed only a limited number of peaks. These were well defined and intensive and often polarised (due to totally symmetric vibrations).
(2) The spectra looked relatively simple (in comparison with the infrared spectra).
(3) There were marked changes as a function of the composition.

These three factors, together with the excellent quality of the spectra, gave a new impulse to research on the structure of glasses by means of vibrational spectroscopy. Some other advantages of laser Raman spectroscopy as compared with infrared spectroscopy are:

(1) Sample preparation is easier; in the infrared only very thin films or a sample suspended in a matrix can be used.
(2) In the infrared measurements the spectrum mainly represents the structure of the surface, because the infrared light is absorbed within a very short distance.
(3) The occurrence of small amounts of water has very little influence.
(4) High-temperature recordings are easier to make.
(5) The lower frequencies (200 cm^{-1}) are easier to measure.

A disadvantage of Raman spectroscopy is the lack of an absolute intensity measurement. Essentially vibrational spectroscopy can provide a great deal of information about structures. The vibrational frequencies provide information about the values of the bonding forces between the vibrating atoms (or between bigger groups). Using the selection rules we can obtain information about the symmetry properties of the vibrations and the vibrating units. The halfwidth of the peaks in the glass spectra is correlated with the degree of disorder of the vitreous network (Brawer [1-11])).

An important advantage of vibrational spectroscopy is the difference in magnitude of the frequencies between the vibrations of the atoms in the network (internal vibrations) and the vibrations as a result of the interaction of the alkali ions and the network (lattice vibrations or external vibrations). This is a consequence of the difference in bonding force (covalent bonding inside the network, ionic bonding between alkali ions and network) and in mass (light atoms in the network, heavy ions in the case of lattice vibrations).

A disadvantage of vibrational spectroscopy is the complicated procedure required to get the information from the experiments. For free molecules and crystals the theory is well understood (see for instance Wilson, Decius and Cross [1-12]) and Shimanouchi [1-13])). Schachtschneider [1-14]) has written a number of computer programs which can be used with the so-called *G-F* matrix method (cf. chapter 3) to perform calculations on free molecules. We have adapted these programs for calculations on crystals, as will be described in chapter 3.

The vibrational spectra of glasses are more difficult to interpret. Brawer [1-11]) has recently developed a theory which describes these vibrations in disordered systems. The starting point of his theory is a comparison of the glass with a regularly built structure (a crystal or a fictive crystal). The short range order in the glass includes the appearance of structural groups, which give rise to rather sharply defined vibrational frequencies. The lack of a long-range order causes small changes in the geometry of these groups and in their coupling. This gives rise to a broadening of the peaks.

In the present investigation we also make a comparison between crystal and glass. The best comparisons are made when crystal and glass have the same composition, and this can be realised with the alkali borates. For several reasons, described in chapter 2, we chose the sodium metaborate ($Na_3B_3O_6$) for our first investigation (chapters 2 and 3). The analysis of the spectra of this crystal yielded much information, although it was practically impossible to make a good glass of the same composition. We were able to calculate some force constants of the boron–oxygen bonds. It was also possible to correlate one special vibration (770 cm^{-1}), which had little coupling with the surrounding, with the same kind of vibration in the alkali borate glasses (chapter 4).

The sodium metaborate is very easy to crystallise. The first correct X-ray analysis of the crystal dates from 1938 (Fang [1-15])). Later Marezio et al.[1-16]) repeated the structure analysis, and found that there were differences in the boron–oxygen distances. The infrared spectra have been described by Hisatsune et al.[1-17]), Goubeau and Hummel [1-18]) and many others. Up to now, however, the Raman spectra were lacking. The new information given by our Raman spectra made it necessary to revise the interpretation of the spectra. This is described in chapter 2. The calculations based on this revised interpretation gave better results than those reported by Kristiansen and Krogh-Moe [1-19]). These new calculations, of which the potential energy distribution was the most important, enabled us to provide an explanation for the vibrational frequencies 770 cm^{-1} and 806 cm^{-1} in alkali borate glasses (chapter 4).

REFERENCES

[1-1]) P. Beekenkamp, Philips Res. Repts Suppl. 1966, No. **4**.
[1-2]) P. J. Bray and J. G. O'Keefe, Phys. Chem. Glasses **4**, 37, 1963.
[1-3]) J. Krogh-Moe, Acta cryst. **B28**, 3089, 1972.
[1-4]) W. L. Konijnendijk, Philips Res. Repts Suppl. 1975, No. **1**.
J. Non-cryst. Solids, in press.
[1-5]) R. R. Shaw and D. R. Uhlmann, J. Am. ceram. Soc. **51**, 377-382, 1968.
[1-6]) W. Vogel, Struktur und Kristallisation der Gläser, VEB Deutscher Verlag für Grundstoffindustrie, Leipzig, 1971, p. 86.
[1-7]) J. Kujumzelis, Z. Phys. **100**, 221, 1936.
[1-8]) J. Etchepare, J. Chim. Physicochim. biol. **67**, 890, 1970.
Spectrochim. Acta **26A**, 2147, 1970.
[1-9]) W. B. White, G. J. McCarthy and J. McKay, Amer. ceram. Soc. Bull. **50**, 411, 1971.

[1-10]) H. C. Tobin and T. Book, J. opt. Soc. Amer. **60**, 368, 1970.
[1-11]) S. Brawer, Phys. Rev. **B11**, 3173, 1975.
[1-12]) E. B. Wilson, J. C. Decius and P. C. Cross, Molecular vibrations, McGraw-Hill Book Company, New York, 1955.
[1-13]) T. Shimanouchi and M. Tsuboi, J. chem. Phys. **35**, 1597, 1961.
[1-14]) J. H. Schachtschneider, Techn. Rep. No. 231-64 (Vol. I and II), Shell Development Company, Emeryville, California, 1966.
[1-15]) Ssu-Mien Fang, Z. kristallogr. Kristallgeom., kristallphys. Kristallchem. **99**, 1, 1938.
[1-16]) M. Marezio, H. A. Plettinger and W. H. Zachariasen, Acta cryst. **16**, 594, 1963.
[1-17]) I. C. Hisatsune and N. H. Suarez, Inorg. Chem. **3**, 168, 1964.
[1-18]) J. Goubeau and D. Hummel, Z. phys. Chem. **20**, 15, 1959.
[1-19]) L. A. Kristiansen and J. Krogh-Moe, Phys. Chem. Glasses **9**, 96, 1968.

2. RING-TYPE METABORATES

2.1. Introduction

In chapter 1 we have explained why the borates are of interest for the purpose of investigating the structural properties of glass. We showed also that vibrational spectroscopy can be of great help to this investigation. In the present chapter we shall first present some arguments for the choice of the metaborates, after which a description of the structure will be given. The major part of this chapter is concerned with the information that can be obtained from the interpretation of the spectra.

As can be seen from the phase diagrams of boron oxide and metal oxides (refs 2–17 to 2–22) there are a great many crystalline compounds.

The materials we need for our investigation are crystalline compounds with known structures. Konijnendijk [2–1]) has given a review of these compounds. A survey of some borates with known crystal structure is given in table 2-I.

TABLE 2-I

Structure of some crystalline alkali borates

$Na_2O.B_2O_3$ and $K_2O.B_2O_3$ are isomorphous, and so are β-$K_2O.5B_2O_3$ and $Rb_2O.5B_2O_3$ (not included in this table). All crystals, except $Na_2O.B_2O_3$ and $K_2O.B_2O_3$, possess networks of boron and oxygen. $Na_2O.B_2O_3$ and $K_2O.B_2O_3$ are built up from isolated rings of boron and oxygen.

All crystals in this table have a structure that is stable at high temperature and normal pressure (and stable or meta-stable at room temperature)

	space group	number of formula units per unit cell	number of atoms per prim. cell	ref.
$Li_2O.B_2O_3$	$P2_1/c$	2	16	2–23
$Li_2O.2B_2O_3$	$I4_1cd$	8	52	2–24
$Na_2O.B_2O_3$	$R\bar{3}c$	3	24	2– 3
$Na_2O.2B_2O_3$	$P\bar{1}$	4	52	2–25
α-$Na_2O.3B_2O_3$	$P2_1/c$	6	108	2–26
β-$Na_2O.3B_2O_3$	$P2_1/c$	6	108	2–27
$Na_2O.4B_2O_3$	$P2_1/a$	4	92	2–28
$K_2O.B_2O_3$	$R\bar{3}c$	3	24	2– 4
$K_2O.2B_2O_3$	$P\bar{1}$	4	52	2–29
$K_2O.3B_2O_3$	triclinic	6	108	2–30
α-$K_2O.5B_2O_3$	$Pbca$	4	112	2–31
β-$K_2O.5B_2O_3$	$Pbca$	4	112	2–32
γ-$K_2O.5B_2O_3$	monoclinic	8	224	2–30

We started our investigation with ring-type metaborates. Although the metaborates do not form glass readily, there are three main arguments in support of the choice:

(1) The first is the simplicity of the vibrational analysis. The symmetry of the crystal and the number of atoms in the primitive unit cell determine the

number of vibrations. It is obvious that the interpretation becomes more difficult as the number of vibrations increases. A higher symmetry can give a greater variety of symmetry species and these can be experimentally separated and recognised. Moreover, a higher symmetry may possess degenerate species, which will diminish the number of frequencies.

(2) The second supporting argument is ease of crystallisation. The borates with more than 66 mole% B_2O_3 do not readily crystallise, since this percentage coincides with the glass-forming region. The tendency to crystallisation decreases with increasing percentage of B_2O_3. Pure B_2O_3 will only crystallise under special conditions (McCulloch [2-34]) and Gurr [2-35])). Cesium ennea borate (Cs_2O . $9B_2O_3$) will crystallise but this can take months. We therefore looked for a compound that would not present problems of crystallisation, especially because we needed single crystals. This meant that we had to choose a compound that lays slightly outside the glass-forming area.

(3) The third consideration was the occurrence of isomorphous compounds. For our purpose it was of particular interest to have isomorphous compounds to work with, both because they enlarge the number of data and because, in our case, they inform us about the influence of the alkali ions. The sodium and potassium compounds of most crystalline borates resemble each other. $Na_3B_3O_6$ and $K_3B_3O_6$ are isomorphous, and the Rb and Cs metaborates are also very probably isomorphous with the first two compounds (v. Grotel [2-2])). Unfortunately, no structural investigations of the latter two compounds have yet been reported. None of the other borates have so many isomorphous compounds as the ring-type metaborates.

An added advantage was the presence of isolated rings of boron and oxygen, which makes the analysis easier.

2.2. Structure considerations

2.2.1. *Description of the structure*

Sodium metaborate and potassium metaborate belong to the same space group $R\bar{3}c$ (D_{3d}^6) (see refs 2–3 and 2–4). This group can be represented in two ways:

(1) with the rhombohedral cell,

(2) with the hexagonal cell.

The hexagonal cell contains six formula units of $Na_3B_3O_6$, the rhombohedral cell contains only two formula units. The rhombohedral cell is also the primitive unit cell (Bravais lattice R, only the cell corners are occupied).

The crystal is built up of plane $B_3O_6^{3-}$ (b_3) rings and Na^+ (or K^+) ions (fig. 2.1). The centre of mass of the ring is on the intersection of a threefold inversion axis with three twofold rotation axes normal to the threefold inversion

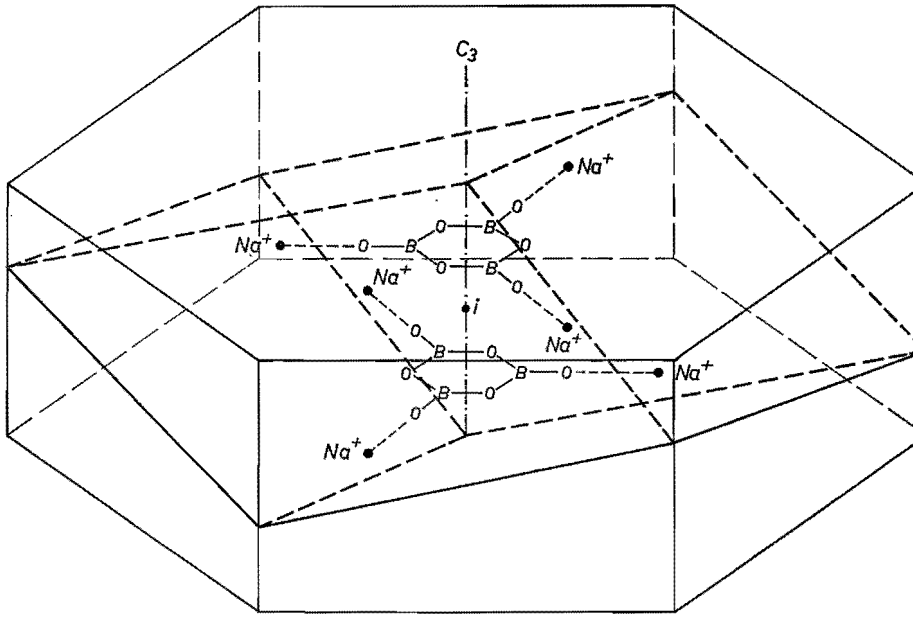

Fig. 2.1

Fig. 2.1. The ***R*** cell of sodiummetaborate. There are two formula units $Na_3B_3O_6$ per primitive unit cell. The hexagonal cell is also drawn.

axis (Wyckoff *a*-position). All atoms are on twofold rotation axis (Wyckoff *e*-position). The centre of inversion, which is located halfway between two rings, causes an alternating orientation of two rings lying one above the other.

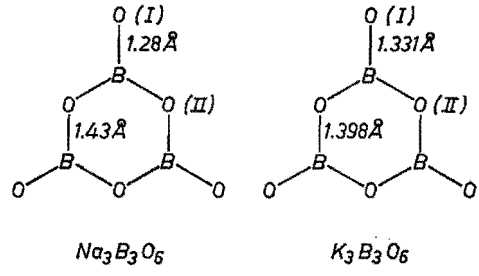

Fig. 2.2

Fig. 2.2. Ring distances in metaborate rings. The rings have symmetry D_{3h}.

As can be seen from fig. 2.2 the boron–oxygen distances in the sodium and potassium metaborates show remarkable differences. The Na^+ (or K^+) ions are surrounded by seven oxygens. The distances according to Marezio et al.[2–3]) and Schneider and Carpenter [2–4]) are:

	$Na_3B_3O_6$	$K_3B_3O_6$	
1×	2.461 Å	2.849 Å	distance M^+–O(I)
2×	2.474 Å	2.801 Å	— do —
2×	2.607 Å	2.835 Å	— do —
2×	2.482 Å	2.775 Å	distance M^+–O(II).

The shortest distances between oxygen and oxygen are:

2.383 Å	2.381 Å	distance O(I)–O(II)
2.410 Å	2.389 Å	distance O(II)–O(II)

and some important angles are:

114.8°	117.3°	angle O(II)–B–O(II)
122.6°	121.3°	angle O(I)–B–O(II)
125.2°	122.6°	angle B–O(II)–B.

O(I) refers to an extra-annular oxygen atom and O(II) to an intra-annular oxygen atom of the metaborate ring.

2.2.2. *Factor group analysis*

Factor group analysis is the method of classifying the modes of a crystal in terms of symmetry species. The method is analogous to that used for free molecules (see e.g. Bhagavantam [2–7]), Woodward [2–9]) or Nakamoto [2–10])). The factor group of a space group is the set of cosets obtained when the space group is decomposed relative to the group of all its primitive translations. The factor group is homomorphous with one of the 32 point groups. The homomorphous point group can be obtained from the Schoenflies notation of the space group by dropping the superscript. Turrell [2–5]) (pp. 103–108) describes why only the irreducible representations of the factor group need be considered in the case of fundamental infrared- and Raman-active vibrations. In the case of an infrared-active vibration the dipole moment vector (or the changes in it) transforms in the same way as the translation vector. The primitive translations belong to the totally symmetric species of the translation group $\boldsymbol{T}$ (this is the group of all primitive translations of the space group). Therefore, the dipole moment vector also belongs to this totally symmetric species. Turrell shows further that the polarisability tensor (with its changes) belongs to this totally symmetric species of the translation group. This means that the fundamental infrared and Raman vibrations belong to this totally symmetric species of $\boldsymbol{T}$ and in this case the wave vector $\boldsymbol{k}$ is equal to zero *). This also means that we only need to consider those representations of the space group which occur as irreducible representations of the factor group (Turrell p. 107) **).

*) The wave vector $\boldsymbol{k}$ is the reciprocal of the wavelength of the standing wave in the crystal. If all primitive cells vibrate in phase, then $\boldsymbol{k} = 0$.

**) For non fundamentals, i.e. for combination tones and overtones (more-phonon processes), a totally different treatment is necessary. The theory can be found in for instance Turrell [2–5]), Poulet and Mathieu [2–6]), Bhagavantam and Venkatarayudu [2–7]) or Nussbaum [2–8]).

These are also the irreducible representations of the homomorphous space group, i.e. the group D_{3d} in the case of $Na_3B_3O_6$, since homomorphous groups have the same representations. Bhagavantam and Venkatarayudu [2–7]) developed a method of calculating the number of vibrations in the different symmetry species. Of course the Wyckoff positions of the atoms in the crystal have to be known. Adams and Newton [2–11]) used this method to tabulate for all 230 space groups and all possible (Wyckoff) positions of the atoms the number of vibrations per symmetry species. In this way we can immediately read in which species the $3N = 72$ modes of the $Na_3B_3O_6$ crystal can be found. The tabulation for the space group $R\bar{3}c$ is given in table 2-II, since all atoms in

TABLE 2-II *)

Space group $R\bar{3}c$, no. 167. Factor group is isomorphous with D_{3d}

	Wyckoff pos.	A_{1g}	A_{2g}	E_g	A_{1u}	A_{2u}	E_u
translation	2*a*	0	1	1	0	1	1
rotation	2*a*	0	1	1	0	1	1
translation	6*e*	1	2	3	1	2	3
rotation	6*e*	1	2	3	1	2	3

*) From Adams and Newton [2–11]).

the crystal are at the Wyckoff *e* position, we readily find that the 72 modes are distributed as follows:

Na(6) $A_{1g} + 2A_{2g} + 3E_g + A_{1u} + 2A_{2u} + 3E_u$
B(6) $A_{1g} + 2A_{2g} + 3E_g + A_{1u} + 2A_{2u} + 3E_u$
O(12) $2A_{1g} + 4A_{2g} + 6E_g + 2A_{1u} + 4A_{2u} + 6E_u$
Total: $4A_{1g} + 8A_{2g} + 12E_g + 4A_{1u} + 8A_{2u} + 12E_u$

Three modes belong to the optically inactive acoustic vibrations. These are vibrations where the whole lattice carries out a translational movement. The modes of the acoustic vibrations belong to the same species as the pure translations. The character table of the point group D_{3d} (table 2-III) shows that these

TABLE 2-III

Character table of the point group D_{3d}

	E	$2C_3$	$3C_2$	i	$2S_6$	$3\sigma_d$		
A_{1g}	1	1	1	1	1	1		$\alpha_{xx} + \alpha_{yy}, \alpha_{zz}$
A_{2g}	1	1	−1	1	1	−1	R_z	
E_g	2	−1	0	2	−1	0	(R_x, R_y)	$(\alpha_{xx} - \alpha_{yy}, \alpha_{xy}), (\alpha_{yz}, \alpha_{zx})$
A_{1u}	1	1	1	−1	−1	−1		
A_{2u}	1	1	−1	−1	−1	1	T_z	
E_u	2	−1	0	−2	1	0	(T_x, T_y)	

must be the species A_{2u} and E_u. From this table we also find the Raman- or infrared-active vibrations. The A_{2g} and A_{1u} species are inactive, so we have left

$$4\,A_{1g}(\mathrm{R}) + 12\,E_g(\mathrm{R}) + 7\,\mathrm{A}_{2u}(\mathrm{IR}) + 11\,E_u(\mathrm{IR}).$$

2.2.3. *Site group analysis*

Factor group analysis supplies the total number of vibrations in the different symmetry species. However, it is worth making a distinction between lattice vibrations and internal vibrations. We are able to do this because the crystal has two distinct structural parts: the covalent bonded boron and oxygen in the ring and the Na^+ ions, which have a much weaker bonding with the $B_3O_6^{3-}$ ions. The strong covalent bond of the boron and oxygen atoms in the ring gives rise to a relatively high vibrational energy as compared to the sodium–oxygen vibrations. This causes a difference in frequency between the two kinds of vibrations. We can easily classify these vibrations by means of site group analysis.

If we consider the $B_3O_6^{3-}$ ring as a whole, we see that it is situated at a Wyckoff *a* position. The ring has $\boldsymbol{D}_3$ site symmetry in the crystal, because one threefold and three twofold rotation axes pass through its centre of mass. The inversion centre in the primitive unit cell delivers two equivalent sites, both having $\boldsymbol{D}_3$ site symmetry. $\boldsymbol{D}_3$ is a subgroup of the point group $\boldsymbol{D}_{3d}$ (with which the factor group is homomorphous). Each ring in a primitive cell contains $N = 9$ atoms and has therefore $3N - 6 = 21$ modes of vibration. Thus, the two rings in the primitive cell give rise to 42 internal vibrations. Their distribution over the symmetry species will be given later.

There remain in this way $72 - 42 = 30$ modes for the lattice vibrations. The acoustic vibrations belong to the species A_{2u} and E_u, as previously deduced. The distribution of the remaining 27 modes can be inferred from table 2-II. We have two rings at a Wyckoff *a* position and six Na^+ ions at the Wyckoff *e* position.

Translations 6 Na^+	:	$A_{1g} + 2\,A_{2g} + 3\,E_g + A_{1u} + 2\,A_{2u} + 3\,E_u$
Translations 2 rings	:	$A_{2g} + E_g + A_{2u} + E_u$
Rotations 2 rings	:	$A_{2g} + E_g + A_{2u} + E_u$
		+
		$A_{1g} + 4\,A_{2g} + 5\,E_g + A_{1u} + 4\,A_{2u} + 5\,E_u$
Acoustic vibrations	:	$A_{2u} + E_u$
		−
Total number of optical lattice vibrations	:	$A_{1g} + 4\,A_{2g} + 5\,E_g + A_{1u} + 3\,A_{2u} + 4\,E_u$
		(= 27 modes)

The A_{2g} and A_{1u} are Raman- and infrared-inactive, so the number of active lattice vibrations is given by

$$A_{1g}(\mathrm{R}) + 5\,E_g(\mathrm{R}) + 3\,A_{2u}(\mathrm{IR}) + 4\,E_u(\mathrm{IR}).$$

These vibrations can be expected in the low frequencyr ange, i.e. below approximately 250 cm^{-1}.

We can specify the rotations and the translations of the rings somewhat better. Fig. 2.3 shows the two rings in a primitive unit cell; the rings are in the

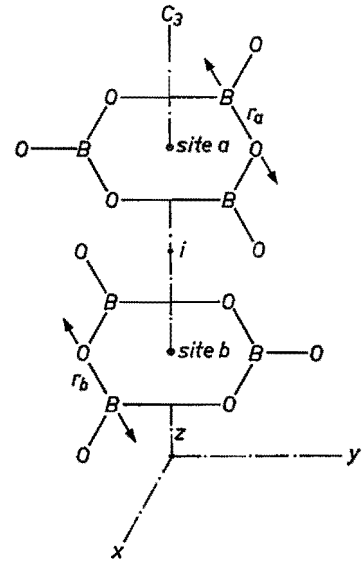

Fig. 2.3. Two $B_3O_6^{3-}$ rings in the primitive unit cell.

X–Y plane and the Z axis is along the threefold inversion axis. For symmetry reasons, the translations in the plane of the ring have to belong to the doubly degenerate species E_g or E_u. The translations along the Z axis belong to the symmetry species A_{2u} or A_{2g}. If both rings shift in the same direction, then this is an anti-symmetric movement with respect to the inversion centre i. For this reason these movements belong to the ungerade species. If both rings move in opposite directions (antiphase) then these vibrations will belong to the gerade species. The rotations can be treated in an analogous way. The rotations around the Z axis belong to the A_{2g} or A_{2u} species and the rotations around an axis in the plane of the ring to the E_g or E_u species. If both rings rotate in the same direction, then this rotation is symmetric with respect to the inversion centre i and the vibration belongs to the gerade species. Whereas if they rotate in opposite directions it is an antisymmetric vibration which belongs to the ungerade species. Summarising we find the following species:

$T_a + T_b$ along the Z axis	: A_{2u}
$T_a + T_b$ in the plane of the rings	: E_u
$T_a - T_b$ along the Z axis	: A_{2g}

$T_a - T_b$ in the plane of the rings : E_g
$R_a + R_b$ around the Z axis : A_{2g}
$R_a + R_b$ around an axis in the plane of the rings : E_g
$R_a - R_b$ around the Z axis : A_{2u}
$R_a - R_b$ around an axis in the plane of the rings : E_u

(T_a and T_b are translations, and R_a and R_b rotations of ring a and ring b, respectively. + = in phase; − = antiphase.)

For the internal vibrations the same arguments can be used. Consider a particular vibration occurring in both ring a and ring b. If the atoms in a move completely in phase with the corresponding atoms in b, the overall vibration is symmetric with respect to i, and belongs to a gerade species. If the atoms in a move in antiphase with the corresponding atoms in b, the overall vibration is antisymmetric with respect to i, and belongs to an ungerade species.

Thus, each particular vibration of the 'free' ring is associated with the occurrence of two vibrations, one of the gerade and one of the ungerade species, in the crystal.

Due to the weak interaction between both rings in the unit cell the frequencies of the gerade and ungerade crystal vibration will differ very little.

2.2.4. *Correlation* D_{3h}–D_3–D_{3d}

Since the sodium metaborate crystal has a centre of inversion, we can use here the rule of mutual exclusion. This rule means that among the active vibrations the Raman-active vibrations belong to the gerade species and the infrared active vibrations belong to the ungerade species. If we use this rule for a pair of vibrations from the two rings, then this pair will be split up into a Raman-active (or inactive) vibration and an infrared-active (or inactive) vibration.

If we take the $B_3O_6^{3-}$ ring as a 'free' ion, then its symmetry is D_{3h}. Placing this ring in the crystal we find that the horizontal mirror plane, the vertical mirror planes and the S_3 axis disappear, that is to say they are locally present but do not form part of the crystal symmetry. We are thus left with symmetry D_3. Because the D_3 site has less symmetry than the free ion, the more differentiated

TABLE 2-IV

Character table of the point group D_{3h}

	E	$2C_3$	$3C_2$	σ_h	$2S_3$	$3\sigma_v$		
A'_1	1	1	1	1	1	1		$\alpha_{xx} + \alpha_{yy}, \alpha_{zz}$
A'_2	1	1	−1	1	1	−1	R_z	
E'	2	−1	0	2	−1	0	(T_x, T_y)	$(\alpha_{xx} - \alpha_{yy}, \alpha_{xy})$
A''_1	1	1	1	−1	−1	−1		
A''_2	1	1	−1	−1	−1	1	T_z	
E''	2	−1	0	−2	1	0	(R_x, R_y)	$(\alpha_{yz}, \alpha_{zx})$

TABLE 2-V

Character table of the point group D_3

	E	$2C_3$	$3C_2$		
A_1	1	1	1		$\alpha_{xx} + \alpha_{yy}, \alpha_{zz}$
A_2	1	1	−1	T_z; R_z	
E	2	−1	0	(T_x, T_y); (R_x, R_y)	$(\alpha_{xx} - \alpha_{yy}, \alpha_{xy})$; $(\alpha_{yz}, \alpha_{zx})$

species of D_{3h} are converted into the species of D_3 with fewer symmetry elements. We can easily find the correlation between D_{3h} and D_3 from the character tables (tables 2-IV and 2-V) (see Turrell [2-5]) for the method), or from the correlation tables of Wilson, Decius and Cross [2-33]) (p. 333). Table 2-VI*a* gives a survey of the correlations between the groups D_{3h}, D_3 and D_{3d} and table 2-VI*b* gives the resulting internal vibrations in the crystal.

TABLE 2-VI

a. Correlation D_{3h}–D_3–D_{3d}

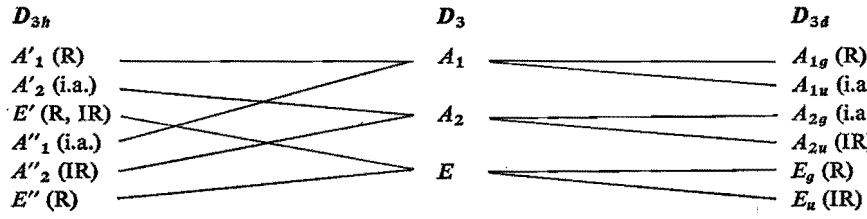

b. Internal vibrations of crystalline $Na_2O.B_2O_3$ ($R\bar{3}c$)

$3A_{1g}$ (A'_1)	R	$3A_{1u}$ (A'_1)	i.a.
$2A_{2g}$ (A'_2)	i.a.	$2A_{2u}$ (A'_2)	IR
$2A_{2g}$ (A''_2)	i.a.	$2A_{2u}$ (A''_2)	IR
$5E_g$ (E')	R	$5E_u$ (E')	IR
$2E_g$ (E'')	R	$2E_u$ (E'')	IR

2.2.5. *Vibrations of the 'free' ion* $B_3O_6^{3-}$

The 'free' $B_3O_6^{3-}$ ion contains 9 atoms and there will be $3N - 6 = 21$ vibrational modes. Starting with the reducible representation of the ion we can reduce this representation to a set of irreducible representations of D_{3h} (see for instance Turrell [2-5]), chapter 2, sec. IX):

$$I^{B_3O_6^{3-}} = 3\,A'_1 + 2\,A'_2 + 5\,E' + 2\,A''_2 + 2\,E'' \quad \text{(totalling 21 modes).}$$

Note: in the case of the planar $B_3O_6^{3-}$ ring, the species A'_1, A'_2 and E' represent the in-plane vibrations and the species A''_2 and E'' the out-of-plane vibrations.

2.2.6. *Displacement configurations*

For the interpretation of the spectra it can be helpful to have a visual representation of the (relative) displacements during the vibrations. We confine ourselves to the $B_3O_6^{3-}$ ion, because, as has been shown in the preceding secs, the movements in the crystal will be very similar.

The influence of the Na^+ ion is expected to be small and is disregarded in this respect. For the purpose of this representation we wish to be informed about:

(1) the directions of the displacements of every atom for every vibration;
(2) the amplitude of these displacements;
(3) the frequency of the vibration whose displacements are known.

We can get all this information from the calculations carried out with the *G-F* matrix method (see chapter 3). But before we can start the calculation we need an assignment of the spectra. As long as we have no assignment (and no calculations) we are deprived of the information on the points 2 and 3, which leaves us with point one — the directions of the displacements. This is primarily a point of symmetry. With this information it is possible to give an approximation of what we shall call the displacement configurations.

For these approximate displacement configurations we make use of the (internal) symmetry coordinates (cf. chapter 3), which can be constructed from the internal coordinates (e.g. stretching, bending and torsion) in such a way that they have the full symmetry of the $B_3O_6^{3-}$ ring. These symmetry coordinates are linear combinations of the normal coordinates, which describe exactly the displacements but have to be calculated as mentioned before. Every symmetry coordinate belongs to one of the species of the symmetry group of the ion. If there are n_γ symmetry coordinates for a species Γ and the number of vibrational modes of species Γ is v_γ, then $n_\gamma \geqslant v_\gamma$ and $n_\gamma - v_\gamma$ is the number of redundant symmetry coordinates for the species. An example of a (completely symmetric) coordinate is $s = r_1 + r_2 + r_3 + r_4 + r_5 + r_6$. It belongs to the A'_1 species, in which r_x refers to stretching of one of the six B–O bonds in the ring. As will be shown in the next chapter, the symmetry coordinates are found by framing a U matrix. The redundant coordinates have to be deleted from this U matrix (see sec. 3.4.1).

One problem encountered in using the U matrix is that it is not unique. It must be chosen to be orthonormal (or unitary if its elements are complex) and in such a way as to give the matrix product $G_s = U G \tilde{U}$ (see sec. 3.2) the diagonal block form, in which each block corresponds to a particular irreducible representation of the group. This leaves us with an infinite number of possibilities for U except in the rare case that each species contains at most one vibrational mode.

Since the normal coordinates are linear combinations of the symmetry coordinates, they are only identical for a vibration which is the only one occurring

in its species. However, if there are more symmetry coordinates per species there is a considerable chance that each of them will make the biggest contribution to a different normal coordinate of the species. If this is not the case then the symmetry coordinates are not representative of the normal coordinates. A calculation of the potential energy distribution over the various symmetry coordinates can settle this question.

A special problem arises from the degenerate species. We already mentioned that the congruence transformation $G_s = U\,G\,\tilde{U}$ yields a diagonal block form. If this transformation is performed with a U matrix obtained with the aid of the projection operator on the basis of the characters of the irreducible representations, the block pattern is often incorrect for the degenerate species. However, for calculation reasons a correct block form is necessary and it also gives more insight into the displacement configurations.

In practice the correct block form can often be realised by constructing the U matrix by means of the projection operator on the basis of the elements of

TABLE 2-VII

U matrix of $B_3O_6^{3-}$ obtained by the method of Nielsen and Berryman [2-36])

symmetry coordinates	↓	internal coordinates																													
		1	2	3	4	5	6	7	8	9	10	11	12	13	14	15	16	17	18	19	20	21	22	23	24	25	26	27	28	29	30	
A'_1	1							1	1	1																						
	2	1	1	1	1	1	1																									
	3										1	1	1																			1 red.
	4													−1	−1	−1																
	5																1	1	1	1	1	1										red.
A'_2	6	1	−1	1	−1	1	−1																									
	7																1	−1	1	−1	1	−1										
A''_1	8																									1	1	1	1	1	1	red.
A''_2	9																						1	1	1							
	10																									1	−1	1	−1	1	−1	
E'	11							2	−1	−1																						
	12	1	1	−2	−2	1	1																									
	13	1	−1			−1	1																									
	14										2	−1	−1																			2 red.
	15													1	−2	1																
	16																1	1	1	−2	−2	1										
	17																1	1	−1			−1										
	18								−1	1																						
	19	−1	−1			1	1																									
	20	1	−1	−2	2	1	−1																									
	21											−1	1																			2 red.
	22													−1		1																
	23																1	−1	−1			1										
	24																−1	1	−1	−2	2	1										
E''	25																							1	−1							
	26																									1	−2	−2	1	1	1	1 red.
	27																									1			1	−1	−1	
	28																						2	−1	−1							
	29																									−1			1	1	−1	1 red.
	30																									1	2	−2	−1	1	−1	

TABLE 2-VII (continued)

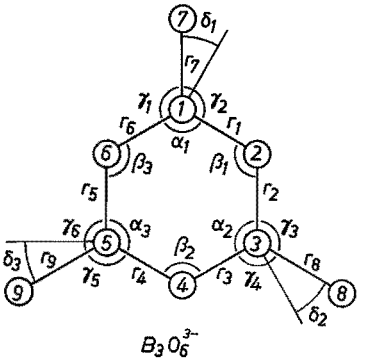

$B_3O_6^{3-}$

r = stretching
α, β, γ = bending
δ = out of plane wag
τ = torsion

Definitions of the internal coordinates

internal coordinate number	kind	atom numbers			
		I	J	K	L
1	r_1	1	2	0	0
2	r_2	2	3	0	0
3	r_3	3	4	0	0
4	r_4	4	5	0	0
5	r_5	5	6	0	0
6	r_6	6	1	0	0
7	r_7	1	7	0	0
8	r_8	3	8	0	0
9	r_9	5	9	0	0
10	α_1	6	1	2	0
11	α_2	2	3	4	0
12	α_3	4	5	6	0
13	β_1	1	2	3	0
14	β_2	3	4	5	0
15	β_3	5	6	1	0
16	γ_1	6	1	7	0
17	γ_2	7	1	2	0
18	γ_3	2	3	8	0
19	γ_4	8	3	4	0
20	γ_5	4	5	9	0
21	γ_6	9	5	6	0
22	δ_1	7	1	2	6
23	δ_2	8	3	4	2
24	δ_3	9	5	6	4
25	τ_1	1	2	3	4
26	τ_2	2	3	4	5
27	τ_3	3	4	5	6
28	τ_4	4	5	6	1
29	τ_5	5	6	1	2
30	τ_6	6	1	2	3

the matrices of the irreducible representations. We call this the method of Nielsen and Berryman [2–36]), who, to our knowledge, were the first to construct the U matrix with this projection operator. In chapter 3 this is done for $B_3O_6^{3-}$ (3.4.1); table 2-VII gives the U matrix of $B_3O_6^{3-}$. The symmetry coordinates nos. 5 and 8 are zero coordinates or straightforward redundant coordinates. This is seen by performing the congruence transformation $G_s = U\,G\,\tilde{U}$. If n is the serial number of a symmetry coordinate and if this coordinate is a zero coordinate, then the nth row and the nth column of G_s will consist of zeros only. However, more redundancies are present among our 30 symmetry coordinates: one more in species A'_1, four in species E' and two in species E'' (table 2-VII). This can be seen at once if we compare the number of symmetry coordinates with the number of modes per species, which have to be equal. They are not straightforwardly redundant in the sense that they do not give rise to the occurrence of rows and columns consisting of only zeros in G_s. This is because, owing to the non-uniqueness of U, zero coordinates are linearly

combined with non-redundant symmetry coordinates of the same species. As for the species A'_1 the linear combination $s_3 - s_4$ is the true redundancy. Because we are allowed to make linear combinations of the symmetry coordinates within a species, we can take $s_3 + s_4$ and $s_3 - s_4$ instead of s_3 and s_4. In this way only $s_3 + s_4$ remains, because $s_3 - s_4$ is redundant.

The redundancies in the degenerate species are not so easy to remove. A method of eliminating the redundancies (which we called the SPC method) is described in chapter 3, sec. 3.3.2. The resulting linear combinations are numerically too complicated to get an easy sketch of the displacement configurations.

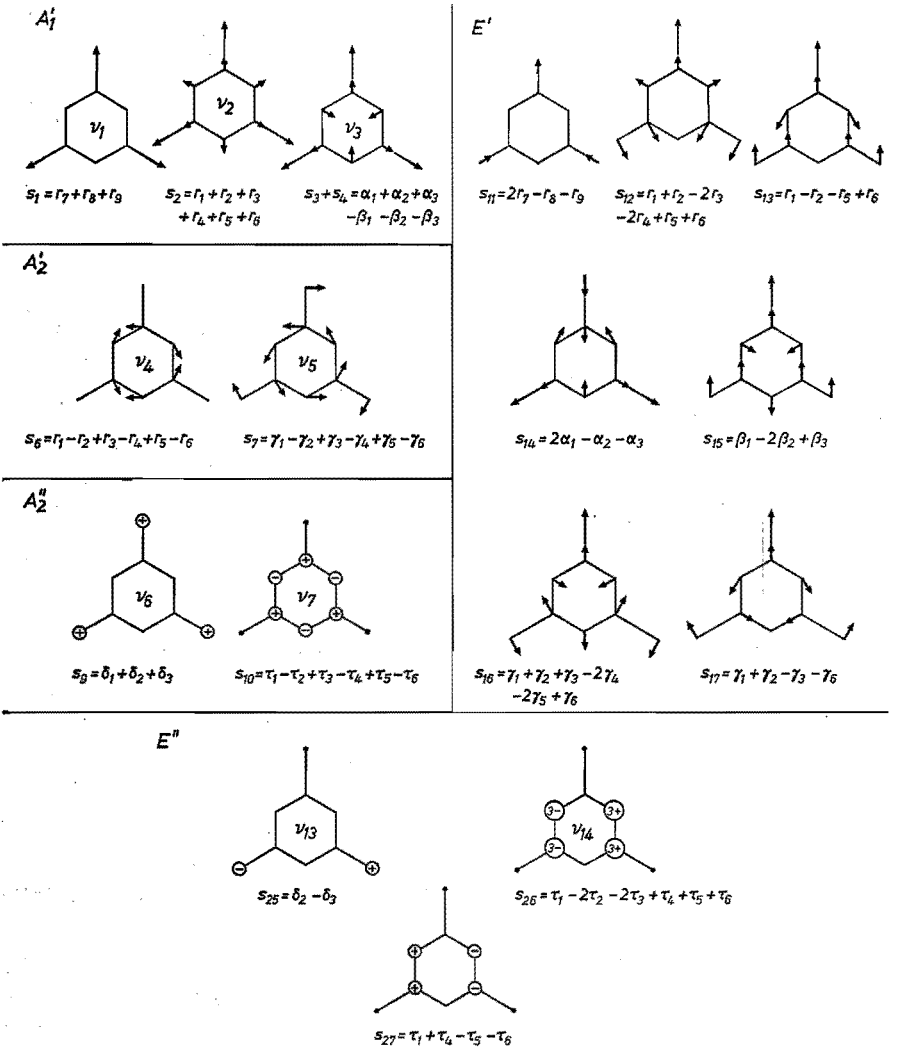

Fig. 2.4. Displacement configurations based on the U matrix of $B_3O_6^{3-}$. ν_8 to ν_{12} belong to species E'.

The symmetry coordinates of a doubly degenerate species may be divided into two sets, each yielding an identical G_s (and F_s) block. Therefore, for each species only one set needs to be considered. For species E' this set is composed of symmetry coordinates nos. 11 to 17 inclusive, and for species E'' of nos. 25, 26 and 27. The coordinates are sketched in fig. 2.4. It can be seen from these figs that s_{26} and s_{27} are identical. Obviously, therefore, a linear combination of these two must be redundant!

2.2.7. *Vibration-intensity relations between ring and crystal*

In secs 2.2.3 and 2.2.4 it has been shown how a vibration of the ring is duplicated in the crystal. To be able to differentiate between the crystal vibrations we will mention their origin: this will be done by placing the original species of the vibration in the $B_3O_6^{3-}$ ion in parentheses behind the symmetry species of the crystal vibration. For instance a crystal vibration belonging to E_g and due to an in-phase vibration of two identical E'' modes of the two rings will be indicated by $E_g\,(E'')$.

It is interesting to see how the inactive vibration A'_2 in the free ring becomes infrared-active in the crystal as $A_{2u}\,(A'_2)$. In this section we will deduce what can be said about the intensity of vibrations of this kind. The theoretical background may be found in Poulet and Mathieu [2–6] (sec. IX.7).

We shall start by looking at the relation between the site (symmetry $\boldsymbol{D}_3$) and the crystal (symmetry $\boldsymbol{D}_{3d}$), after which we shall consider the relations between the free ring (symmetry $\boldsymbol{D}_{3h}$) and the site. For a vibration on site a (see fig. 2.3) we can define the normal coordinate Q_a, the derived polarisability tensor, $\mathbf{P}_a$, and the derived dipole moment vector, $\boldsymbol{M}_a$. This can also be done for the same vibration on site b, giving Q_b, $\mathbf{P}_b$ and $\boldsymbol{M}_b$. We know that the combination of these vibrations in the crystal gives rise to a gerade and an ungerade vibration. These can be represented by the symmetry coordinates

$$s_g = (Q_a + Q_b)/\sqrt{2},$$
$$s_u = (Q_a - Q_b)/\sqrt{2}.$$

The derived polarisability tensors and dipole moment vectors can be combined in the same way to get the derived crystal polarisability tensor and dipole moment vector of each vibration. This may be done in the following way.

Let a rectangular coordinate system O_{xyz} be fixed in the crystal, and a local coordinate system O_a be chosen with its origin on site a and its axes parallel to the corresponding axes of O_{xyz}. If a second local coordinate system O_b is chosen with its origin on site b and in such an orientation that O_a and O_b transform into each other under the inversion operation, and if $\mathbf{P}_a$ and $\boldsymbol{M}_a$ are defined in O_a and $\mathbf{P}_b$ and $\boldsymbol{M}_b$ in O_b, then

$$\mathbf{P}_a = \mathbf{P}_b \equiv \mathbf{P} \quad \text{and} \quad \boldsymbol{M}_a = \boldsymbol{M}_b \equiv \boldsymbol{M}.$$

The transformation matrices T_a and T_b which transform O_a and O_b to the crystal coordinate system O_{xyz} are given by

$$T_a = \begin{pmatrix} 1 & 0 & 0 \\ 0 & 1 & 0 \\ 0 & 0 & 1 \end{pmatrix}, \qquad T_b = \begin{pmatrix} -1 & 0 & 0 \\ 0 & -1 & 0 \\ 0 & 0 & -1 \end{pmatrix}.$$

The contributions from the ring tensor and vector in the crystal tensor and vector will now be

site a

$$\begin{aligned} \mathbf{P}_a^{\text{cryst}} &= T_a \mathbf{P} T_a^{-1} = \mathbf{P} \\ M_a^{\text{cryst}} &= T_a M = M \end{aligned}$$

site b

$$\begin{aligned} \mathbf{P}_b^{\text{cryst}} &= T_b \mathbf{P} T_b^{-1} = \mathbf{P} \\ M_b^{\text{cryst}} &= T_b M = -M. \end{aligned}$$

The total derived polarisability tensor and dipole moment of the crystal become now

for the gerade species $\quad \mathbf{P}^{\text{cryst}} = (\mathbf{P}_a^{\text{cryst}} + \mathbf{P}_b^{\text{cryst}})/\sqrt{2} = \sqrt{2}\,\mathbf{P}$,
$\qquad\qquad\qquad\qquad M^{\text{cryst}} = (M_a^{\text{cryst}} + M_b^{\text{cryst}})/\sqrt{2} = 0$;

for the ungerade species $\quad \mathbf{P}^{\text{cryst}} = \mathbf{0}$,
$\qquad\qquad\qquad\qquad M^{\text{cryst}} = \sqrt{2}\,M$.

This deduction shows that gerade species cannot be infrared-active and ungerade species cannot be Raman-active.

The next thing we have to do is to give the relations between the vibration of the 'free' ion and the ion on the site D_3. In table 2-VI it can be seen that there are different symmetry species of the group D_{3h} (of the 'free' ring) which contribute to one species of the site group D_3. We will now, after Mathieu and Poulet [2–6]) (sec. XI.8.1) make the following assumptions: Let a vibration of the 'free' $B_3O_6^{3-}$ ion belong to the species Γ_1 and another to the species Γ_2 (Γ_1 and Γ_2 are species of D_{3h}). We then assume that both, if incorporated in the crystal, pass into Γ of D_3. Two crystal vibrations will now result. One will be basically the Γ_1 ring vibration with a slight admixture of the Γ_2 ring vibration, the other will be basically the Γ_2 vibration with a slight admixture of the Γ_1 vibration. We will denote them by $\Gamma(\Gamma_1)$ and $\Gamma(\Gamma_2)$, respectively. If we represent the vectors of the derived dipole moment and the tensors of the derived polarisability in D_{3h} by $M(\Gamma_1)$ and $M(\Gamma_2)$, and $\mathbf{P}(\Gamma_1)$ and $\mathbf{P}(\Gamma_2)$ respectively, then vectors and tensors from the vibrations $\Gamma(\Gamma_1)$ in D_3 are

$$\begin{aligned} M(\Gamma(\Gamma_1)) &= M(\Gamma_1) + \lambda\, M(\Gamma_2); \\ \mathbf{P}(\Gamma(\Gamma_1)) &= \mathbf{P}(\Gamma_1) + \lambda\, \mathbf{P}(\Gamma_2); \end{aligned}$$

where λ is a small number. For the $\Gamma(\Gamma_2)$ vibrations in D_3 we have

$$\boldsymbol{M}(\Gamma(\Gamma_2)) = \lambda\, \boldsymbol{M}(\Gamma_1) + \boldsymbol{M}(\Gamma_2);$$
$$\mathbf{P}(\Gamma(\Gamma_2)) = \lambda\, \mathbf{P}(\Gamma_1) + \mathbf{P}(\Gamma_2)\ ;$$

The λ's in these four expressions will in principle be different, but that is not relevant to this discussion.

Let us now see how this works out for the vibrations of the $B_3O_6^{3-}$ ion. Taking the crystal vibrations $E_g(E')$ and $E_u(E')$ we see that they are correlated with the E species of $\boldsymbol{D}_3$. Thus

$$\boldsymbol{M}(E(E')) = \boldsymbol{M}(E') + \lambda\, \boldsymbol{M}(E'').$$

The character table 2-IV gives the components of the derived dipole moment vector (M_x, M_y and M_z):

$$\boldsymbol{M}(E') = \{M_x, M_y, 0\} \quad \text{and} \quad \boldsymbol{M}(E'') = \{0, 0, 0\}.$$

so that in this case $\boldsymbol{M}(E(E')) = \{M_x, M_y, 0\}$.

We represent the non-zero components of the (derivative) of the polarisability tensor by a, b, c and d, and have

$$\mathbf{P}(E(E') = \mathbf{P}(E') + \lambda\, \mathbf{P}(E'').$$

The tensors $\mathbf{P}(E')$ and $\mathbf{P}(E'')$ may be found in Poulet and Mathieu [2–6], p. 245, for the following setting of the local coordinate system O_a: $O_z//C_3$, $O_x//C_2$. They are

$$\mathbf{P}(E', x) = \begin{pmatrix} c & 0 & 0 \\ 0 & -c & 0 \\ 0 & 0 & 0 \end{pmatrix} \quad \text{and} \quad \mathbf{P}(E', y) = \begin{pmatrix} 0 & -c & 0 \\ -c & 0 & 0 \\ 0 & 0 & 0 \end{pmatrix},$$

$$\mathbf{P}(E'', 1) = \begin{pmatrix} 0 & 0 & 0 \\ 0 & 0 & d \\ 0 & d & 0 \end{pmatrix} \quad \text{and} \quad \mathbf{P}(E'', 2) = \begin{pmatrix} 0 & 0 & -d \\ 0 & 0 & 0 \\ -d & 0 & 0 \end{pmatrix}.$$

We now obtain

$$\mathbf{P}(E,x(E')) = \begin{pmatrix} c & 0 & 0 \\ 0 & -c & \lambda \\ 0 & \lambda & 0 \end{pmatrix} \quad \text{and} \quad \mathbf{P}(E, y(E')) = \begin{pmatrix} 0 & -c & -\lambda \\ -c & 0 & 0 \\ -\lambda & 0 & 0 \end{pmatrix}.$$

Combining these results with the results of the first part of this section, we can write for the crystal vibrations

species $E_g(E')$ (gerade species, i.e. $\boldsymbol{M} = \boldsymbol{0}$)

$$\mathbf{P}(E_g, 1) = 1/2\, \mathbf{P}(E, x(E')) = 1/2 \begin{pmatrix} c & 0 & 0 \\ 0 & -c & \lambda \\ 0 & \lambda & 0 \end{pmatrix}$$

and

$$\mathbf{P}(E_g, 2) = 1/2 \begin{pmatrix} 0 & -c & -\lambda \\ -c & 0 & 0 \\ -\lambda & 0 & 0 \end{pmatrix};$$

species E_u (E') (ungerade species, i.e. $\mathbf{P} = \mathbf{0}$)

$$M(E_u, 1) = M(E_u, 2) = 1/2\,\{M_x, M_y, 0\}.$$

There are two polarisability tensors for the degenerate species (and also two dipole moment vectors), because these vibrations are composed of two vibrations (with the same frequency), both possessing their own tensor (and vector). In the same way we can deduce the M and $\mathbf{P}$ for the other species of the crystal:

species A_{1g} (A'_1): $M(A_{1g}) = 0$; $\mathbf{P}(A_{1g}) = 1/2 \begin{pmatrix} a & 0 & 0 \\ 0 & a & 0 \\ 0 & 0 & b \end{pmatrix}$;

species A_{2u} (A'_2): $M(A_{2u}) = 1/2\,\{0, 0, \lambda\}$; $\mathbf{P}(A_{2u}) = \mathbf{0}$.

species A_{2u} (A''_2): $M(A_{2u}) = 1/2\,(0, 0, M_z)$; $\mathbf{P}(A_{2u}) = \mathbf{0}$;

species E_g(E'') : $\mathbf{P}(E_g, 1) = 1/2 \begin{pmatrix} \lambda & 0 & 0 \\ 0 & -\lambda & d \\ 0 & d & 0 \end{pmatrix}$

and $\mathbf{P}(E_g, 2) = 1/2 \begin{pmatrix} 0 & -\lambda & -d \\ -\lambda & 0 & 0 \\ -d & 0 & 0 \end{pmatrix}$;

$M(E_g, 1) = M(E_g, 2) = \mathbf{0}$.

species E_u (E'') : $M(E_u, 1) = M(E_u, 2) = 1/2\,\{\lambda, \lambda, 0\}$;

$\mathbf{P}(E_u, 1) = \mathbf{P}(E_u, 2) = \mathbf{0}$;

It is clear now why the infrared-inactive vibration A'_2 of the ring has become active in the crystal as an A_{2u} vibration: its derived dipole moment is not equal to zero. However, it is unlikely that the species A_{2u} (A'_2) and E_u (E'') can be seen in the infrared, because in their case all contributions to the derived dipole moment vector are small.

2.2.8. *Single crystals*

In the factor group analysis we have distributed the normal vibrations among the different symmetry species. Every active species is characterised by one or more non-zero components — specific to the species — of the derivative of the polarisability tensor or dipole moment vector. The components can be measured separately if we take into account the directions that define these components. This is only possible if we use polarised light and single crystals for our measurements. If the components are found for every vibration, then

we are able to decide what the symmetry species of the vibrations are. This is of course an important tool for the assignment of the vibrational spectra.

We succeeded in growing single crystals of sodium metaborate from the melt and also in recording the Raman spectra of these crystals. We decided not to align the crystal for several reasons.

(1) Since the alkali metaborates are very hygroscopic, the alignment would have involved taking special precautions to protect the crystal against moisture.
(2) The alignment is time consuming.
(3) The information can be obtained without an alignment, as will be shown in this section.

We did not try to make infrared spectra from the single crystals, because the crystals were too small.

In this section we will calculate the expected intensities of the different vibrations in a non-aligned single crystal. Before starting the calculation of the intensity we define a right handed coordinate system O_{pqr}. This is placed in such a way that the laser beam enters along the r axis and the observed radiation leaves the sample along the p axis. The entering beam is polarised parallel to the q axis. The coordinate system of the crystal, which is independent of O_{pqr}, will be O_{xyz} (see fig. 2.5).

The derivative of the polarisability tensor $\mathbf{P}_{xyz}$ can be transposed to the coordinate system O_{pqr} with the transformation matrix T:

$$\mathbf{P}_{pqr} = T^{-1}\,\mathbf{P}_{xyz}\,T \tag{2.1}$$

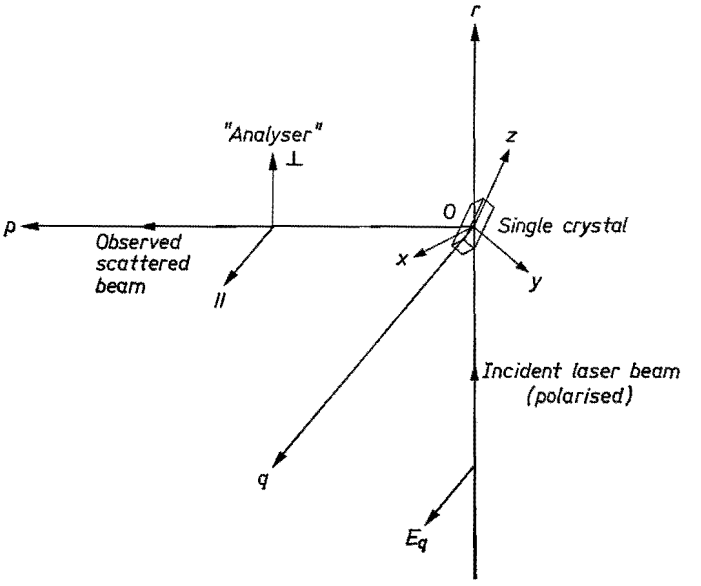

Fig. 2.5

$$T = \begin{pmatrix} t_{11} & t_{12} & t_{13} \\ t_{21} & t_{22} & t_{23} \\ t_{31} & t_{32} & t_{33} \end{pmatrix} = \begin{pmatrix} \cos(p, x) \cos(q, x) \cos(r, x) \\ \cos(p, y) \cos(q, y) \cos(r, y) \\ \cos(p, z) \cos(q, z) \cos(r, z) \end{pmatrix}. \qquad (2.2)$$

The relations between the direction cosines are

$$\sum_{j=1}^{3} t_{ij}\, t_{kj} = \delta_{ik} \quad \text{and} \quad \sum_{j=1}^{3} t_{ji}\, t_{jk} = \delta_{ik} \quad (i, k = 1, 2, 3)$$

This implies the orthonormality of the matrix T and will be used below. According to Poulet and Mathieu [2–6]) the intensity of the scattered Raman radiation for a vibration belonging to the species $\Gamma^{(i)}$ with a degree of degeneracy l_i is given by

$$I = k \sum_{n=1}^{l_i} \Big| \sum_{\alpha,\beta} e_{2\alpha}\, e_{1\beta}\, P_{\alpha\beta}((i), n) \Big|^2. \qquad (2.3)$$

In this equation $e_{1\beta}$ and $e_{2\alpha}$ ($\alpha, \beta = p, q, r$) are the components of the unit vectors $\boldsymbol{e}_1$ and $\boldsymbol{e}_2$, which define the respective directions of the entering polarised beam and the polarisation direction of the analyser. $P_{\alpha\beta}((i), n)$ is the component on row α and in column β of the tensor $\mathbf{P}$ for member n from the degenerate set of vibrations of species $\Gamma^{(i)}$; k is a constant. We know for the entering beam that $e_{1p} = 0$, $e_{1q} = 1$ and $e_{1r} = 0$ and for the components of the observed scattered beam, after it has passed through the analyser, we have *)

$$I_{\parallel}\colon\ e_{2p} = 0,\ e_{2q} = 1 \quad \text{and} \quad e_{2r} = 0;$$
$$I_{\perp}\colon\ e_{2p} = 0,\ e_{2q} = 0 \quad \text{and} \quad e_{2r} = 1;$$

There are two symmetry species we are interested in: A_{1g} and E_g. The scattered intensities $I_{\parallel}$ and $I_{\perp}$ are (from eq. (2.3))

$$A_{1g}\colon \quad I_{\parallel} = k\,[P_{qq}(A_{1g})]^2, \qquad (2.4)$$
$$I_{\perp} = k\,[P_{rq}(A_{1g})]^2; \qquad (2.5)$$

$$E_g\ :\quad I_{\parallel} = k\,\{[P_{qq}(E_g, 1)]^2 + [P_{qq}(E_g, 2)]^2\}, \qquad (2.6)$$
$$I_{\perp} = k\,\{[P_{rq}(E_g, 1)]^2 + [P_{rq}(E_g, 2)]^2\}. \qquad (2.7)$$

($\mathbf{P}$ is symmetric, hence $P_{rq} = P_{qr}$.)

The polarisability tensors $\mathbf{P}_{xyz}$ for the different symmetry species are (see Mathieu and Poulet [2–6]), pp. 244–245 or Turrell [2–5]), p. 359)

*) $I_{\parallel}$ is the intensity of the scattered light polarised in the q direction (by means of an analyser). $I_{\perp}$ is the intensity of the scattered beam polarised in the r direction.

$$\mathbf{P}_{xyz}(A_{1g}) = \begin{pmatrix} a & 0 & 0 \\ 0 & a & 0 \\ 0 & 0 & b \end{pmatrix}, \tag{2.8}$$

$$\mathbf{P}_{xyz}(E_g, 1) = \begin{pmatrix} c & 0 & 0 \\ 0 & -c & d \\ 0 & d & 0 \end{pmatrix}, \tag{2.9}$$

$$\mathbf{P}_{xyz}(E_g, 2) = \begin{pmatrix} 0 & -c & -d \\ -c & 0 & 0 \\ -d & 0 & 0 \end{pmatrix}. \tag{2.10}$$

From eqs (2.4), (2.5), (2.6) and (2.7) we know that only P_{qq} and P_{rq} are of interest. For the intensities we now obtain the following expressions with the help of eq. (2.1):

$$A_{1g}: I_{\parallel} = k P_{qq}^2 = k \left[(t_{12}, t_{22}, t_{32}) \mathbf{P}_{xyz}(A_{1g}) \begin{pmatrix} t_{12} \\ t_{22} \\ t_{32} \end{pmatrix} \right]^2 =$$

$$= k (a t_{12}^2 + a t_{22}^2 + b t_{32}^2)^2 = k [a (1 - t_{32}^2) + b t_{32}^2]^2, \tag{2.11}$$

$$A_{1g}: I_{\perp} = k P_{rq}^2 = k \left[(t_{13}, t_{23}, t_{33}) \mathbf{P}_{xyz}(A_{1g}) \begin{pmatrix} t_{12} \\ t_{22} \\ t_{32} \end{pmatrix} \right]^2 =$$

$$= k [a (t_{12} t_{13} + t_{22} t_{23}) + b t_{32} t_{33}]^2 = k [t_{32} t_{33} (a - b)]^2, \tag{2.12}$$

$$E_g: \quad I_{\parallel} = k \left\{ \left[(t_{12}, t_{22}, t_{32}) \begin{pmatrix} c & 0 & 0 \\ 0 & -c & d \\ 0 & d & 0 \end{pmatrix} \begin{pmatrix} t_{12} \\ t_{22} \\ t_{32} \end{pmatrix} \right]^2 + \right.$$

$$\left. + \left[(t_{12}, t_{22}, t_{32}) \begin{pmatrix} 0 & -c & d \\ -c & 0 & 0 \\ -d & 0 & 0 \end{pmatrix} \begin{pmatrix} t_{12} \\ t_{22} \\ t_{32} \end{pmatrix} \right]^2 \right\} =$$

$$= k \{ [c (t_{12}^2 - t_{22}^2) + 2d t_{32} t_{22}]^2 + [2c t_{12} t_{22} + 2d t_{12} t_{32}]^2 \}, \tag{2.13}$$

$$I_{\perp} = k \left\{ \left[(t_{13}, t_{23}, t_{33}) \begin{pmatrix} c & 0 & 0 \\ 0 & -c & d \\ 0 & d & 0 \end{pmatrix} \begin{pmatrix} t_{12} \\ t_{22} \\ t_{32} \end{pmatrix} \right]^2 + \right.$$

$$\left. + \left[(t_{13}, t_{23}, t_{33}) \begin{pmatrix} 0 & -c & -d \\ -c & 0 & 0 \\ -d & 0 & 0 \end{pmatrix} \begin{pmatrix} t_{12} \\ t_{22} \\ t_{32} \end{pmatrix} \right]^2 \right\} =$$

$$= k \{ [c (t_{12} t_{13} - t_{22} t_{23}) + d (t_{23} t_{32} + t_{22} t_{33})]^2 +$$

$$+ [c (t_{12} t_{22} + t_{12} t_{23}) + d (t_{13} t_{32} + t_{12} t_{33})]^2 \}. \tag{2.14}$$

With the last four equations it is possible to say something about the intensity ratio $\varrho \equiv I_{\perp}/I_{||}$, also called the degree of depolarisation. For A_{1g}:

$$\varrho = \frac{k\,[t_{32}\,t_{33}\,(a-b)]^2}{k\,[a\,(1-t_{32}{}^2)+b\,t_{32}{}^2]^2}. \tag{2.15}$$

For the A_{1g} vibrations it seems reasonable to suppose that

$$a \gg b\,(P_{xx} = P_{yy} \gg P_{zz}),$$

since the three internal A_{1g} vibrations of the ring are all in the x–y plane. If it is further supposed that t_{32} is sufficiently smaller than 1 we have

$$a \gg b\,t_{32}{}^2/(1-t_{32}{}^2).$$

Then

$$\varrho \cong \frac{t_{32}{}^2\,t_{33}{}^2\,a^2}{a^2\,(1-t_{32}{}^2)^2} = \frac{t_{32}{}^2\,t_{33}{}^2}{(1-t_{32}{}^2)^2}. \tag{2.16}$$

If $t_{32}{}^2$ approaches 1, we can write

$$\varrho \cong \frac{t_{32}{}^2\,t_{33}{}^2\,a^2}{b^2\,t_{32}{}^4} = \frac{t_{33}{}^2\,a^2}{t_{32}{}^2\,b^2} \tag{2.17}$$

and because $t_{33}{}^2 + t_{32}{}^2 + t_{31}{}^2 = 1$, $t_{33}{}^2$ and $t_{31}{}^2$ have to be very small. Then, it is evident that

$$\frac{t_{33}{}^2}{t_{32}{}^2} \ll 1.$$

Since $a^2/b^2 \gg 1$, ϱ cannot be predicted. But in this case $I_{\perp}$ and $I_{||}$ are very small because $t_{32}{}^2 \cdot t_{33}{}^2 \ll 1$, $(1-t_{32}{}^2) \ll 1$ and also $b\,t_{32}{}^2 \ll a$. Provided we take a direction of the crystal with enough intensity we can use eq. (2.16). Figure 2.6 gives the value of ϱ from eq. (2.16) for values of the direction cosines t_{32} and t_{33} ranging from 0 to 1. In this figure it can be seen that $\varrho < 1$ for most angles. Only in the shaded area is $\varrho > 1$, and this was the part where eq. (2.17) had to be used. This last area is not of practical interest. *Conclusion:* For the internal A_{1g} vibrations with sufficient intensity is $\varrho < 1$ ($I_{||} > I_{\perp}$).

The treatment for the E_g vibrations is somewhat more complicated. From the preceding section we know that there are two kinds of internal E_g vibrations: $E_g\,(E')$ and $E_g\,(E'')$. In sec. 2.2.7 it has been shown that for $E_g\,(E')$ the value for d in eq. (2.9) and (2.10) is small ($d = \lambda$) and for $E_g\,(E'')$ we found $c = \lambda$. Filling in these values in eqs (2.13) and (2.14) we obtain the following intensities:

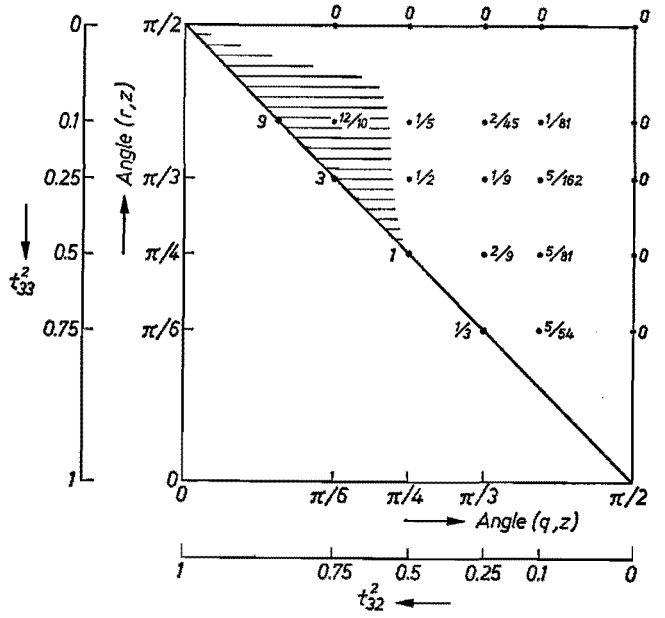

Fig. 2.6. ϱ-values for $0 \leqslant t_{32}^2, t_{33}^2 \leqslant 1$.

$$E_g(E'): \quad I_{\parallel} = k\{[c(t_{12}^2 - t_{22}^2) + 2\lambda t_{22} t_{32}]^2 + [2c t_{12} t_{22} + 2\lambda t_{12} t_{32}]^2\},$$
$$I_{\perp} = k\{[c(t_{12} t_{13} - t_{22} t_{23}) + \lambda(t_{23} t_{32} + t_{22} t_{33})]^2 +$$
$$+ [c(t_{12} t_{23} + t_{22} t_{13}) + \lambda(t_{13} t_{32} + t_{12} t_{33})]^2\};$$

$$E_g(E''): \quad I_{\parallel} = k\{[2d t_{22} t_{32} + \lambda(t_{12}^2 - t_{22}^2)]^2 + [2d t_{12} t_{32} + 2\lambda t_{12} t_{22}]^2\},$$
$$I_{\perp} = k\{[d(t_{22} t_{33} + t_{23} t_{32}) + \lambda(t_{12} t_{13} - t_{22} t_{23})]^2 +$$
$$+ [d(t_{12} t_{33} + t_{13} t_{32}) + \lambda(t_{22} t_{13} + t_{12} t_{23})]^2\}.$$

Since the λ's are small quantities we assume them to be zero and obtain for the ϱ's

$$\varrho(E_g(E')) = \frac{1 - t_{33}^2}{1 - t_{32}^2} \tag{2.18}$$

$$\varrho(E_g(E'')) = \frac{t_{32}^2 + t_{33}^2 - 4 t_{32}^2 t_{33}^2}{4 t_{32}^2 (1 - t_{32}^2)}. \tag{2.19}$$

It can be seen that these equations for $\varrho(E_g(E'))$ and $\varrho(E_g(E''))$ are independent of c and d and that in general they will not be equal.

Conclusion: The value of ϱ for the E_g species is only dependent on the angles and not on the values of c or d. In the general case $E_g(E')$ and $E_g(E'')$ have a different ϱ.

2.3. Experiments

2.3.1. *Preparation of the samples*

The majority of the samples were obtained by melting together anhydric B_2O_3 and alkali carbonates (if possible borax). The chemicals used were reagent grade from Merck; the chemicals enriched with ^{10}B were delivered by 20th Century Electronics Ltd. The metaborate crystals were made by cooling the melt about 50 °C below their melting point and annealing for several hours at this temperature. The single crystals were formed by cooling the melt very slowly (0.5 °C/hr) to a temperature below the melting point (Bronswijk [2–37]).

The structure was checked with X-ray diffraction (Debye–Sherrer exposures). Because of the hygroscopic behaviour of the metaborates, the sample was enclosed in a Lindemann capillary. The measured d values of $Na_3B_3O_6$ and $K_3B_3O_6$ agreed well with the calculated values from the crystal structure (and the values of the ASTM system). A detailed structure of the rubidium metaborate and the cesium metaborate is not known. Schneider and Carpenter [2–4]) found that these compounds were isostructural with $Na_3B_3O_6$ and $K_3B_3O_6$, which agrees well with our measurements (v. Grotel [2–2])).

The glass samples were made by cooling the melt in air. There was no measurable influence of small amounts of water or carbon dioxide in the Raman spectra. Samples were melted in the normal way and also in a vacuum furnace (10^{-4} Torr, 1000 °C) but no difference in the Raman spectra was found between them.

For the Raman measurements (and also for the infrared measurements) the crystals were powdered in an agate mortar. The powder was placed in the Raman spectroscope at an angle of 60° with the laser beam. The infrared measurements were done by suspending the powder in a polyethylene matrix (for the frequency region below 600 cm^{-1}) or in an alkali-halide matrix (above 600 cm^{-1}). This alkali-halide was usually KBr. The single-crystal samples were only measured in the Raman spectroscope and irradiated at different angles. The glass samples were made by drawing a thin bar (some millimetres thick and about 5 cm long) from the melt. The bars were irradiated by the laser beam along their length axis. In this way a maximum output was obtained, because the whole sample was irradiated by the beam and the path of the scattered light through the sample was very short. No infrared measurements were made on these glasses, recent infrared measurements on borate glasses having been made by Konijnendijk [2–1]).

2.3.2. *Raman and infrared measurements*

All Raman scattering measurements were made on a Cary 82 Raman spectrograph (from Varian). The spectrograph was equipped with an Ar^+ laser (Spectra Physics model 165) giving a maximum output of about two watts for the used

lines. The wavelength of the incident laser beam generally used was the green line at 514.5 nm. In a few cases the blue line at 488.0 nm was used, in order to be sure that no plasma lines (or other interference) had been recorded. The bandwidth used was normally 5 cm^{-1}.

The infrared measurements were done with a Hitachi EPI-L spectrograph for the frequency region from 200 cm^{-1} up to 700 cm^{-1}. The measurements in the frequency region from 400 cm^{-1} up to 4000 cm^{-1} were done on a type MK-3 double-beam grating spectrophotometer from Grubb–Parsons. The infrared spectrum of $Na_3B_3O_6$ in the region from 40 cm^{-1} up to 280 cm^{-1} was recorded by H. v.d. Boom (Philips Research Laboratories). A cooling cell equipped with KBr windows was used for infrared measurements at liquid nitrogen temperatures.

For the Raman spectroscopy two special cells were developed by E. Strijks: one for liquid nitrogen temperature and one for temperatures up to 500 °C. The Raman spectra of $Na_3B_3O_6$ (with three different ratios of $^{10}B/^{11}B$), $K_3B_3O_6$, $Rb_3B_3O_6$ and $Cs_3B_3O_6$ are given in figs 2.7 to 2.13. The peak frequencies of $Na_3B_3O_6$ are tabulated in tables 2-VIII and 2-IX with an indication of the intensity. Tables 2-X and 2-XI give the infrared frequencies and intensities. Table 2-XII shows the Raman frequencies of the four metaborates.

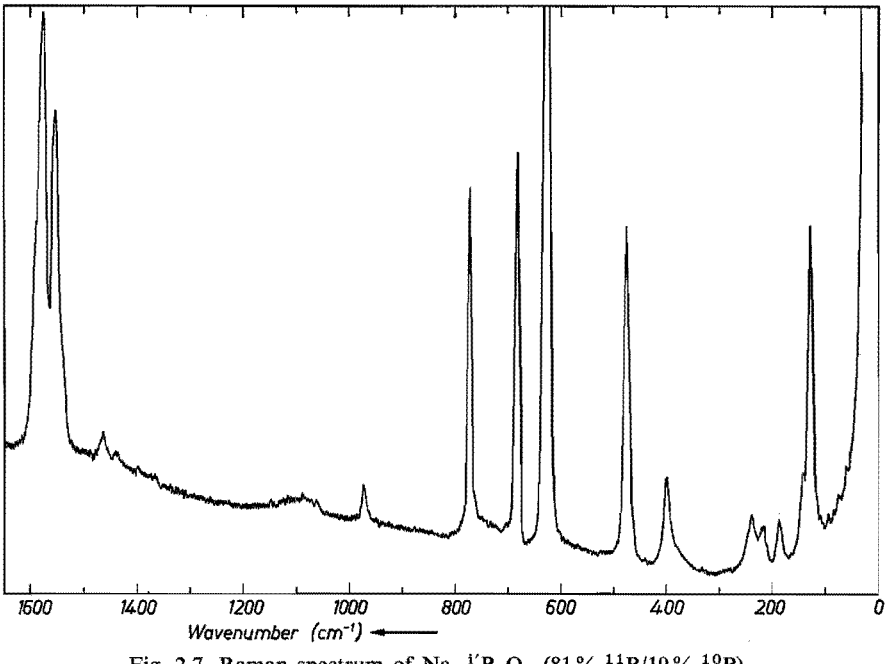

Fig. 2.7. Raman spectrum of $Na_3{}^{i'}B_3O_6$ (81% ^{11}B/19% ^{10}B).

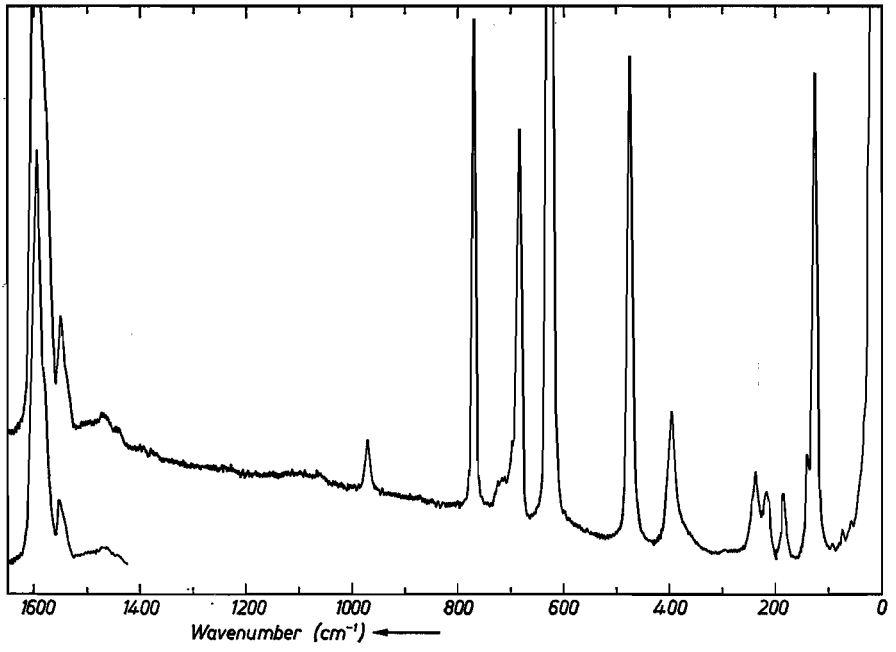

Fig. 2.8. Raman spectrum of $Na_3{}^{1''}B_3O_6$ (56% ^{10}B/44% ^{11}B).

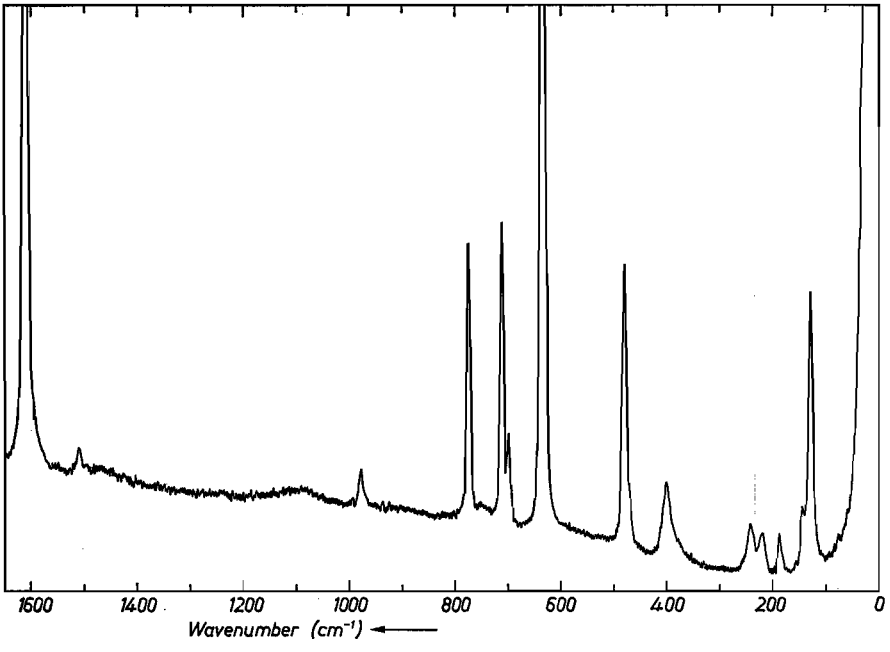

Fig. 2.9. Raman spectrum of $Na_3{}^{1}B_3O_6$ (93% ^{10}B/7% ^{11}B).

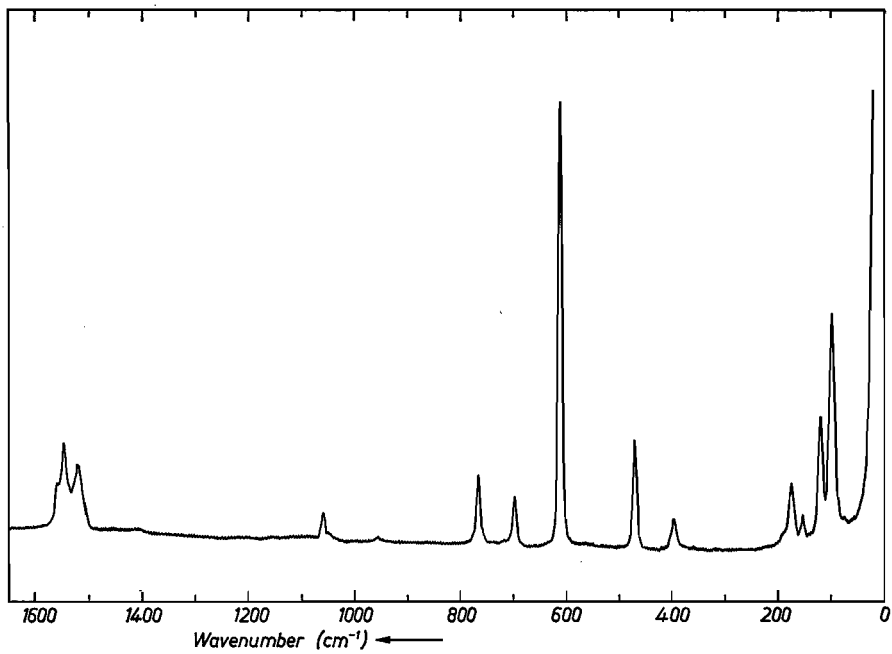

Fig. 2.10. Raman spectrum of K_3BO_6 (81% ^{10}B/19% ^{11}B).

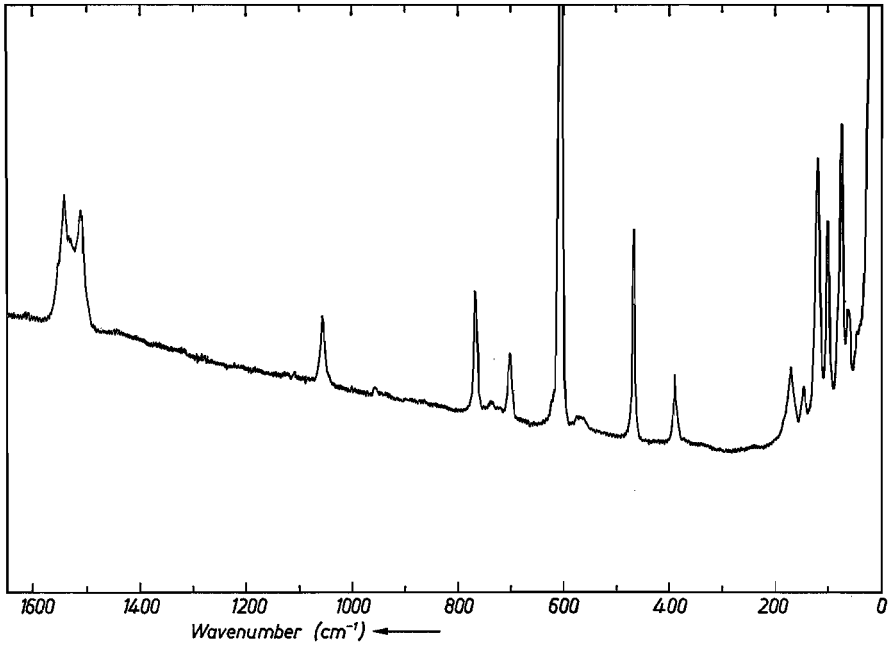

Fig. 2.11. Raman spectrum of RbB_3O_6 (81% ^{10}B/19% ^{11}B).

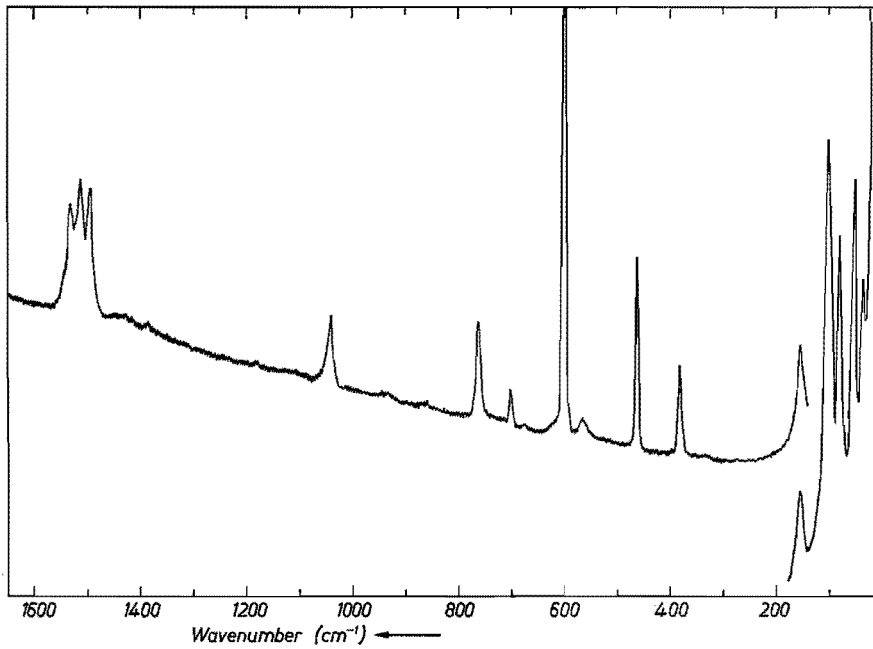

Fig. 2.12. Raman spectrum of CsB_3O_6 (81% ^{10}B/19% ^{11}B).

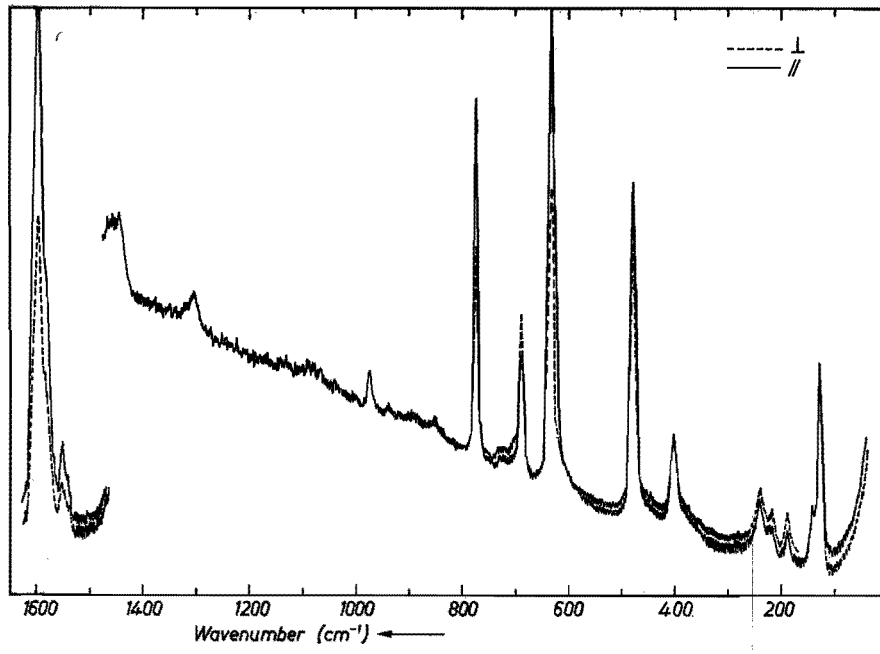

Fig. 2.13. Single crystal Raman spectrum of $Na_3{}^{i''}B_3O_6$ (56% ^{10}B/44% ^{11}B).

TABLE 2-VIII

Raman frequencies of $Na_3\ ^{i}B_3O_6$ (93% ^{10}B). The values between brackets are the differences between the maximum and the minimum value of three observations

127[4] (0.9) cm^{-1} s	694[0] (0.6) cm^{-1} m
140[5] (1.0) cm^{-1} m, sh	706[4] (0.9) cm^{-1} s
185[6] (0.8) cm^{-1} w	769[4] (1.3) cm^{-1} s
217[3] (1.4) cm^{-1} w	973[2] (2.3) cm^{-1} w
238[7] (1.2) cm^{-1} w	(1468?) cm^{-1} vw
397[4] (0.9) cm^{-1} m	(1490?) cm^{-1} vw, sh
476[2] (0.5) cm^{-1} s	1503[8] cm^{-1} w
630[6] (0.4) cm^{-1} ss	1604[7] (0.2) cm^{-1} ss

s = strong, m = medium, w = weak, ? = uncertain, sh = shoulder.

TABLE 2-IX

Raman frequencies of $Na_3\ ^{i'}B_3O_6$ (81% ^{11}B, natural abundance). The values between brackets are the differences between two observations

25 °C	230 °C	25 °C	230 °C
126 (1.1) cm^{-1} s	125 (0.1) cm^{-1}	679 (1.5) cm^{-1} s	679 (0.1) cm^{-1}
142 (0.8) cm^{-1} m, sh	139 (1.2) cm^{-1}	769 (1.1) cm^{-1} s	768 (1.5) cm^{-1}
186 (0.4) cm^{-1} w	183 (0.5) cm^{-1}	969 (1.0) cm^{-1} w	—
217 (1.0) cm^{-1} w	213 (—) cm^{-1}	1440(?) cm^{-1} vw	
239 (1.5) cm^{-1} w	235 (—) cm^{-1}	1461 cm^{-1} vw	
397 (1.0) cm^{-1} m	398 (3.0) cm^{-1}	1550 (0.8) cm^{-1} s	1549 (—) cm^{-1}
473 (0.4) cm^{-1} s	474 (0.0) cm^{-1}	1573 (1.0) cm^{-1} s	1572 cm^{-1}
624 (0.4) cm^{-1} ss	624 (0.3) cm^{-1}	1585 (0.0) cm^{-1} m, sh	1584 (—) cm^{-1}

TABLE 2-X

Infrared frequencies of $Na_3\ ^{i}B_3O_6$ (93% ^{10}B). The values are the average of two observations

225 cm^{-1} very broad	955 cm^{-1} m
380 cm^{-1} s	1240 cm^{-1} s
480 cm^{-1} w	1275 cm^{-1} ss
690 cm^{-1} w	1440 cm^{-1} s
738 cm^{-1} s	1480 cm^{-1} ss

TABLE 2-XI

Infrared frequencies of $Na_3\ ^{i'}B_3O_6$ (81% ^{11}B, natural abundance). The values are the average of two observations

225 cm^{-1} very broad	950 cm^{-1} m
380 cm^{-1} s	1217 cm^{-1} s
480 cm^{-1} vw	1250 cm^{-1} s
707 cm^{-1} m	1390 cm^{-1} m
722 cm^{-1} m	1450 cm^{-1} ss, broad maximum

TABLE 2-XII

Raman frequencies of $Na_3B_3O_6$, $K_3B_3O_6$, $Rb_3B_3O_6$ and $Cs_3B_3O_6$ (81 % ^{11}B and 19 % ^{10}B, natural abundance). The Raman spectra of $Na_3B_3O_6$ and $K_3B_3O_6$ were also recorded at liquid nitrogen temperature. No change was observed in the spectrum of $Na_3B_3O_6$. In the case of $K_3B_3O_6$ the peaks at 100 cm^{-1} and 612 cm^{-1} were split up

$Na_3B_3O_6$	$K_3B_3O_6$	$Rb_3B_3O_6$	$Cs_3B_3O_6$
126 cm^{-1} s	100 cm^{-1} s	44 cm^{-1} ?	39 cm^{-1} s
142 cm^{-1} m, sh	120 cm^{-1} m	64 cm^{-1} m	58 cm^{-1} s
186 cm^{-1} w	154 cm^{-1} w	76 cm^{-1} s	85 cm^{-1} s
217 cm^{-1} w	176 cm^{-1} w	102 cm^{-1} s	105 cm^{-1} s
239 cm^{-1} w	190 cm^{-1} w, sh	122 cm^{-1} s	158 cm^{-1} ms
		148 cm^{-1} m	
		172 cm^{-1} m	
397 cm^{-1} m	397 cm^{-1} w	390 cm^{-1} m	384 cm^{-1} ms
473 cm^{-1} s	471 cm^{-1} m	467 cm^{-1} s	465 cm^{-1} s
624 cm^{-1} ss	612 cm^{-1} ss	606 cm^{-1} ss	601 cm^{-1} ss
679 cm^{-1} s	697 cm^{-1} m	700 cm^{-1} m	702 cm^{-1} m
769 cm^{-1} s	766 cm^{-1} m	766 cm^{-1} ms	763 cm^{-1} ms
969 cm^{-1} w	960 cm^{-1} vw	956 cm^{-1} ?	935 cm^{-1} ?
		1055 cm^{-1} m	1040 cm^{-1} m
1440? cm^{-1} vw			
1461 cm^{-1} vw			1430 cm^{-1} ?
1550 cm^{-1} s	1522 cm^{-1} s	1507 cm^{-1} s	1494 cm^{-1} s
1573 cm^{-1} ss	1548 cm^{-1} ss	1527 cm^{-1} m, sh	1512 cm^{-1} s
		1536 cm^{-1} s	1530 cm^{-1} m
1585 cm^{-1} m, sh	1558 cm^{-1} s	1550 cm^{-1} m, sh	1543 cm^{-1} ?, sh

2.4. Assignment of spectra

2.4.1. *Introduction*

In the following part of this chapter we give an assignment of the crystal spectra of sodium metaborate. Our assignment was based in the first place on the established data of the preceding secs. Since these data were not sufficient for a complete assignment we used other methods, such as a comparison with the tri-substituted benzenes, to complete the picture.

2.4.2. *Isotope effects*

As already mentioned in sec. 2.3, we used samples with different $^{10}B/^{11}B$ ratios. Both isotopes are stable and found in the natural boron compounds in the ratio $^{10}B/^{11}B = 19/81$. If we assume that both isotopes are randomly distributed over all boron positions, we can distinguish four different rings with percentages as given in table 2-XIII.

In these compounds we expect at least four peaks from every fundamental vibration, one for every ring of different isotopic composition. It is even possible that as a result of lowering the symmetry of the ring containing both isotopes the doubly degenerate species will split up into two non-degenerate

TABLE 2-XIII

Frequencies and intensities of two ring vibrations for the rings with different isotope composition

sample	composition ^{10}B	^{11}B	ring $^{10}B_3O_6^{3-}$	frequencies 1606	707 cm^{-1}	ring $^{10}B_2{}^{11}BO_6^{3-}$	frequencies 1593	698 cm^{-1}	ring $^{10}B^{11}B_2O_6^{3-}$	frequencies 1576	682 cm^{-1} *)	ring $^{11}B_3O_6^{3-}$	frequencies 1550	682 cm^{-1} *)
$Na_3{}^{i}B_3O_6$	93%	7%	80.4%	ss	ss	18.2%	—	ms	1.4%	—	—	0.03%	—	—
$Na_3{}^{i'}B_3O_6$	19%	81%	0.8%	w	—	9.4%	ms	w	38.2%	ss	(ss)	51.6%	s	(ss)
$Na_3{}^{i''}B_3O_6$	56%	44%	17.9%	w	—	41.6%	ss	m	32.3%	ms	(ss)	8.3%	m	(ss)

*) The peak at 682 cm^{-1} is probably the sum of the peaks for $^{11}B_3O_6^{3-}$ and $^{10}B^{11}B_2O_6^{3-}$.

species. Unfortunately this symmetry splitting is much smaller than the width of the peaks and cannot be observed, so that only isotope shifts are visible. Moreover, the peaks due to rings occurring in a low concentration will merge into the background. It is also possible that there will be fewer than four peaks owing to the overlap of two or more peaks.

From the Raman spectra of the three compounds it is clear that there are two vibrations, which show the isotope splitting (Bronswijk [2-37]). The infrared spectra are less suited to the study of this effect because of the poor resolution of the different peaks. The two split Raman vibrations occur in the region from 1550 to 1600 cm^{-1} and around 700 cm^{-1}. It can be seen from the spectra (figs 2.7, 2.8 and 2.9) that the peak intensities agree rather well with the percentages of the different rings *) as can be seen in table 2-XIII. The frequency increases as the mass of the ring decreases, as must be expected.

2.4.3. *Infrared and Raman spectra*

The first thing we can do is to separate the lattice vibrations from the internal vibrations of the $B_3O_6^{3-}$ ring. Table 2-XII shows the Raman frequencies of the four alkali metaborates (Na, K, Rb and Cs). As was stated in sec. 2.1, these crystals are all isomorphous. It is easy to see from this table that the peaks with a frequency lower than 250 cm^{-1} show great differences, whereas the peaks above 250 cm^{-1} resemble each other very much in frequency and intensity. Therefore we assign the peaks below 250 cm^{-1} to the lattice vibrations **).

In the spectrum of $Na_3B_3O_6$ we can see five lattice vibrations, which is one less than the expected number of six. Of these six, five belong to E_g and one to A_{1g}. Bagavantam [2-7] and Harrand [2-38] establish that a libration (belonging to the lattice vibrations) of an optical anisotropic group gives rise to an intensive Raman line, while the translational vibrations are usually weak. If we apply this rule to our spectra, then the peak with the frequency of 126 cm^{-1} will be the libration of the $B_3O_6^{3-}$ group. The remaining lattice vibrations are not easy to assign. The infrared spectra do not help; in the low frequency region only a broad band around 225 cm^{-1} was detected.

The infrared spectra do give information about the internal vibrations. The infrared-active vibrations belong to the species A_{2u} and E_u (see table 2-VI). If we assume that the intensities of A_{2u} (A'_2) and E_u (E'') are low (see sec. 2.2.7) we are left with the vibrations belonging to A_{2u} (A''_2) and E_u (E'). The five vibrations belonging to E_u (E') should correspond in frequency to the five

*) The rings with both ^{10}B and ^{11}B (frequencies 1576 cm^{-1} and 1593 cm^{-1}) have a relatively too high intensity. It is not possible to give a comparison of the peak heights owing to the overlap of the peaks.

**) As will be seen later, internal vibrations with frequencies below 250 cm^{-1} are not to be excluded. Actually, our normal coordinate analysis of the compound provided strong evidence that the frequencies of two internal vibrations do fall in this region.

Raman-active vibrations E_g (E') (see sec. 2.2.3). The assignment of these species is done in secs 2.4.5 and 2.4.6.

The three internal vibrations belonging to A_{1g} are assigned in the next section.

2.4.4. *Single-crystal Raman spectra*

In sec. 2.2.8 we derived some expressions for the ϱ of the two Raman-active species (internal vibrations)A_{1g} and E_g. If we take the same assumptions, hence a $\gg$ b and enough intensity for the A_{1g} vibrations, and for the E_g vibrations $\lambda = 0$, then the ϱ's are only dependent on the orientation of the crystal with respect to the incident laser beam. Within each symmetry species (A_{1g}, E_g (E'), or E_g (E'')), the value of ϱ does not depend on the modes.

In the spectra, three peaks possessed an equal value for ϱ (< 1) for each orientation of the crystal. One of these spectra is shown in fig. 2.13. The peaks referred to have a $\varrho = \frac{1}{2}$ in this case. They are found at 1547 cm^{-1} to 1606 cm^{-1} (isotope shift), at 769 cm^{-1} and at 630 cm^{-1}. Moreover, they are the strongest peaks in the spectrum. For both these reasons it is reasonable to suppose that they are the three internal A_{1g} vibrations.

The ϱ of all the other peaks in the spectrum is ≈ 1. The intensity of the majority of these peaks is too low for more precise measurements of ϱ. Two strong peaks, which have a measurable ϱ, are the peaks at 478 cm^{-1} and 686 cm^{-1}. From fig. 2.13 it is easy to see that their ϱ's are different, hence we conclude that they belong to different species, i.e. E_g (E') and E_g (E'').

The lattice vibrations (with frequencies lower than 250 cm^{-1}) cannot be divided among the symmetry species. Five of them belong to E_g and one to A_{1g}. In the spectrum five peaks can be seen, mostly too weak for a measurement of ϱ. The A_{1g} lattice vibration does not need to have a ϱ-value equal to that of the other internal A_{1g} vibrations, because there is no certainty that in this case the components of the polarisability tensor will have the property a $\gg$ b. The vibration is again in the x–y plane (Na–O stretching) but there is a considerable influence from the Na^+ ions, which are not all in the x–y plane and have the same distances to the oxygen atom as the in-plane Na^+ ion. The single crystal in this case can provide no further information.

2.4.5. *Out-of-plane vibrations A_{2u} (A''_2) and E_g (E'')*

From the character table of the group D_{3h} (table 2-IV) we see that the vibrations that are antisymmetric with respect to the horizontal mirror plane belong to (A''_1), A''_2 or E''. These are the out-of-plane vibrations. The $B_3O_6^{3-}$ ring possesses only four of these vibrations (two belonging to A''_2, two to E'' and none to A''_1; see sec. 2.2.5), and in consequence the crystal has eight, viz. $2A_{2g}$ (A''_2), $2A_{2u}$ (A''_2), $2E_g$ (E'') and $2E_u$ (E''); see also table 2-VIb. In sec. 2.2.7 we have seen that a reasonable intensity can only be expected for A_{2u} (A''_2) and the E_g (E'') vibrations. The two A_{2g} (A''_2) vibrations are not active, either

in the Raman or in the infrared spectrum. The E_u (E'') is infrared active. However, the small value of the change in dipole moment (sec. 2.2.7) makes it very probable that these vibrations are lacking in the infrared.

If we are able to indicate the out-of-plane vibrations we only need to check whether the remaining peaks belong to the E_g/E_u (E') *) vibrations. We will now assign these out-of-plane vibrations one at a time.

Discussion of the vibration ν_{14} (E_g/E_u (E''))

A good start for the identification of the out-of-plane vibrations is provided by the peaks around 700 cm^{-1}. As mentioned in sec. 2.4.2, the three Raman frequencies in this region belong to only one fundamental vibration of the E_g species (2.4.3). In the same region we must encounter the corresponding infrared vibration of species E_u.

Hisatsune and Suarez [2-40]) studied the infrared spectrum of the metaborate ion very thoroughly, varying the $^{10}B/^{11}B$ ratio up to high degrees of enrichment for both isotopes. They concluded that the peak should belong to E'' by reasoning as follows. In the highly enriched ^{10}B and ^{11}B compounds the peak at 707 cm^{-1} is lacking. In the compounds with both ^{10}B and ^{11}B the peak is present. Hence the conclusion is that this peak is due to a vibration, which becomes active if the symmetry of the $B_3O_6^{3-}$ group is lowered. If we introduce two kinds of boron atoms the symmetry changes from D_{3h} to C_{2v}. The correlation table between these groups is:

D_{3h}	C_{2v}
A'_1 (R)	A_1 (IR, R)
A'_2 (inactive)	B_2 (IR, R)
E' (R, IR)	A_1 (IR, R) + B_2 (IR, R)
A''_1 (inactive)	A_2 (R)
A''_2 (IR)	B_1 (IR, R)
E'' (R)	A_2 (R) + B_1 (IR, R).

Only the symmetry species that are not infrared-active in D_{3h}, but are active in C_{2v}, need to be considered, i.e. A'_1, A'_2 and E''. Species A'_1 drops out, since it corresponds to the species A_{1g} (and A_{1u}) of the crystal and this has already been assigned. The species A'_2 and E'' remain. Hisatsune and Suarez motivate their choice for E'' with an intensity argument. They assigned the peak at 722 cm^{-1} (738 cm^{-1} for the ^{10}B compound) to a vibration of A''_2. With the symmetry lowering to C_{2v} this species is also correlated with the species B_1 of C_{2v}, just as is E''. In this case there is a possibility of Fermi resonance, which may explain the relatively high intensity of the 707 cm^{-1} peak.

*) This notation stands for: vibrations belonging to E' in the case of the 'free' $B_3O_6^{3-}$ ion and split in the crystal into an E_g (E') and an E_u (E') vibration.

The arguments for assigning the ν_{14} to the peaks around 700 cm^{-1} may be summarised as follows:

(1) The peaks are only Raman-active in the compounds with a high degree of isotope enrichment, as was expected from sec. 2.2.7.

(2) In the case of symmetry lowering (by isotope substitution) a peak is found in the infrared spectrum. The intensity may be enhanced by Fermi resonance. The frequency of this peak is similar to the frequencies in the Raman spectrum. Moreover, according to Hisatsune and Suarez, the infrared peak shifts to higher frequencies as the ratio $^{10}B/^{11}B$ increases. This is similar to the behaviour of the Raman peaks, if we regard this infrared peak as the envelope of two peaks, one corresponding to the $^{10}B_2{}^{11}BO_6{}^{3-}$ and the other to the $^{10}B^{11}B_2O_6{}^{3-}$ ring.

On these grounds we assign the peaks around 700 cm^{1-} to E_g (E'') (R) and E_u (E'') (IR). If we had an orientated single crystal at our disposal it would be possible to designate peaks belonging to E_g (E'') and E_g (E'), which could confirm this assignment.

The choice between ν_{13} and ν_{14}, both E_g (E'') vibrations, is easy to make. If we look at the displacement configurations (sec. 2.2.6 and fig. 2.4) we see that the boron atoms play an important part in the vibration only in ν_{14}. Therefore ν_{14} alone can give a measurable isotope shift. Moreover, if we make a comparison with the tri-substituted benzenes *) we see that ν_{14} has a comparable frequency (see table 2-XIV). In these spectra ν_{13} has a lower frequency than ν_{14}. This will also be found from our calculations in chapter 3 for $B_3O_6{}^{3-}$.

Discussion of the vibration ν_7 (A_{2u} (A''_2))

The next peak to be considered is the strong absorption in the infrared at 722 cm^{-1} (^{11}B) and 738 cm^{-1} (^{10}B). This peak is not visible in the Raman spectrum and therefore it must belong to the A_{2u} species, because this is the only symmetry species that is active only in the infrared. The vibration can be derived from the A'_2 or the A''_2 species of the free ion. We did not expect a

*) It is possible to compare the tri-substituted benzene ring ($C_6H_3X_3$) with the $B_3O_6{}^{3-}$ ring because they have much in common:
(1) D_{3h} symmetry;
(2) sp^2-hybridisation of the ring atoms and therefore a comparable electronic structure. The charge distribution over the ring atoms is slightly different; electrons of the benzene ring have a homogeneous distribution, while the $B_3O_6{}^{3-}$ ring has an extra charge on the oxygen atoms in the ring;
(3) the distances in the ring are almost equal;
(4) in the compounds $C_6H_3F_3$ and $C_6H_3(OH)_3$ the substituents have almost the same mass as the extra-annular oxygen atoms of the $B_3O_6{}^{3-}$ ring. Nor does the distance C–F (1.30 Å) differ very much from B–O (1.28 Å).
Where they differ is in the binding between substituent and ring. In the $B_3O_6{}^{3-}$ ring this binding has a π bond character (Coulson and Dingle [2–48]), which is not the case with the tri-substituted benzenes. Table 2-XIV gives an assignment of some tri-substituted benzenes based on a comparison of published data of these compounds. This comparison will not be published here; only the results are given in the table.

TABLE 2-XIV

Assignment of some tri-substituted benzenes

	references		$C_6H_3D_3$ 2–41, 2–44)		$C_6H_3(CH_3)_3$ 2–47)		$C_6H_3F_3$ 2–42, 2–47)		$C_6D_3F_3$ 2–42, 2–47)	
description		ν	IR	Raman	IR	Raman	IR	Raman	IR	Raman
	sym C–H stretch	—		3055 p		3020 p		3080 m,p		2309
	sym C–X stretch	ν_1		2384 p		1299 p		1350 s,p		1344
A'_1	sym ring bend	ν_3		1002 p		997 p		1010 vs,p		966
	sym ring stretch	ν_2		955 p		579 p		578 vs,p		576
		—		1226?		(1290)		(1294)		(1189)
A'_2	ring stretch	ν_4		—		(1260)		(1163)		(998)
		ν_5		—		(495)		(565)		(516)
	asym C–H stretch	—		3055	3017		3108 m			2308
	ring stretch	ν_9		1574	1613	1606 dp	1624 vs			1606
E'	ring bend-stretch	ν_{10}		1405	1472		1475 s			1420
	asym C–H bend	—		1166	1166	1164	1122 vs			1046
	asym C–X stretch	ν_8		2272	930	930	993 vs			792
	ring bend	ν_{11}		592	516	517 dp	500 s			484
	asym C–X bend	ν_{12}		833	275	275 dp	326 –			322
	out-of-plane C–H	—	917		835		845 vs			771
A''_2	ring torsion	ν_7	697		686		665 s			520
	out-of-plane C–X	ν_6	531		181		214			—
	out-of-plane C–H	—		933?	880	879	(860)			699
E''	ring torsion	ν_{14}		375		(533)		595 s		547
	out-of-plane C–X	ν_{13}		714		224		253 vs		238

perceptible intensity from the A_{2u} (A'_2) (sec. 2.2.7), so that the only possibility is A_{2u} (A''_2).

There are some other infrared peaks that do not have Raman peaks either and could also belong to A_{2u} (A''_2) (see table 2-XV). These are the peaks at 1250 cm^{-1} and possibly at 375 cm^{-1} (there is a Raman peak at 397 cm^{-1}) and at 950 cm^{-1} (there is again a Raman peak in the neighbourhood at 970 cm^{-1}). There are only two vibrations belonging to A_{2u} (A''_2): ν_6 and ν_7. Taking the frequencies of the tri-substituted benzenes into account, ν_6 is expected to have a low frequency. The 375 cm^{-1} could be ν_6. For ν_7 the three other frequencies remain. The peak at 950 cm^{-1} drops out because it has no isotope shift, while the occurrence of an isotope shift for ν_7 is to be expected from the displacement configurations (sec. 2.2.6). The peak at 1250 cm^{-1} (in fact there are two peaks) has too high a frequency with respect to ν_{14}, which has a displacement configuration similar to that of ν_7.

The arguments for the assignment of the peak at 722 cm^{-1} to ν_7 of the species A_{2u} (A''_2) may be summarised as follows:

(1) There is an isotope shift from 722 cm^{-1} (^{11}B) to 738 cm^{-1} (^{10}B), which is expected from the displacement configurations.

$C_6H_3Cl_3$ [2-45, 2-47]		$C_6D_3Cl_3$ [2-45, 2-47]		$C_6H_3Br_3$ [2-46, 2-47]		$C_6D_3Br_3$ [2-46, 2-47]		$C_6H_3(OH)_3$ [2-41]
IR	Raman	IR	Raman	IR	Raman	IR	Raman	
	3084 s,p		2296 s,p		3073 s,p		2296	
	1149 p		1146 s,p		1115 p		1113	
	995 vs,p		956 vs,p		985 p		956	
	379 m,p		376 s,p		241 p		241	
(1333)				(1319)		(1222)		
(1194)				(1194)		(982)		
(464)				(435)		(407)		
3089		2312 m		3090		2313		
1570 vvvs		1552 vvs	1552 s,dp	1557 vvs	1553 s	1540		
1420 vs		1342 vvs		1408 vvs	1408 vw	1324		
1098 vs	1095 vw,dp	840 vs		1099 s	1082 w	836		
810 vs		800 vs	806	742 vvs	745 vw	736		
429 s	429 w,dp	418 s	417 m,dp	348–	348 w	340		
190 s	191 s,dp		191 vvs,dp	118–	118 vs	118		
853 vs		763 s		849 vvs		775		815
662 vs		534 vs		659 vvs		534		668
149 s				(113)		(110)		(187?)
869 m			713 w,dp		870 vvw	713		(923?)
530 vw			498 w,dp		509 vvw	478		566
	215 ms,dp		203 m,dp		193 s	182		249

s = strong, m = medium, w = weak, ? = uncertain, p = polarised, dp = depolarised ( ) =calculated.

TABLE 2-XV

Frequencies of internal vibrations used for the assignment (for detailed data see tables 2-VIII–2-XI). The final assignment is given between brackets (based on $B_3O_6^{3-}$)

Infrared		Raman	
375 cm^{-1} (s)	(E')		
		397 cm^{-1} (m)	(E')
480 cm^{-1} (vw)	(E')	476 cm^{-1} (s)	(E')
		630 cm^{-1} (ss)	(A'_1)
707 cm^{-1} (w) *)	(E'')	679–698–706 cm^{-1} (s)	(E'')
722 cm^{-1} (s)	(A_2'')	769 cm^{-1} (s)	(A'_1)
950 cm^{-1} (m)	(E')	970 cm^{-1} (m)	(E')
1217 cm^{-1} (s)	?		
1250 cm^{-1} (s)	(E'?)		
1441 cm^{-1} (sh) **)	(E'?)	1440 cm^{-1} (vw)	(E'?)
1466 cm^{-1} (s) **)	(E')	1460 cm^{-1} (w)	(E')
		1547 cm^{-1}–1606 cm^{-1}	(A'_1)

*) A broad tail of the peak at 707 cm^{-1} to lower frequencies suggests that this peak envelops the peaks of different isotope compositions.

**) These frequencies are taken from Cole [2-39]. Our spectra give a broad band.

(2) The peak shows a great resemblance with that at 707 cm^{-1} (ν_{14}) as regards the displacement configuration and hence the frequency.
(3) There is a Fermi resonance with ν_{14} in the case of symmetry lowering to C_{2v}.
(4) The infrared absorption is very strong. According to Nonnenmacher [2-44]) the infrared-active out-of-plane peaks are very strong, at least in the case of the tri-substituted benzenes.
(5) Hisatsune and Suarez, Parsons [2-49]) and Fisher et al.[2-50]) have also assigned this peak to the A''_2 species.

The frequency of ν_7 shows a similarity with the tri-substituted benzenes (table 2-XIV). The frequency of ν_{14} (E_g/E_u (E'')) is higher than the frequencies for these benzenes. The tri-substituted benzenes that show the greatest resemblance with the $B_3O_6^{3-}$ ring have a frequency difference between ν_7 and ν_{14} of 70 cm^{-1} ($C_6H_3F_3$) and 100 cm^{-1} ($C_6H_3(OH)_3$). For $Na_3B_3O_6$ this difference is 722 cm^{-1} — 680 cm^{-1} = 42 cm^{-1}.

Discussion of the vibrations ν_6 (A_{2u} (A''_2)) *and* ν_{13} (E_g (E''))

These vibrations too show a similarity, as can be seen from the displacement configurations. Table 2-XIV shows that in the case of the tri-substituted benzenes these vibrations usually have very low frequencies. They depend, moreover, on the kind of substituent, as is to be expected from the displacement configurations. We do not expect an important isotope shift because the boron atoms do not play an important part in the vibrations. The internal vibrations with the lowest frequencies larger than 250 cm^{-1} are the infrared peak at 375 cm^{-1} and the Raman peak at 397 cm^{-1}. Except for the relatively high frequencies, these peaks satisfy the mentioned conditions. In this case the peak at 375 cm^{-1} (IR) should be ν_6 (A_{2u} (A''_2)) and the peak at 397 cm^{-1} ν_{13} (E_g (E'')).

It is also possible that these vibrations are influenced by the alkali ion. This seems reasonable if we look at the displacement configurations; the most important part of the vibration is formed by the extra-annular oxygen atoms. These oxygen atoms have a relatively strong connection with the alkali atoms as compared with the ring oxygen atoms and the boron atoms. Therefore these vibrations may be among the vibrations below 250 cm^{-1}, which depend on the alkali ion. The strong and broad infrared absorption found at 225 cm^{-1} may partly be due to ν_6. Not all the peaks with a frequency below 250 cm^{-1} necessarily belong to lattice vibrations. There are six lattice vibrations and only five peaks below 250 cm^{-1}. The translational vibrations are usually weak (sec. 2.2.4) and some might be absent from the spectrum. Thus, one or two of the frequencies in this area might belong to internal vibrations. However, there is no way to decide which one of them could be ν_{13}.

Our conclusion is that we have to check two possibilities for these vibrations. In the next chapter we will show that the latter possibility (ν_6 and ν_{13} lower than 250 cm^{-1}) is the right one.

2.4.6. *Species E_g (E') and E_u (E')*

There remain five internal vibrations of the species E_g/E_u (E') to assign. The peaks not yet assigned are

infrared	Raman
375 cm^{-1} (s)	397 cm^{-1} (m) (possibly the out-of-plane vibrations ν_6 and ν_{13})
480 cm^{-1} (vw)	473 cm^{-1} (s)
950 cm^{-1} (m)	969 cm^{-1} (m)
1217 cm^{-1} (s)	
1250 cm^{-1} (s)	
1441 cm^{-1} (sh)	1440 cm^{-1} (vw)
1466 cm^{-1} (s)	1460 cm^{-1} (w)

There are several uncertainties in this row of frequencies. The first one has been mentioned in the preceding section: the peaks at 375 cm^{-1} (IR) and 397 cm^{-1} (R) can be two out-of-plane vibrations A_{2u} (A''_2) and E_g (E'') or one in-plane vibration E_g/E_u (E'). The second uncertainty concerns the peaks at 1217 cm^{-1} (IR) and 1250 cm^{-1} (IR), which have no counterparts in the Raman spectrum. They are possibly vibrations of the type A_{2u} (A'_2), which were expected to have little or no intensity (see sec. 2.2.7). Another possibility is that the Raman activity is too small to detect and that the vibration belongs to E_g/E_u (E'). Both possibilities are checked in the next chapter. The third uncertainty is the peak at 1440 cm^{-1} (R). This peak is very weak in the Raman spectrum and it is not certain that it really exists. In the infrared this peak is a shoulder of the peak at 1466 cm^{-1}. In our spectra it was not always possible to separate it from the peak at 1466 cm^{-1}.

Because of these uncertainties we will not try to assign the peaks to the displacement configurations. We conclude by summarising three assignments for the E_g/E_u (E') vibrations, which will be used in our normal coordinate analysis in the following chapter (natural abundance of $^{11}B/^{10}B$).

model 1	model 2	model 3
1460 cm^{-1}	1460 cm^{-1}	1460 cm^{-1}
1440 cm^{-1}	1440 cm^{-1}	1250 cm^{-1}
1250 cm^{-1}	969 cm^{-1}	969 cm^{-1}
969 cm^{-1}	473 cm^{-1}	473 cm^{-1}
473 cm^{-1}	397 cm^{-1}	397 cm^{-1}

Note: Since we need five internal vibrations in the species E_g/E_u (E'), we do not consider the possibility of all three uncertain peaks being skipped.

REFERENCES

2-1) W. L. Konijnendijk, Philips Res. Repts Suppl. 1975, no. 1.
2-2) C. van Grotel, Report Silicate Chemistry of the Eindhoven University of Technology, 1974.

[2-3] M. Marezio, H. A. Plettinger and W. H. Zachariasen, Acta cryst. **16**, 594, 1963
[2-4] W. Schneider and G. B. Carpenter, Acta cryst. **B26**, 1189, 1970.
[2-5] G. Turrell, Infrared and raman spectra of crystals, Academic Press, London, 1972.
[2-6] H. Poulet and J. P. Mathieu, Spectres de vibration et symétrie des cristaux., Gordon & Breach, Paris, 1970.
[2-7] S. Bhagavantam and T. Venkatarayudu, Theory of groups and its application to physical problems, Academic Press, New York, 1969.
[2-8] A. Nussbaum, Applied group theory for chemists, physicists and engineers, Prentice-Hall, Englewood Cliffs, N.J., 1971.
[2-9] L. A. Woodward, Introduction to the theory of molecular vibrations and vibrational spectroscopy, Oxford University Press, London, 1972.
[2-10] K. Nakamoto, Infrared spectra of inorganic and coordination compounds, second ed., John Wiley & Sons (Wiley interscience), New York, 1970.
[2-11] D. M. Adams and D. C. Newton, Tables for factor-group and point-group analysis, Beckman-RIIC, Sunley House, Croydon, England, 1970.
[2-12] International tables for X-ray crystallography vol. I, The Kynoch Press, Birmingham, England, 1959.
[2-13] C. E. Weir and E. R. Lippincott, J. Res. natl Bur. Stand. **65A**, 173, 1961.
[2-14] C. E. Weir and R. A. Schroeder, J. Res. natl Bur. Stand. **68A**, 465, 1964.
[2-15] J. Kocher, Bull. Soc. chim. 1968, 919.
[2-16] R. Bouaziz, Bull. Soc. chim. 1962, 1451.
[2-17] A. P. Rollett and R. Bouaziz, Compt. rend. **240**, 2417, 1955.
[2-18] B. S. R. Sastry and F. A. Hummel, J. Amer. ceram. Soc. **41**, 7, 1958.
[2-19] B. S. R. Sastry and F. A. Hummel, J. Amer. ceram. Soc. **42**, 216, 1959.
[2-20] G. W. Morey, and H. E. Merwin, J. Amer. chem. Soc. **58**, 2248, 1936.
[2-21] T. Milman and R. Bouaziz, Ann. Chim. **3**, 311, 1968.
[2-22] E. M. Levin, C. R. Robbins and H. F. McMurdie, Phase diagrams for ceramists, The American Ceramic Society, 1964.
[2-23] W. H. Zachariasen, Acta cryst. **17**, 749, 1964.
[2-24] J. Krogh-Moe, Acta cryst. **15**, 190, 1962.
J. Krogh-Moe, Acta cryst. **B24**, 179, 1968.
[2-25] J. Krogh-Moe, Acta cryst. **B30**, 578, 1974.
[2-26] J. Krogh-Moe, Acta cryst. **B30**, 747, 1974.
[2-27] J. Krogh-Moe, Acta cryst. **B28**, 1571, 1972.
[2-28] A. Hyman, A. Perloff, F. Mauer and S. Block, Acta cryst. **22**, 815, 1967.
[2-29] J. Krogh-Moe, Acta cryst. **B28**, 3089, 1972.
[2-30] J. Krogh-Moe, Acta cryst. **14**, 68, 1961.
[2-31] J. Krogh-Moe, Acta cryst. **B28**, 168, 1972.
[2-32] J. Krogh-Moe, Acta cryst. **18**, 1088, 1965.
[2-33] E. B. Wilson, J. C. Decius and P. C. Cross, Molecular vibrations, McGraw-Hill Book Company, New York, 1955.
[2-34] L. McCulloch, J. Amer. chem. Soc. **59**, 2650, 1939.
[2-35] G. E. Gurr, P. W. Montgomery, C. D. Knutson and B. T. Gorres, Acta cryst. **B26**, 906, 1970.
[2-36] J. R. Nielsen and L. H. Berryman, J. chem. Phys. **17**, 659, 1949.
[2-37] J. P. Bronswijk, Spectroscopie aan alkali-boraten, Report Eindhoven Technological University, 1974.
[2-38] M. Harrand, J. Raman Spectrosc. **2**, 15, 1974.
[2-39] C. P. Cole, Collections of Laporte Chemicals Ltd., Luton.
[2-40] I. C. Hisatsune and N. H. Suarez, Inorg. Chem. **3**, 168, 1964.
[2-41] K. S. Pitzer and D. W. Scott, J. Amer. chem. Soc. **65**, 803, 1943.
[2-42] J. R. Nielsen, Ching-Yu Liang and D. C. Smith, Trans. Faraday Soc. **9**, 177, 1950.
[2-43] E. J. Ferguson, J. chem. Phys. **21**, 5, 1953.
[2-44] G. Nonnenmacher and R. Mecke, Spectrochim. Acta **17**, 1049, 1961.
[2-45] J. R. Scherer, J. C. Evans, W. W. Muelder and J. Overend, Spectrochim. Acta **18**, 57, 1962.
[2-46] J. R. Soerer, J. C. Evans and W. W. Muelder, Spectrochim. Acta **18**, 1579, 1962.
[2-47] J. H. S. Green, D. J. Harrison and W. Kynaston, Spectrochim. Acta **27A**, 793, 1971.
[2-48] C. A. Coulson and T. W. Dingle, Acta cryst. **B24**, 153, 1968.
[2-49] J. L. Parsons, J. chem. Phys. **33**, 1860, 1960.
[2-50] H. D. Fisher, W. J. Lehmann and I. Shapiro, J. phys. Chem. **65**, 1166, 1961.

3. NORMAL COORDINATE ANALYSIS

3.1. Introduction

This chapter describes the manner in which the force or interaction constants of a crystal of known structure can be calculated from the vibrational frequencies. The importance of a calculation of the force constants in relation to the structure and vibrational frequencies of glasses has already been explained in chapter 1.

The chapter is divided into three parts. The first part (3.2) gives a short review of the principles underlying the method of calculation and the computer programs used for the purpose. The second part (3.3) describes the manner in which the computer programs were made suitable for crystals and for eliminating the redundant coordinates. The third part (3.4 and 3.5) deals with the application of the method of calculation to the $B_3O_6^{3-}$ ion and crystalline $Na_2O.B_2O_3$.

3.2. *G-F* matrix method and the Schachtschneider programs

The *G-F* matrix method developed by E. B. Wilson Jr. is a method of calculating the vibrational frequencies starting from the kinetic and the potential energy of a molecule (represented in the *G* and *F* matrices respectively). A detailed derivation and description of the method is given in Wilson, Decius and Cross [3-1]). We shall confine ourselves here to a brief review of the method.

Schachtschneider [3-3]) has described a number of computer programs which, based on the *G-F* matrix method, can calculate the vibrational frequencies of a free molecule or, using experimentally determined frequencies, give an approximation of the force constants with the aid of an iteration program.

The classical method of determining the vibrational frequencies starts from the equations of motion:

$$\frac{\mathrm{d}}{\mathrm{d}t}\left(\frac{\partial T}{\partial \dot{Q}_i}\right)+\frac{\partial V}{\partial Q_i}=0 \quad (i=1,\ldots,3N-6), \tag{3.1}$$

where T is the kinetic energy of the vibration, V the potential energy of the vibration and Q_i the normal coordinate, describing the displacements of all atoms vibrating with frequency ν_i.

The solution of eq. (3.1) is given by

$$Q_i = Q_{i0}\cos(\lambda_i^{\frac{1}{2}}\, t+\delta),$$

where $\lambda_i = 4\pi\,\nu_i^2$.

Unfortunately, the normal coordinates are not known in advance, so that we are obliged to describe the equations of motion with a different coordinate system.

The kinetic energy of the molecule or crystal can easily be expressed in cartesian coordinates:

$$2T = \tilde{\dot{X}}\, M\, \dot{X}, \tag{3.2}$$

where M is a diagonal matrix with the masses of the atoms on the diagonal. The column vector X is composed of the cartesian components of the atomic displacements.

The potential energy, based on the forces between the atoms, can best be described with internal coordinates. Internal coordinates are the changes in distance (stretching), angle (bending) or dihedral angle (torsion) between the atoms. Since we are interested in the forces (interaction between atoms) our obvious procedure is to start from internal coordinates.

The kinetic energy expressed in internal coordinates can be written as

$$2T = \tilde{\dot{R}}\, G^{-1}\, \dot{R}, \tag{3.3}$$

where R represents the column vector of the internal coordinates. If G is singular, G^{-1} does not exist. The theory for this case will not be treated here. R can be determined from X using the transformation matrix B:

$$R = B\, X. \tag{3.4}$$

With eqs (3.2), (3.3) and (3.4) we can define the G matrix as

$$G \equiv B\, M^{-1}\, \tilde{B}. \tag{3.5}$$

In order to express the potential energy V in internal coordinates we shall expand V in a Taylor series:

$$\begin{aligned} V(R_1, R_2, R_3, \ldots) = V_0 + \left(\frac{\partial V}{\partial R_1}\right)_0 R_1 + \left(\frac{\partial V}{\partial R_2}\right)_0 R_2 + \ldots + \\ + \tfrac{1}{2}\left(\frac{\partial^2 V}{\partial {R_1}^2}\right)_0 {R_1}^2 + \tfrac{1}{2}\left(\frac{\partial^2 V}{\partial {R_2}^2}\right)_0 {R_2}^2 + \ldots + \\ + \left(\frac{\partial^2 V}{\partial R_1\, \partial R_2}\right)_0 R_1\, R_2 + \left(\frac{\partial^2 V}{\partial R_2\, \partial R_3}\right)_0 R_2\, R_3 + \ldots + \\ + \text{higher derivatives.} \end{aligned} \tag{3.6}$$

R_1, R_2, R_3 etc. are the individual internal coordinates, which together form the internal coordinate vector R. In the harmonic approximation we will neglect the higher derivatives. The first term V_0 is the potential energy in the equilibrium position, which is arbitrarily chosen equal to zero. The first derivative with respect to an internal coordinate must be zero in the equilibrium position, since

the potential energy is then a minimum. If we define the quadratic terms as force or interaction constants:

$$\left(\frac{\partial^2 V}{\partial R_i \partial R_j}\right)_0 = f_{ij} \quad (i,j = 1, 2, \ldots)$$

then the expression for the potential energy becomes

$$2V = f_{11} R_1^2 + f_{22} R_2^2 + \ldots 2f_{12} R_1 R_2 + 2f_{23} R_2 R_3 + \ldots \quad (3.7)$$

or, in matrix notation

$$2V = \tilde{\boldsymbol{R}} \boldsymbol{F} \boldsymbol{R}, \quad (3.8)$$

where F is the matrix that comprises the above-mentioned force and interaction constants. For a set of r internal coordinates the equations of motion are

$$\frac{\mathrm{d}}{\mathrm{d}t}\left(\frac{\partial T}{\partial \dot{R}_i}\right) + \frac{\partial V}{\partial R_i} = 0 \quad (i = 1, \ldots, r) \quad (3.9)$$

with, as the general solution,

$$R_i = A_i \cos(\lambda^{\frac{1}{2}} t + \delta) \quad (i = 1, \ldots, r), \quad (3.10)$$

where $\lambda = 4\pi \nu^2$, ν again being the frequency of a normal vibration. Substitution of eq. (3.10) in eq. (3.9) gives a set of linear equations in $A_1, \ldots, A_r$. This set of equations has only a non-trivial solution for the amplitudes A_i if the following secular equation is satisfied:

$$\begin{vmatrix} F_{11} - \lambda G_{11}^{-1} & F_{12} - \lambda G_{12}^{-1} & F_{13} - \lambda G_{13}^{-1} \ldots \\ F_{21} - \lambda G_{21}^{-1} & F_{22} - \lambda G_{22}^{-1} & F_{23} - \lambda G_{23}^{-1} \ldots \\ \vdots & & \end{vmatrix} = 0$$

or $|F - \lambda G^{-1}| = 0$. Multiplication by $|G|$ then gives the familiar notation of the secular equation

$$|GF - E\lambda| = 0, \quad (3.11)$$

where E is the identity matrix of order r.

Using the foregoing treatment, and given the masses, the position and the force and interaction constants of the atoms, it is possible to determine the vibrational frequencies of a molecule or crystal.

The problem can be greatly simplified, however, by making use of the symmetry of the molecule or crystal. We shall explain this with the G matrix; similar considerations apply to the F matrix.

So far we have proceeded from a coordinate system based on the internal coordinates. We can also use so-called internal symmetry coordinates as basis vectors. The relation with the internal coordinates is given by

$$\boldsymbol{s} = U\boldsymbol{R}, \tag{3.12}$$

where $\boldsymbol{s}$ is the symmetry coordinate column vector and U a transformation matrix.

A typical characteristic of these symmetry coordinates is that they belong to one of the symmetry species of the factor or point group of the crystal or molecule. The kinetic energy can now be written as

$$2T = \tilde{\dot{\boldsymbol{s}}}\, G_s^{-1}\, \dot{\boldsymbol{s}}, \tag{3.13}$$

where G_s is the G matrix based on the symmetry coordinates. If we ensure that U is orthonormal (or unitary), then the relation between G_s and G is

$$G_s = U G \tilde{U}. \tag{3.14}$$

Writing out eq. (3.13) we get

$$\begin{aligned} 2T = {} & s_1^2\, g_{11}^{-1} + s_2^2\, g_{22}^{-1} + s_3^2\, g_{33}^{-1} + \\ & + 2s_1 s_2\, g_{12}^{-1} + 2s_1 s_3\, g_{13}^{-1} + 2s_2 s_3\, g_{23}^{-1} + \ldots \end{aligned} \tag{3.15}$$

with

$$G_s^{-1} \equiv \begin{pmatrix} g_{11}^{-1} & g_{12}^{-1} & g_{13}^{-1} & \ldots \\ g_{21}^{-1} & g_{22}^{-1} & g_{23}^{-1} & \ldots \\ g_{31}^{-1} & g_{32}^{-1} & g_{33}^{-1} & \ldots \\ \vdots & \vdots & \vdots & \end{pmatrix}, \tag{3.16}$$

$s_1, s_2, \ldots$ are the individual symmetry coordinates.

We assume now that s_1 and s_2 belong to the same symmetry species and s_3 to a different species. We see that a number of squares occur in eq. (3.15) and a number of cross products. These products are zero if the symmetry coordinates occurring in the product do *not* belong to the same symmetry species. This is because the kinetic energy is invariant under each symmetry operation of the group. Since s_1 and s_3 do not belong to the same species, an operation may always be found that leaves s_1 unchanged and causes s_3 to transform to $-s_3$. The product $s_1 s_3\, g_{13}^{-1}$ should change sign under that operation. Since the kinetic energy does not change under a symmetry operation we have $g_{13}^{-1} = 0$. The appearance of zero elements causes G_s^{-1} to assume a block form, provided the symmetry coordinates are grouped together according to their species. The blocks with non-zero elements are situated along the main diagonal of the matrix and each particular block is of order n, where n is the number of symmetry coordinates belonging to that block.

We have not yet taken any account of the degenerate species. It may be noted in this connection that a degenerate block can in turn be divided up into a number of m identical blocks, where m represents the degeneracy. For a more detailed description, reference may be made to Woodward [3–2]), p. 183.

The F matrix factorises into blocks in the same way.

The great advantage of this procedure is the splitting up of the secular equation into a number of equations of smaller dimensions, making it possible to relate the calculated frequencies to their symmetry species.

The Schachtschneider computer programs are based on the G-F matrix method described above. Fig. 3.1 illustrates schematically how the various programs yield the desired result from the basic data. The functions of these programs are briefly described below.

(1) CART. This program calculates from a given geometry of a molecule the cartesian coordinates of all atoms. There are also options for computing the centre of mass and moments of inertia. The origin of the coordinate system can be placed at the centre of mass.

(2) GMAT calculates the (Wilson) G matrix for a 'free' molecule. The input consists of the cartesian coordinates of the atoms (called X matrix and can be obtained from CART) and the internal coordinates chosen.

With eq. (3.4) the B matrix is then determined, after which, using eq. (3.5) and the stated masses of the atoms, the G matrix is calculated, schematically:

$$\boldsymbol{R} = B\,X \rightarrow B \rightarrow G = B\,M^{-1}\,\tilde{B}.$$

The U matrix may also be optionally introduced, after which G_s is calculated from eq. (3.14).

(3) VSEC calculates the vibrational frequencies from the G matrix and Z matrix. The Z matrix is a three-dimensional matrix with elements Z_{ijk}. The indices i and j refer to the row and column numbers of the F matrix and the index k refers to a force constant Φ_k. The element Z_{ijk} is the coefficient of the force constant Φ_k in the expression

$$F_{ij} = \sum_k Z_{ijk}\,\Phi_k.$$

The advantage of this representation of the F matrix is the ease with which F matrices based on e.g. symmetry coordinates can be introduced. Later, moreover, it is easier to see which force constants refer to a particular coordinate and vibrational frequency.

The G and Z input may be block-diagonalised or not. By way of option the amplitudes of the vibration, the potential energy distribution over the force constants, the cartesian displacements for each normal coordinate and the coriolis coefficients can be computed.

(4a) FPERT is an iteration program. The input consists of the G matrix,

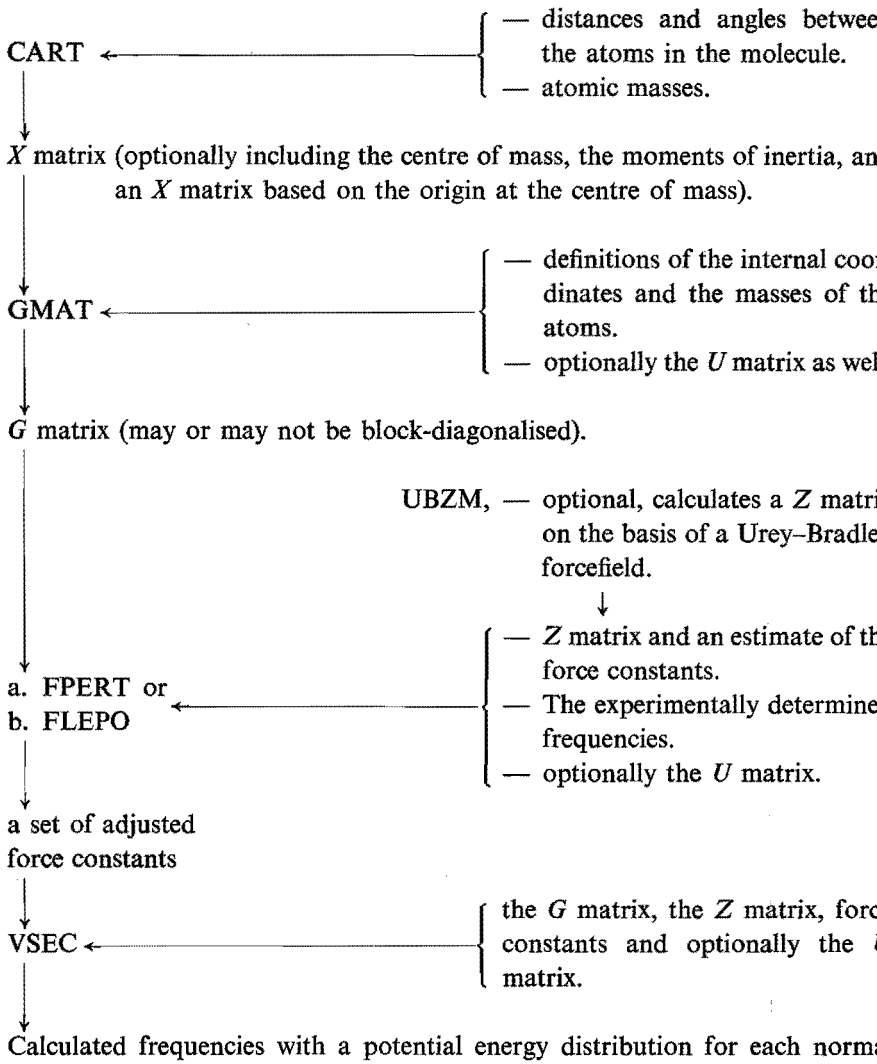

Fig. 3.1. Diagram illustrating the Schachtschneider programs. Basic data: the geometry of the molecule, the masses of the atoms and the experimentally determined frequencies.

the Z matrix, and the force constants Φ_i. For the force constants Φ_i the best possible estimates of their real values are taken. The input should also include the experimentally determined frequencies. The program calculates the frequencies, ν_i(calc), and compares them with the observed values, ν_i(obs). Following a method proposed by King and Crawford (refs 3–3 and 3–4) the differences

$|\lambda_i(\text{calc}) - \lambda_i(\text{obs})|$ are used to adjust the force constants ($\lambda = 4\pi\ \nu^2$). This process is repeated until

$$\sum_i |\lambda_i(\text{calc}) - \lambda_i(\text{obs})|^2$$

is a minimum.

(4b) FLEPO is also an iteration program. It is based on a minimisation method developed by Fletcher and Powell [3-15]). The algorithm for this method (FLEPOMIN) is given by Wells [3-16]) and corrected by Fletcher [3-17]). The input is identical with the input for FPERT. FLEPO has some advantages over FPERT. The minimisation procedure in FPERT diverges very easily, and therefore it is often difficult to get results from this program. Moreover, FLEPO is more rapid then FPERT. A more detailed description has been given by Dikhoff [3-18]). For the calculations in this chapter we used FLEPO instead of FPERT.

3.3. GMOP, the subroutine SPC and *GZ* conversion

Schachtschneider [3-3]) has written a program for the calculation of the *G* matrix for polymers and crystals (program GMATP). For the polymer polyethylene he has given an example, showing that 20 atoms and 60 internal coordinates are required for this simple substance. However, he does not indicate how the input of a crystal should be composed. The method described below requires only 8 atoms and 20 internal coordinates for the polyethylene problem.

To make up for this shortcoming in Schachtschneider's programs we have written a new program, called GMOP, which is a substitute for GMAT and CART at the same time. Program GMOP is based on Schachtschneider's GMAT and CART.

An important procedure included in the new program is the subroutine SPC. This subroutine develops a transformation matrix which ensures that redundant coordinates can be eliminated.

A supplementary program, *GZ* conversion, removes the zero and redundant degenerate coordinates from the *G* and *Z* matrices. The new, much smaller *G* and *Z* matrices are suitable for input in VSEC and FLEPO.

3.3.1. *GMOP*

Shimanouchi et al.[3-5]) describe how the *G-F* matrix method can be applied to the optically active vibrations of crystals. As already pointed out in sec. 2.2.2, the optically active vibrations are vibrations which are in phase in all primitive cells ($\boldsymbol{k} = \boldsymbol{0}$). It is therefore sufficient to compose *G* and *F* matrices for only one primitive cell, including interactions with neighbouring cells in so far as these are different from zero. Doing this for a cell *i*, *j*, *k* we find

$$G_{\text{op}} = \sum_{i',j',k'} G_{ijk,i'j'k'} \quad \text{and} \quad F_{\text{op}} = \sum_{i'j'k'} F_{ijk,i'j'k'}, \tag{3.17}$$

where G_{op} is the G matrix for the optically active vibrations. According to Shimanouchi, we may write $i' = i$, $i \pm 1$ or $i \pm 2$, $j' = j$, $j \pm 1$ or $j \pm 2$, and $k' = k$, $k \pm 1$ or $k \pm 2$, i.e. the interactions extend over nearest-neighbour cells and next-neighbour cells. It may be necessary to add $i' = i \pm 3$ to this if the torsions are also taken into account. For the F matrix the interaction could theoretically extend further than next-next-neighbouring cells. However, the force constants will be very small in that case. In the program GMATP, G_{op} is in fact obtained by such an addition of G matrices. For this purpose the input must also comprise the neighbour cells. If we include all nearest-neighbour cells and next-neighbour cells in the calculation, this would give us a maximum of 125 primitive cells. Usually we can do with fewer than this, as will be clear from the example of diamond given in the article by Shimanouchi et al.

The solution worked out by us is based on the following consideration.

The kinetic energy of the optical vibrations in cell i, j, k is

$$2T = \tilde{\dot{\boldsymbol{X}}}_{ijk} \, \boldsymbol{M}_{ijk} \, \dot{\boldsymbol{X}}_{ijk}, \tag{3.18}$$

where $\boldsymbol{X}_{ijk}$ is the cartesian displacement coordinate vector of the atoms *in cell ijk* and $\boldsymbol{M}_{ijk}$ is the diagonal matrix of the masses of the atoms *in cell ijk*.

In cell *ijk* we can define a number of internal coordinates, represented by the vector $\boldsymbol{R}_{ijk}$. The kinetic energy is now

$$2T = \tilde{\dot{\boldsymbol{R}}}_{ijk} \, \boldsymbol{G}_{op}^{-1} \, \dot{\boldsymbol{R}}_{ijk}. \tag{3.19}$$

The internal coordinates $\boldsymbol{R}_{ijk}$ are defined by atoms that may also lie *outside the cell ijk*, hence

$$\boldsymbol{R}_{ijk} = \boldsymbol{B}_{ijk,ijk} \, \boldsymbol{X}_{ijk} + \boldsymbol{B}_{ijk,i'j'k'} \, \boldsymbol{X}_{i'j'k'} + \boldsymbol{B}_{ijk,i''j''k''} \, \boldsymbol{X}_{i''j''k''} + \ldots \tag{3.20}$$

Since the displacement coordinate vector $\boldsymbol{X}$ is identical for all cells, eq. (3.20) may also be written as

$$\boldsymbol{R}_{ijk} = \Big(\sum_{i'j'k'} \boldsymbol{B}_{ijk,i'j'k'} \Big) \, \boldsymbol{X}_{ijk} = \boldsymbol{B}_{op} \, \boldsymbol{X}_{ijk}. \tag{3.21}$$

After substitution in eq. (3.18) we obtain

$$\boldsymbol{G}_{op} = \boldsymbol{B}_{op} \, \mathrm{M}_{ijk}^{-1} \, \tilde{\boldsymbol{B}}_{op} \tag{3.22}$$

(see e.g. Woodward [3-2]), p. 76 ff).

The problem has now been converted into the determination of $\boldsymbol{B}_{op}$, that is to say into the addition of the B matrices. Now in eq. (3.20) only those elements $\boldsymbol{B}_{ijk,i'j'k'}$ and $\boldsymbol{B}_{ijk,i''j''k''}$ are different from zero that involve atoms in the neighbour cells which are part of an internal coordinate $\boldsymbol{R}_{ijk}$ of cell i, j, k. It is therefore not necessary to consider more atoms than are needed for the definition of all coordinates $\boldsymbol{R}_{ijk}$.

Each element of the matrices $\boldsymbol{B}_{ijk,pqr}$ from eq. (3.20) is characterised by a row number corresponding to the serial number of an internal coordinate in the vector $\mathbf{R}_{ijk}$, and a column number corresponding to an atom coordinate. For

the nth atom in the primitive cell the atom coordinate numbers are $3(n-1)+1$ for Δx, $3(n-1)+2$ for Δy and $3(n-1)+3$ for Δz. The B_{op} is now obtained by adding the B elements with the same row numbers that are recorded under identical atom coordinate numbers in the various cells ijk, $i'j'k'$, $i''j''k''$, ... The row number of the sum remains of course the same, and the column number becomes equal to the number of the atom coordinate in the cell ijk. To summarise, it is sufficient to include in the input those atoms which are needed for the definitions of $\boldsymbol{R}_{ijk}$ and to indicate which atoms are equivalent to the atoms in the cell ijk. The great advantage of the procedure outlined above is that it limits the number of atoms that need to be considered in the calculation to a strict minimum. Furthermore, we are always sure that sufficient atoms have been included, as otherwise the definition of one or more internal coordinates is impossible.

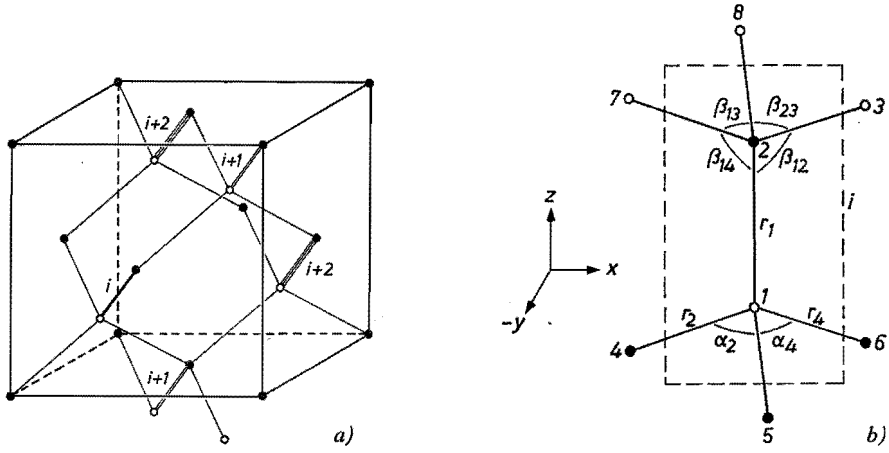

Fig. 3.2. Diamond. (*a*) Diamond lattice. The two f.c.c. sublattices of which diamond is composed are indicated by C atoms shown as open and solid circles. There are six $i+1$ nearest-neighbour cells and six $i+2$ next-neighbour cells. (*b*) Schematic representation of a primitive cell. The atom numbering and various internal coördinates are defined in this figure.

We shall illustrate this procedure by taking diamond as an example, as was also done by Shimanouchi [3–5]). The primitive cell (Bravais cell) of diamond contains two carbon atoms. In this primitive cell we can define 16 internal coordinates, namely four stretchings and twelve bendings. The primitive cell is shown schematically in fig. 3.2, which also illustrates the location of the neighbouring cells in the diamond lattice.

Shimanouchi obtains G_{op} by adding the $G_{ijk,i'j'k'}$'s, for which purpose he has to determine and add 13 matrices! *) We need a total of 8 atoms in order

*) It should be noted here that Shimanouchi also gives a shorter method which makes use of cartesian coordinates. The cartesian force constant matrix F_{cart} is then determined by $F_{cart} = \widetilde{B}_{op} F_{intern} B_{op}$. The drawback of this is that the force constants no longer have any physical meaning. In our case this would imply that we could no longer use the programs FLEPO and VSEC directly.

to define the 16 internal coordinates as can be inferred from fig. 3.2. If we calculate the B matrix in the ordinary way for this 'eight atom molecule' using the internal coordinates defined for it, we obtain the B matrix of table 3-I.

TABLE 3-I

The B matrix of the 'eight atom molecule' for calculating the B_{op} of diamond. The internal coordinates are defined in fig. 3.2, as well as the atom numbers. The coordinate numbers are only of relevance to the calculations. Atoms 1 and 2 are in cell i, the other atoms are in different $i + 1$ cells

no. atom	3			7			8			1		
coord. no.	7	8	9	19	20	21	22	23	24	1	2	3
r_1												−1
r_2										.943		.333
r_3										−.471	.816	.333
r_4										−.471	−.816	.333
α_{12}										−.866		.612
α_{13}										.433	−.750	.612
α_{14}										.433	.750	.612
α_{34}										.866		−.612
α_{42}										−.433	.750	−.612
α_{23}										−.433	−.750	−.612
β_{12}	−.216		.612							−.649		
β_{13}				.325			.108	.187	.612		−.562	
β_{14}				.108	.187	.612				.325	.562	
β_{34}				.433	−.375	−.306	.433	.375	−.306			
β_{42}	.108	.562	−.306	−.541	.187	−.306						
β_{23}	.108	−.562	−.306				−.541	−.187	−.306			

Table 3-I clearly shows the division into cells. A division can also be made in terms of the position of an atom in the primitive cell. We shall call atom 1 and the equivalent atoms in the neighbour cells A atoms, and atom 2 with its equivalent atoms B atoms (in fig. 3.2 the open circles are the atoms A and the solid circles the atoms B). Atom numbers 3, 7 and 8 are A atoms and 4, 5 and 6 are B atoms.

Matrix B_{op} is obtained by adding the $B_{i,i+1}$'s to $B_{i,i}$. Table 3-I gives six (half) $B_{i,i+1}$'s, the other halves consist of zero elements. These half matrices have to be added to the proper half of the (complete) $B_{i,i}$. For example, in the case of the column with atom coordinate number 5 the columns with the atom coordinate numbers 11, 14 and 17 have to be added to this column (the 'y-coordinate' of the atoms B). After addition, the values we obtain for the elements of B_{op} are those listed in table 3-II. The matrix multiplication:

$$G_{op} = B_{op}\, M^{-1}\, \tilde{B}_{op}$$

then yields G_{op}. We shall not work out this matrix here; the values are found to agree with the G_{op} values obtained by Shimanouchi [3–5]).

3.3.2. *Sun–Parr–Crawford method*

3.3.2.1. Introduction

The purpose of this method is to find a set of symmetry coordinates that contain no redundancies. A set of symmetry coordinates contains redundancies if the coordinates are not all independent. It is often particularly useful (for symmetry reasons) to introduce one or more redundancies. A familiar example is the use of six bending coordinates in the case of methane, where one of these

2			4			5			6		
4	5	6	10	11	12	13	14	15	16	17	18
		1									
			−.943		−.333						
						.471	−.816	.333			
									.471	.816	−.333
.649			.216		−.612						
−.325	.562					−.108	.187	−.612			
−.325	−.562								−.108	−.187	−.612
						−.433	−.375	.306	−.433	.375	.306
			−.108	−.562	.306				.541	−.187	.306
			−.108	.562	.306	.541	.187	.306			
.866		−.612									
−.433	.750	−.612									
−.433	−.750	−.612									
−.866		.612									
.433	−.750	.612									
.433	.750	.612									

TABLE 3-II

B_{op} of diamond

atom no.	1 (A)			2 (B)		
coord. no.	1	2	3	4	5	6
r_1			− 1		1	
r_2	.943		.333	−.943		−.333
r_3	−.471	.816	.333	.471	−.816	−.333
r_4	−.471	−.816	.333	.471	.816	−.333
α_{12}	−.866		.612	.866		−.612
α_{13}	.433	−.750	.612	−.433	.750	−.612
α_{14}	.433	.750	.612	−.433	−.750	−.612
α_{34}	.866		−.612	−.866		.612
α_{42}	−.433	.750	−.612	.433	−.750	.612
α_{23}	−.433	−.750	−.612	.433	.750	.612
β_{12}	−.866		.612	.866		−.612
β_{13}	.433	−.750	.612	−.433	.750	−.612
β_{14}	.433	.750	.612	−.433	−.750	−.612
β_{34}	.866		−.612	−.866		.612
β_{42}	−.433	.750	−.612	.433	−.750	.612
β_{23}	−.433	−.750	−.612	.433	.750	.612

symmetrically equivalent coordinates is redundant in the description of the vibrations.

In framing the symmetry coordinates (U matrix) we shall include the redundancies. Without the redundant coordinates it would in many cases be quite impossible to set up the U matrix.

The solution of the secular equation is rendered cumbersome by the occurrence of redundancies. In the first place the dimension of the determinant ($|GF - E\lambda| = 0$) increases unnecessarily, and moreover, the first derivative of the potential energy with respect to the coordinate is no longer necessarily zero (see eq. (3.6)). The consequences of the latter problem have been treated by Wilson, Decius and Cross [3-1]) (p. 171 ff) and by Jones [3-6]) (sec. 1.10.2).

It is therefore appropriate to eliminate these redundancies before beginning with the solution of the secular equation.

The procedure adopted for this purpose was first suggested by Sun, Parr and Crawford [3-7]). It is based on the transformation of the old symmetry coordinates (s) to a set of new coordinates $\bar{s}$ which contain the redundancies as zero coordinates (e.g. $\bar{s}_1 = 0$, and possibly $\bar{s}_2 = 0$, etc.).

The following calculation has been elaborated by Vogel [3-8]) and is based on the suggestion of Sun, Parr and Crawford.

3.3.2.2. Calculation

We assume that the G matrix is based on symmetry coordinates and that the matrix is consequently in the block-diagonal form. The transformation to a new set of coordinates $\bar{s}$ can now be carried out per block. The number of redundancies per block is known beforehand and thus provides a check on the correctness of the result. It is not essential that the G matrix be in the block-diagonal form, but if it is not we are unable to make any distinction in terms of symmetry species.

Let G be a block of the G matrix pertaining to the symmetry species Γ. A known number of independent modes, r, will pertain to Γ. r is equal to the rank of G, while the order of G is equal to the number of symmetry coordinates, k, which pertain to G ($k \geqslant r$). The symmetry coordinates are collected in the column vector $s = \{s_1, \ldots, s_k\}$. The number of redundant coordinates is equal to $k - r$. The zero coordinates are in general linear combinations of the symmetry coordinates. For CH_4 the symmetry coordinate

$$s = \alpha_1 + \alpha_2 + \alpha_3 + \alpha_4 + \alpha_5 + \alpha_6$$

happens to be a straightforward zero coordinate, since

$$\alpha_1 + \alpha_2 + \alpha_3 + \alpha_4 + \alpha_5 + \alpha_6 = 0$$

in this case.

The kinetic energy (for the block) expressed in the old symmetry coordinates is:

$$2T = \tilde{\dot{s}}\, G^{-1}\, \dot{s}. \tag{3.23}$$

We can also express the kinetic energy in the space spanned by the new symmetry coordinates $\bar{s}_1, \ldots, \bar{s}_k$ pertaining to the block. The new space is obtained from the old one by means of a linear transformation using an orthonormal transformation matrix C:

$$\bar{s} \equiv \{\bar{s}_1, \ldots, \bar{s}_k\} = C\, s. \tag{3.24}$$

The kinetic energy is now

$$2T = \tilde{\dot{\bar{s}}}\, \bar{G}^{-1}\, \dot{\bar{s}}. \tag{3.25}$$

The relation between the old and new G matrix block is

$$G^{-1} = \tilde{C}\, \bar{G}^{-1}\, C \tag{3.26}$$

as is seen after substitution of (3.24) in (3.25) and comparison with (3.23). Since C is orthonormal, $\tilde{C} = C^{-1}$, and we get upon inversion of (3.26):

$$G = \tilde{C}\, \bar{G}\, C.$$

Pre- and post-multiplying this by C and $\tilde{C}$, respectively we obtain

$$\bar{G} = C\, G\, \tilde{C}. \tag{3.26'}$$

If C is properly chosen the new G block, $\bar{G}$, will reflect the zero coordinates through the appearance of corresponding rows and columns of zeros. A correct choice for C can be made along the lines now to be described.

If $\tilde{x}_i = \{x_{1i}, \ldots, x_{ki}\}$ is a solution of the set of linear equations

$$G\, \tilde{x}_i = 0_k, \tag{3.27}$$

where 0_k is the k-dimensional zero vector, then according to Sun, Parr and Crawford [3–7]), the linear combination of old symmetry coordinates $\bar{s}_i = \tilde{x}_i\, s$ is a zero coordinate. The number of linear independent solutions x_i for (3.27) is equal to $k - r$. Thus, $k - r$ zero coordinates may be found. Generally, they are not orthonormal, but may be chosen to be so. The $(k - r)$ orthonormal solutions $\tilde{x}_i$ together form a matrix X:

$$X \equiv \begin{pmatrix} x_{11}, & \ldots, & x_{1,k-r} \\ \vdots & & \\ x_{k,1}, & \ldots, & x_{k,k-r} \end{pmatrix}. \tag{3.28}$$

We may write

$$s_0 = \tilde{X}\, s, \tag{3.29}$$

where $s_0 \equiv \{s_{1,0}, \ldots, s_{k-r,0}\}$ is the column vector of the $k-r$ zero coordinates. Equation (3.27) can now be written as

$$G\,X = O_{k,k-r}, \tag{3.30}$$

where $O_{k,k-r} = r \times (k-r)$ zero matrix.

We must now solve X from eq. (3.30), and this is done by transforming the matrix G into its row-echelon form (see B. Noble [3–9], sec. 3.7). This row-echelon form will be indicated here by M:

$$M = \begin{bmatrix} 1 & x & 0 & 0 & x & x & x & 0 & 0 & x & 0 & \ldots \\ 0 & 0 & 1 & 0 & x & x & x & 0 & 0 & x & 0 & \ldots \\ 0 & 0 & 0 & 1 & x & x & x & 0 & 0 & x & 0 & \ldots \\ 0 & 0 & 0 & 0 & 0 & 0 & 0 & 1 & 0 & x & 0 & \ldots \\ 0 & 0 & 0 & 0 & 0 & 0 & 0 & 0 & 1 & x & 0 & \ldots \\ 0 & 0 & 0 & 0 & 0 & 0 & 0 & 0 & 0 & 0 & 1 & \ldots \\ 0 & 0 & 0 & 0 & 0 & 0 & 0 & 0 & 0 & 0 & 0 & \ldots \\ \ldots & \ldots & \ldots & \ldots & \ldots & \ldots & \ldots & \ldots & \ldots & \ldots & \ldots & \ldots \\ 0 & 0 & 0 & 0 & 0 & 0 & 0 & 0 & 0 & 0 & 0 & \ldots \end{bmatrix} \begin{matrix} \left.\vphantom{\begin{matrix}a\\a\\a\\a\\a\\a\\a\end{matrix}}\right\} r \text{ rows} \\ \left.\vphantom{\begin{matrix}a\\a\end{matrix}}\right\} (k-r) \text{ rows of zeros} \end{matrix} \tag{3.31}$$

Here the symbol x stands for a numeral, which is not necessarily equal to zero. The equation

$$M\,X = O \tag{3.32}$$

is equivalent to eq. (3.30) (see Noble, sec. 4.8).

By interchanging columns, i.e. by renumbering the columns, we obtain from M the *normal* row-echelon form M^n:

$$M^n = \left(\begin{array}{c|c} I_r & B \\ \hline O_{k-r,r} & O_{k-r,k-r} \end{array}\right), \tag{3.33}$$

where I_r = identity matrix of order r,

B = $r \times (k-r)$ matrix, with at least one element unequal to zero, and

$O_{i,j} = i \times j$ zero matrix.

We must remember here which columns have been interchanged in order to obtain M^n, and this can be represented as follows:

$$M^n = M\, I_k^{i,j}\, I_k^{l,m} \ldots . \tag{3.34}$$

Here $I_k^{p,q}$ is a matrix of order k, which is obtained from the identity matrix by interchanging the pth and qth columns.

For example

$$I_5^{3,4} = \begin{pmatrix} 1 & 0 & 0 & 0 & 0 \\ 0 & 1 & 0 & 0 & 0 \\ 0 & 0 & 0 & 1 & 0 \\ 0 & 0 & 1 & 0 & 0 \\ 0 & 0 & 0 & 0 & 1 \end{pmatrix}.$$

Since $I_k^{p,q}$ is equal to its own inverse, we have

$$M = M^n \ldots I_k^{l,m} I_k^{i,j}. \tag{3.35}$$

We had to determine the solutions of eq. (3.30): $GX = O$, which is equivalent to $MX = O$ and hence also to

$$M^n \ldots I_k^{l,m} I_k^{i,j} X = O. \tag{3.36}$$

If we write

$$X' = \ldots I_k^{l,m} I_k^{i,j} X, \tag{3.37}$$

this is further equivalent to

$$M^n X' = O_{k,k-r}. \tag{3.38}$$

The solutions for this equation are given by

$$x'_i(r) = -Bx'_i(k-r) \quad (i = 1, \ldots, k-r), \tag{3.39}$$

where

$$x'_i(r) = \{x'_{1,i}, \ldots, x'_{r,i}\}$$

and

$$x'_i(k-r) = \{x'_{r+1,i}, \ldots, x'_{k,i}\},$$

hence

$$x'_i = \begin{pmatrix} x'_i(r) \\ \cdots\cdots \\ x'_i(k-r) \end{pmatrix}.$$

B is taken from eq. (3.33). The $x'_i(k-r)$ can be chosen arbitrarily, but will be taken in such a way as to form a set of linear independent vectors. This may be done by putting them equal to

$$\begin{aligned} x'_1(k-r) &= \{1, 0, 0 \ldots, 0\} \\ x'_2(k-r) &= \{0, 1, 0 \ldots, 0\} \\ &\vdots \\ x'_{k-r}(k-r) &= \{0, 0 \ldots, 0, 1\}. \end{aligned}$$

Substitution of these relations in eq. (3.39) yields

$$\begin{aligned} x'_1 &= \{-\tilde{B}_1, \quad 1, 0, 0 \ldots, 0\} \\ x'_2 &= \{-\tilde{B}_2 \quad , 0, 1, 0 \ldots, 0\} \\ &\vdots \\ x'_{k-r} &= \{-\tilde{B}_{k-r}, 0, 0 \ldots, 0, 1\}, \end{aligned}$$

where $\tilde{B}_i$ represents the ith row of the transposed matrix $\tilde{B}$ (or the ith column of B). Collecting these $k - r$ independent solutions again in a matrix X' we obtain

$$X' = \begin{pmatrix} -B \\ \cdots\cdots \\ I_{k-r} \end{pmatrix} \tag{3.40}$$

as the solution of (3.38). If we compare eq. (3.38) with its equivalent, eq. (3.32) it follows, using eq. (3.34), that

$$X = I_k^{i,j} I_k^{l,m} \ldots X'. \tag{3.42}$$

Since we know X' from eq. (3.40), we also know X. We only need to make all vectors of X orthonormal.

In the normal coordinate analysis we are interested in a set of coordinates $\bar{s}$ which are mutually orthonormal and which contain all $(k - r)$ zero coordinates. We can obtain this new set of coordinates as follows from the old set of symmetry coordinates s.

The $k - r$ generally non-orthonormal zero coordinates are given by eq. (3.29). To these we add r linear combinations from the set s, which are mutually independent and also independent of the $(k - r)$ zero coordinates. We do this by means of the linear transformation

$$\bar{s}' = C' s, \tag{3.43}$$

where

$$C' = \begin{pmatrix} \tilde{X} \\ \cdots\cdots \\ I_r \;\vdots\; O_{r,k-r} \end{pmatrix}. \tag{3.44}$$

In other words, we take the zero coordinates given by eq. (3.29) and, in addition, the symmetry coordinates $s_1, \ldots, s_r$ from the original set s (these symmetry coordinates must be independent of the zero coordinates, otherwise others would have to be chosen).

Using the relation

$$\tilde{X} = \tilde{X}' \ldots I_k^{l,m} I_k^{i,j} \tag{3.45}$$

and

$$\tilde{X}' = (-\tilde{B} \;\vdots\; I_{k-r}), \tag{3.46}$$

we can write C' as

$$C' = \begin{pmatrix} (-\tilde{B} \;\vdots\; I_{k-r}) \ldots I_k^{l,m} I_k^{i,j} \\ \cdots\cdots\cdots\cdots\cdots\cdots\cdots\cdots \\ r \;\vdots\; O_{r,k-r} \end{pmatrix}. \tag{3.47}$$

By subjecting C' to a Gram–Schmidt orthogonalisation we obtain an orthonormal matrix C, which we shall call the Sun–Parr–Crawford transformation

matrix. The symmetry coordinate $\bar{s}$, which we shall call the Sun–Parr–Crawford symmetry coordinates, are now given by eq. (3.24):

$$\bar{s} = C\,s,$$

where $\bar{s}$ is an orthonormal set as well, provided that s formed an orthonormal set. If $\bar{G}_s$ refers to the total, block-diagonalised G matrix with respect to the new coordinates $\bar{s}$, we obtain from eq. (3.26′) and eq. (3.14), sec. 3.2

$$\bar{G}_s = C\,G_s\,\tilde{C} = C\,U\,G\,\tilde{U}\,\tilde{C}, \tag{3.48}$$

where C is now taken over all species.

We will call $\bar{G}_s$ the Sun–Parr–Crawford G matrix, and

$$\bar{U} \equiv C\,U, \tag{3.49}$$

the Sun–Parr–Crawford U-matrix. $\bar{U}$ is evaluated in the subroutine SPC of program GMOPSECONDVERSION. From (3.48) and (3.49) we obtain

$$\bar{G}_s = \bar{U}\,G\,\tilde{\bar{U}}. \tag{3.50}$$

3.4. Calculations on $B_3O_6^{3-}$

3.4.1. *GMOPSECONDVERSION*

As has been pointed out in the foregoing, it is useful to consider first the internal vibrations of the $Na_2O.B_2O_3$ crystal as vibrations of the 'free' ion $B_3O_6^{3-}$.

The force constants obtained in this approximation will serve as initial values for calculations on the crystal itself. In table 2-VII the 30 internal coordinates of the $B_3O_6^{3-}$ ion are defined. The geometry of the ring is described in sec. 2.2.1, so that working out the G matrix does not offer any further problem. The numerical data are listed in appendix 1.

Drawing up a good U matrix is rather more complicated. We use for this the method given by Nielsen and Berryman [3–12]. (Nussbaum [3–19]) has also given a good description of it.) The symmetry coordinates must be ordered very carefully because upon interchanging them the matrix may not assume the correct block form or degenerate blocks may arise that are not subdivided. This method calls for the complete matrices of the irreducible representations of the symmetry group D_{3h} (the characters alone are not sufficient). Cornwell [3–10]) (p. 237) and Bradley and Cracknell [3–11]) (p. 61) have given these matrices for the various point groups. For the degenerate species of symmetry group D_{3h} they are the following *)

*) + stands for a rotation in the right-hand screw sense, seen from the origin.

D_{3h}	E	C_3^+	C_3^-	C_{2x}	C_{2a}	C_{2b}	σ_h	S_3^+	S_3^-	σ_{vx}	σ_{va}	σ_{vb}
E'	a	b	c	d	e	f	a	b	c	d	e	f
E''	a	b	c	d	e	f	$-a$	$-b$	$-c$	$-d$	$-e$	$-f$

where

$$a = \begin{pmatrix} 1 & 0 \\ 0 & 1 \end{pmatrix}; \quad b = \begin{pmatrix} -\frac{1}{2} & \frac{1}{2}\sqrt{3} \\ -\frac{1}{2}\sqrt{3} & -\frac{1}{2} \end{pmatrix}; \quad c = \begin{pmatrix} -\frac{1}{2} & -\frac{1}{2}\sqrt{3} \\ \frac{1}{2}\sqrt{3} & -\frac{1}{2} \end{pmatrix};$$

$$d = \begin{pmatrix} -1 & 0 \\ 0 & 1 \end{pmatrix}; \quad e = \begin{pmatrix} \frac{1}{2} & -\frac{1}{2}\sqrt{3} \\ -\frac{1}{2}\sqrt{3} & -\frac{1}{2} \end{pmatrix}; \quad f = \begin{pmatrix} \frac{1}{2} & \frac{1}{2}\sqrt{3} \\ \frac{1}{2}\sqrt{3} & -\frac{1}{2} \end{pmatrix};$$

C_{2x} and C_{vx} are respectively the twofold axis and the vertical mirror plane through the atoms 7, 1 and 4 (fig. in table 2-VII). C_{2a} and C_{va} are respectively the twofold axis and the vertical mirror plane through the atoms 8, 3 and 6. C_{2b} and C_{vb} are respectively the twofold axis and the vertical mirror plane through the atoms 9, 5 and 2. The matrices of the non-degenerate symmetry species correspond to the characters in the character table.

The U matrix given in table 2-VII is now compiled by applying to a number of internal coordinates the projection operator proposed by Nielsen and Berryman [3–12]).

This projection operator contains, instead of the character, the same matrix element a_{ij} $(i,j = 1, 2)$ from the 2×2 matrix for each symmetry operator. There are thus four projection operators for each doubly degenerate symmetry species; we shall call these p_{11}, p_{12}, p_{21} and p_{22} (the subscripts correspond to the chosen element from the 2×2 matrices). For the non-degenerate species the projection operator is the familiar one based on the characters.

Before the projection operators can be applied, it is useful to make first a table of the transformation properties of a number of internal coordinates. Not all internal coordinates are required for this purpose; one of each kind (r, R, α, β, γ, δ and τ) is sufficient. The application of the projection operators upon a second internal coordinate of a given kind only provides linear combinations of the symmetry coordinates already obtained. In the specific case of the $B_3O_6^{3-}$ ring (plane) is it not necessary to include in the table the symmetry elements σ_h, S_3^+, S_3^-, σ_{vx}, σ_{va} snd σ_{vb}. For the in-plane coordinates these symmetry operations yield the same result as the operations E, C_3^+, C_3^-, C_{2x}, C_{2a} and C_{2b}. After application of the former operations (σ_h, etc.) to the out-of-plane coordinates, the sign is changed with respect to the application of the latter operations (E, C_3^+, etc.).

Table of symmetry coordinates developed by using Nielsen and Berryman's method

	projection operator	applied to	sym. coord.	internal coordinates 1	2	3	4	5	6	7	8	9	10	11	12	13	14	15	16	17	18	19	20	21
E'	p_{11}	r_3	s_{20}	−1	1	2	−2	−1	1															
	p_{12}	r_3	s_{19}	−1	−1	0	0	1	1															
	p_{21}	r_3	s_{13}	1	−1	0	0	−1	1															
	p_{22}	r_3	s_{12}	−1	−1	2	2	−1	−1															
	p_{12}	R_1	s_{18}							0	1	−1												
	p_{22}	R_1	s_{11}							2	−1	−1												
	p_{12}	α_1	s_{21}										0	1	−1									
	p_{22}	α_1	s_{14}										2	−1	−1									
	p_{12}	β_2	s_{22}													−1	0	1						
	p_{22}	β_2	s_{15}													−1	2	−1						
	p_{11}	γ_4	s_{24}																1	−1	1	2	−2	−1
	p_{12}	γ_4	s_{23}																1	−1	−1	0	0	1
	p_{21}	γ_4	s_{17}																1	1	−1	0	0	−1
	p_{22}	γ_4	s_{16}																−1	−1	−1	2	2	−1

	projection operator	applied to	sym. coord.	22	23	24	25	26	27	28	29	30
E''	p_{11}	δ_1	s_{28}	2	−1	−1						
	p_{12}	δ_1	s_{25}	0	1	−1						
	p_{11}	τ_2	s_{26}				−1	2	2	−1	−1	−1
	p_{12}	τ_2	s_{27}				−1	0	0	1	1	−1
	p_{21}	τ_2	s_{29}				1	0	0	−1	−1	1
	p_{22}	τ_2	s_{30}				1	2	−2	−1	1	−1

Transformation properties of a number of internal coordinates

Symmetry operation:		E	C_3^+	C_3^-	C_{2x}	C_{2a}	C_{2b}
Internal coord. no. ↓							
r_3	3	3	5	1	4	2	6
R_1	7	7	8	9	7	9	8
α_1	10	10	11	12	10	12	11
β_2	14	14	15	13	14	13	15
γ_4	19	19	21	17	20	18	16
δ_1	22	22	23	24	−22	−24	−23
τ_2	26	26	28	30	−27	−25	−29

Remarks:

— Coordinates r_7, r_8 and r_9 (defined in table 2-VII) are also represented by R_1, R_2 and R_3.

— r_3, γ_4 and τ_2 have been chosen in order to obtain agreement with the U matrix earlier set up for crystalline $Na_2O.B_2O_3$, where the definitions of the internal coordinates differed slightly from the definitions for the ring given in table 2-VII.

— β_2 was chosen with a view to the factorising of the E' species into two identical blocks. This choice is not arbitrary since the α's and the β's together yield a number of redundancies which must be properly divided among the two identical blocks.

For the E' and the E'' blocks we now obtain the symmetry coordinates as presented in the table. They have also been listed in table 2-VII and have not been normalised.

It is evident that the out-of-plane coordinates must yield zero in species E', just as the in-plane coordinates do in species E''. The U matrix is given in table 2-VII. The serial order of the symmetry coordinates must be found by inspection of the form of the G matrix. In each species, symmetry coordinates must be interchanged until the correct block form is obtained.

With the above data we can now run the computer program GMOPSECONDVERSION (i.e. GMOP including the SPC transformation described in the foregoing). The B matrix, the G matrix (for the natural isotope ratio of boron), the block-diagonalised G matrix and the Sun–Parr-Crawford G matrix are given in appendix 1. The latter matrix is obtained from the G matrix and the Sun–Parr–Crawford U matrix, $\bar{U}$ (sec. 3.3.2.2), with the help of program *GZ* conversion.

3.4.2. *F matrix (Z matrix)*

The force field chosen is the General Quadratic Valence Force Field (GQVFF) This is the force field most generally used in vibrational analysis. It might be possible to use other force fields, such as the MUBFF (Modified Urey Bradley Force Field), but that would only be meaningful if the GQVFF did not provide satisfactory results.

The force and interaction constants (further simply referred to as force constants) from eq. (3.7) in sec. 3.2 are defined in table 3-III, for the $B_3O_6^{3-}$ ion.

TABLE 3-III

Definitions of the force constants of the 'free' ion $B_3O_6^{3-}$, with an estimate of their initial values (in mdyn/Å). O = intra-annular O atom; O′ = extra-annular O atom

no.	explanation principal force constants	estimated value (mdyn/Å)
f_1	f_r, B–O (stretching)	6.5
f_2	f_R, B–O′ (stretching)	9.5
f_3	f_α, O–B–O (bending)	0.33
f_4	f_β, B–O–B (bending)	0.33
f_5	f_γ, O–B–O′ (bending)	0.33
f_6	f_τ, O–B–O–B (torsion)	0.8
f_7	f_δ, out-of-plane wagging	0.3
	interaction constants	
f_8	f_{rr}, common B atom	1
f_9	f_{rr}' common O atom	1
f_{10}	f_{Rr},	1.5
f_{11}	$f_{r\alpha}$, with r as part of α	0.5
f_{12}	$f_{r\alpha}'$, r and α having an O atom in common	0
f_{13}	$f_{r\beta}$, with r as part of β	0.5
f_{14}	$f_{r\beta}'$, r and β having a B atom in common	0
f_{15}	$f_{r\gamma}$, with r as part of γ	0.5
f_{16}	$f_{r\gamma}'$, r and γ having a B atom in common	0
f_{17}	$f_{r\gamma}''$, r and γ having an O atom in common	0
f_{18}	$f_{R\alpha}$, adjacent R and α	0
f_{19}	$f_{R\beta}$, adjacent R and β	0
f_{20}	$f_{R\gamma}$, with R as part of γ	small
f_{21}	$f_{\alpha\alpha}$, adjacent α's	0
f_{22}	$f_{\alpha\beta}$, r common	0.12
f_{23}	$f_{\alpha\gamma}$, r common	0
f_{24}	$f_{\alpha\gamma}'$, O atom common	0
f_{25}	$f_{\beta\beta}$, adjacent β's	0
f_{26}	$f_{\beta\gamma}$, r common	0
f_{27}	$f_{\beta\gamma}'$, B atom common	0
f_{28}	$f_{\gamma\gamma}$, R common	0
f_{29}	$f_{\gamma\gamma}'$, O atom common	0
f_{30}	$f_{\tau\tau}$, B–O–B common	?
f_{31}	$f_{\tau\tau}'$, O–B–O common	?
f_{32}	$f_{\tau\tau}''$, r common	?
f_{33}	$f_{\tau\tau}'''$, end atoms common	0
f_{34}	$f_{\delta\delta}$, an O atom common	0
f_{35}	$f_{\delta\tau}$, r common	?
f_{36}	$f_{\delta\tau}'$, two r's common	?
f_{37}	$f_{\delta\tau}''$, O atom common	0

r = stretching B–O
R = stretching B–O′
α = bending O–B–O
β = bending B–O–B
γ = bending O–B–O′
δ = out-of-plane wag *)
τ = torsion O–B–O–B

*) Is defined by a boron atom and its three covalently bonded atoms.

The force constants that represent an interaction between an out-of-plane and an in-plane coordinate must be zero. This is readily understood if we consider the potential energy before and after reflection with respect to the plane of the $B_3O_6^{3-}$ ring (σ_h). The potential energy before and after reflection must be identical:

Before reflection in σ_h: $2V = \ldots + f_{io}\, R_i\, R_o + \ldots$
after reflection in σ_h : $2V = \ldots + f_{io}\, R_i\, (-R_o) + \ldots$

hence $f_{io}\, R_i\, R_o = -f_{io}\, R_i\, R_o$, which is only true for $f_{io} = 0$. Here, f_{io} is the force constant of the interaction between an in-plane (R_i) and an out-of-plane coordinate (R_o).

There are a total of 37 different force constants, and with these the Z matrix can be drawn up. For each element of the F matrix we must determine which of the 37 force constants is represented in that element. In the F matrix each element consists of only one force constant. The Z matrix for $B_3O_6^{3-}$ is given in appendix 1.

3.4.3. *GZ CONVERSION*

We now have at our disposal the G and Z matrices and the SPC U matrix, $\tilde{U}$. The next thing to do is to reduce the size of the secular equation as far as possible. For this purpose the superfluous coordinates from the SPC matrix must be eliminated, i.e. the zero coordinates and one of each pair of degenerate blocks. We can also delete the non-active symmetry species, such as the A'_2 block. The dimension of the G and Z matrices obtained in this way (after transformation with the reduced SPC U matrix) is only 12. This is because we are only left with the following new symmetry coordinates:

A'_1 : coordinates 1, 2 and 3
A''_2: coordinates 4 and 5
E' : coordinates 6, 7, 8, 9 and 10
E'' : coordinates 11 and 12.

The elimination of the superfluous coordinates is done by the program *GZ* conversion. This program will not be described here. With the G and F matrices and the SPC U matrix as an input, it yields the SPC G and F matrices. These are given in appendix 1.

As was to be expected, the two symmetry species that contain only out-of-plane coordinates (A''_2 and E'') are completely independent of the 'in-plane symmetry species' (A'_1 and E'). The blocks A''_2 and E'' only contain force constants that relate to the out-of-plane motion, and these force constants do not occur in the blocks A'_1 and E', and vice versa.

This means that the problem is divided into two smaller sub-problems: the out-of-plane problem (dimension 4), and the in-plane problem (dimension 8).

3.4.4. *Out-of-plane vibrations*

The SPC G and F matrices that relate to the out-of-plane vibrations may be represented as follows:

F matrix

	4	5	11	12
4	F_1		0	
5		F_2		
11	0		F_3	
12				F_4

G matrix

	4	5	11	12
4	a_1	b_1	0	0
5	b_1	c_1	0	0
11	0	0	a_2	b_2
12	0	0	b_2	c_2

where $F_1 = f_7 + 2f_{34}$

$F_2 = f_6 - f_{30} - f_{31} + 2f_{32} - f_{33}$

$F_3 = f_7 - f_{34}$

$F_4 = f_6 - 0.582125f_{30} - 0.4131f_{31} - f_{32} + 0.995227f_{33}$

and $a_1 = 0.881480$; $b_1 = 1.721677$; $c_1 = 3.792065$

$a_2 = 0.754024$; $b_2 = 0.832911$; $c_2 = 1.256209$

(these-data have been taken from appendix 1).

The four F's can be calculated from four observed frequencies. However, the observed frequencies are required to satisfy certain conditions, and these will first be derived.

The above F and G matrices can each be subdivided into two blocks (the A''_2 and the E'' blocks), and for each block we may write

$$|FG - E\lambda| = 0 \quad \text{or} \quad \left| \begin{pmatrix} F_x & 0 \\ 0 & F_y \end{pmatrix} \begin{pmatrix} a & b \\ b & c \end{pmatrix} - \begin{pmatrix} 1 & 0 \\ 0 & 1 \end{pmatrix} \lambda \right| = 0 \tag{3.50}$$

or:

$$(ac - b^2) F_x F_y - \lambda (aF_x + cF_y) + \lambda^2 = 0. \tag{3.51}$$

If ν_1 and ν_2 are two observed frequencies appertaining to the block (= species), we have $\lambda_1 = 4\pi \nu_1{}^2 c^2$, $\lambda_2 = 4\pi \nu_2{}^2 c^2$, and

$$(ac - b^2) F_x F_y - \lambda_1 (aF_x + cF_y) + \lambda_1{}^2 = 0 \tag{3.52}$$

$$(ac - b^2) F_x F_y - \lambda_2 (aF_x + cF_y) + \lambda_2{}^2 = 0. \tag{3.53}$$

Subtraction of the above equations, and dividing by $(\lambda_1 - \lambda_2)$ yields

$$aF_x + cF_y = \lambda_1 + \lambda_2. \tag{3.54}$$

Multiplying eq. (3.52) by λ_2 and eq. (3.53) by λ_1 followed by subtraction and division by $(\lambda_2 - \lambda_1)$ yields

$$(ac - b^2)\, F_x\, F_y = \lambda_1\, \lambda_2. \tag{3.55}$$

From eqs (3.54) and (3.55) we can solve F_x and F_y:

$$aF_x^2 - (\lambda_1 + \lambda_2)\, F_x + \lambda_1\, \lambda_2\, c/(ac - b^2) = 0 \tag{3.56}$$

(F_y gives a similar equation). If this equation is to yield a real value for F_x the determinant must be $\geqslant 0$, i.e.

$$(\lambda_1 + \lambda_2)^2 - p\lambda_1\, \lambda_2 \geqslant 0, \tag{3.57}$$

where $p = 4ac/(ac - b)^2$, and p depends only on the values from the G block (F_y gives the same determinant). Equation (3.57) can also be written as

$$\frac{\lambda_1}{\lambda_2} + \frac{\lambda_2}{\lambda_1} \geqslant (p - 2), \tag{3.58}$$

where $p - 2 = 33.33$ for the A''_2 block and
$p - 2 = 12.95$ for the E'' block.

In sec. 2.4.5 the frequencies 722 cm^{-1} and 678 cm^{-1} of the crystal were assigned to the modes $\nu_7(A_{2u}\,(A''_2))$ and $\nu_{14}(E_g/E_u\,(E''))$, respectively. The frequencies of the modes $\nu_7(A''_2)$ and $\nu_{14}(E'')$ of the 'free' $B_3O_6^{3-}$ ion will be approximately equal to these values. Therefore we can calculate the frequencies $\nu_6(A''_2)$ and $\nu_{13}(E'')$ of the ion from eq. (3.58). The result is that ν_6 and ν_{13} must be less than 126 cm^{-1} and 198 cm^{-1}, respectively. In the far-infrared spectrum (sec. 2.3.2), however, no band could be observed in this region, so that the precise value of the infrared active ν_6-mode is not known and the force constants of the block A''_2 cannot be determined.

In the Raman spectrum, however, we do find a number of peaks at the lower frequencies, but these have been assigned to the lattice vibrations. It is possible that one of these peaks belong to the internal vibration $\nu_{13}(E'')$, in spite of the fact that the frequency is strongly influenced by the alkali ion.

Thus, for the E'' block, we cannot calculate any force constants either. Since, however, in the case of the crystal the frequency of ν_{13} pertains to the same species as most of the lattice vibrations (E_g), it may be possible to find the relevant force constants and establish the frequency from a calculation on the crystal.

3.4.5. *In-plane vibrations*

In sec. 3.4.3 we reduced the dimension of this problem to 8. This is too large, however, to allow of a derivation of similar relations between the frequencies as we have done for the out-of-plane vibrations.

This problem must therefore be solved directly with the iteration program

FLEPO. For this purpose the observed frequencies from the A'_1 and E' species are needed. As already explained in chapter 4, there are still a few uncertainties as regards the assignment of the symmetry species E'. The various possibilities that arise will be separately calculated.

A problem in the calculations is the larger number of force constants that occur in the two blocks. Appendix 1 gives the SPC Z matrix and shows that 27 different force constants occur in blocks A'_1 and E'. This number must be reduced. To do this, we shall assume as a first approximation that the force constants relating to interactions between internal coordinates having only one atom in common are equal to zero *). The number of force constants is then reduced to 16. Since this is still too large, a further approximation is needed. If we look at the force constants in table 3-III we notice that f_8 and f_9 are rather similar (they are both f_{rr}'s but have a different central atom). The same thing is true for f_{11} and f_{13} and for f_{23} and f_{26}. We shall therefore take these force constants pairwise equal, which can easily be realised in the Z matrix. We are now left with 13 force constants.

From this point onwards the problem can be solved in two steps, firstly by calculating the A'_1 block and secondly by calculating the two blocks A'_1 and E' together. The great advantage of this is that the frequencies from the A'_1 block, which have been assigned with high certainty, yield a limited number of force constants that are no longer varied in the second step. Furthermore, for the A'_1 block we have well-defined frequencies for both the natural isotope composition of the ring and the ^{10}B-enriched composition. The E' block does not have this advantage, because the infrared spectrum often has no sharply defined peaks, and we do need a number of values from this spectrum.

The F matrices of the various isotope compositions are the same, but the G matrices differ. From the two A'_1 blocks we can now make a single large block:

F matrix

	1	2	3	4	5	6
1	F_1	F_4	F_6			
2		F_2	F_5		0	
3			F_3			
4				F_1	F_4	F_6
5					F_2	F_5
6						F_3

G matrix

	1	2	3	4	5	6
1	a	b	c			
2		d	e		0	
3			f			
4				a′	b′	c′
5					d′	e′
6						f'

where the first three 'coordinates' relate to the ^{10}B composition and the last three to the natural isotope composition. The force constants in the F matrix,

*) With the exception of f_{rr} (the interaction constants between two adjacent stretchings), which often have a relatively high value.

which is the SPC F matrix, are related to the original GQVFF force constants (as may be seen in appendix 1) as follows:

$F_1 = f_2$; $F_2 = f_1 + f_8 + f_9$; $F_3 = 0.41f_3 + 0.41f_4 + 0.18f_5 - 1.63f_{22} + 0.18f_{28}$; $F_4 = 1.41f_{10}$; $F_5 = 0.43f_{15}$ and $F_6 = -0.60f_{20}$.

The G matrix elements have the following values (where a to f originate from the G matrix of $^{10}B_3O_6^{3-}$ and a′ to f′ from $B_3O_6^{3-}$ with $m_B = 10.811$):

a = 0.162374; b = –0.076510; c = 0.262618; d = 0.08473; e = 0.088770; f = 1.17448.
a′ = 0.155001; b′ = –0.070862; c′ = 0.243231; d′ = 0.080406; e′ = 0.073918; f′ = 1.123468.

The appertaining frequencies are: 1605, 769, 631, 1573, 769, 624 cm^{-1}.

These frequencies show a few small discrepancies compared with the associated G matrix blocks. The frequencies 769 cm^{-1} and 631 cm^{-1} belong to the ^{10}B-enriched sample (93% ^{10}B), whereas the G matrix is that of 100% ^{10}B. The frequency of 1573 cm^{-1} is due to $^{10}B^{11}B_2O_6^{3-}$, and thus pertains to 33% ^{10}B instead of 20% ^{10}B, on which the G matrix is based. (The small error which this involves is to some extent compensated by the overlap of the peaks of $^{10}B^{11}B_2O_6^{3-}$ and $^{11}B_3O_6^{3-}$.)

At first sight we should now be able to calculate the force constants F_1 to F_6, since we have just as many unknown F's as frequencies. This is not entirely true, however (see Jones [3–6]), p. 34), because the frequencies are not independent of each other. The rule of Teller and Redlich (the isotope product rule) gives the relation between the frequencies and the G matrices (blocks):

$$\frac{\nu_1}{\nu_1'}\,\frac{\nu_2}{\nu_2'}\,\frac{\nu_3}{\nu_3'} = \sqrt{\frac{|G|}{|G'|}},$$

which means that one of the frequencies is dependent on the other frequencies. This problem is solved by applying an approximation, namely by choosing $F_6 = 0$ and leaving this force constant out of the iterations. In this way five independent force constants remain to be solved.

The drawback of this method is that one force constant (F_6) has wrongly been taken equal to zero. Another method is to work towards a minimum sum of squared residuals,

$$\text{SUMDD} = \sum_{i}^{6} [\lambda_i(\text{obs}) - \lambda_i(\text{calc})]^2 ,$$

with six variable force constants using the FLEPO program. This gives a solution that is *not* strictly correct mathematically but is physically more acceptable than the previous approximation. Both solutions are given in appendix 2, and show very little difference (A2 and A3 in appendix 2).

Before running the program FLEPO we had to choose a number of initial values for the force constants. These values have to be estimated as accurately as possible, otherwise the number of iterations that have to be performed increases enormously. Starting with six variable force constants with unrealistic initial values there is even a great chance that the program will find another minimum. An example is given in appendix 2 (A4), where all six F's have zero as their initial value. The solution is seen to be physically unrealistic (e.g. F_6 is relatively very large in this case).

Firstly, therefore, we estimated the force constants (see table in sec. 3.4.1), taking $F_6 = 0$ (and constant), and then used the resultant improved values (appendix 2, A1) in order to:

(1) refine these values still further (appendix 2, A2) and

(2) to run the program with the six variable force constants (appendix 2, A3).

We can now move on to the second step of the calculations, i.e. the treatment of the blocks A'_1 and E' together. For this, we need the values of the GQVFF force constants f_1, f_2, etc. Since $F_1 = f_2$, $F_4 = 1.41 f_{10}$, $F_5 = 0.43 f_{15}$ and $F_6 = -0.60 f_{20}$, the values of f_2, f_{10}, f_{15} and f_{20} are immediately obtained from F_1, F_4, F_5 and F_6, taking for the latter the physically most meaningful values (appendix 2, A3). F_2 and F_3 are composed of a larger number of GQVFF force constants and therefore provide only limited information. However, we can calculate f_1, f_8 and f_9 from F_2 assuming that the ratio $f_1 : f_8 : f_9$ is equal to that for their initial values. Analogously, f_3, f_4, f_5, f_{22} and f_{28} may be obtained from F_3. In the calculation we have fixed f_2, f_{10} and f_{20} at the calculated values, but have left f_{15} variable, since this force constant occurs in very many elements of the E' block and probably plays only a minor role in the A'_1 block. In this way we are left with 10 variable force constants and we have 8 frequencies. In mathematical terms the solution will not be unique, and there is a chance that we shall arrive at an entirely wrong minimum. The chance of this happening is smaller the better are the initial values of the force constants. The solution obtained was evaluated afterwards for its physicochemical relevance. In doing so, we were guided by the following criteria:

(1) Force constants relating to the stretchings usually have the largest values;

(2) Principal force constants, i.e. force constants on the diagonal of the F matrix (on the basis of the internal coordinates) are positive *);

(3) Principal force constants are usually larger than interaction constants;

(4) As far as the $B_3O_6^{3-}$ ring is concerned f_1 (intra-annular B–O stretching) will be smaller than f_2 (extra-annular B–O stretching) owing to the difference in distances between the two bonds.

*) At first sight it is entirely logical that a deviation from the equilibrium state for one of the bonding distances, angles etc. will give rise to an increased potential energy. In spite of this, there are authors who have found negative values for a diagonal constant (Pandey and Sharma [3-13]) and Ramaswamy and Muthusubramanian [3-14]). So has Dikhoff [3-18]) for Na_2WO_4, and he has given a possible explanation for this case.

If all these conditions are satisfied we may consider that we have obtained a good force field for the $B_3O_6^{3-}$ ion. The frequencies in the E' block have been given in sec. 2.4.6. There were some doubts, however, about the assignment of the frequencies at 397 cm^{-1} (R), 1240 + 1275 cm^{-1} (IR), and 1440 cm^{-1} (IR + R?). There remain three possibilities which have all been tested.

(1) The peak at 397 cm^{-1} does not belong to the E' block, but the peaks at 1440 cm^{-1} and at 1275 cm^{-1} do.

(2) The peak at 397 cm^{-1} belongs to the E' block (with the peak at 375 cm^{-1} as corresponding vibration in the infrared). The peak at 1440 cm^{-1} also belongs to the E' block. Neither the peak at 1240 nor the one at 1275 cm^{-1} belongs to E'.

(3) The peak at 397 cm^{-1} (with that at 375 cm^{-1}) again belongs to the E' block, as does 1275 cm^{-1}. The peaks at 1440 cm^{-1} and at 1240 cm^{-1} do not.

The three possibilities are now (^{10}B):

	1	2	3
	1605 cm^{-1}	1605 cm^{-1}	1605 cm^{-1}
A'_1	769 cm^{-1}	769 cm^{-1}	769 cm^{-1}
	631 cm^{-1}	631 cm^{-1}	631 cm^{-1}
	1480 cm^{-1}	1480 cm^{-1}	1480 cm^{-1}
	1440 cm^{-1}	1440 cm^{-1}	1275 cm^{-1}
E'	1275 cm^{-1}	973 cm^{-1}	973 cm^{-1}
	973 cm^{-1}	476 cm^{-1}	476 cm^{-1}
	476 cm^{-1}	397 cm^{-1}	397 cm^{-1}

The frequencies used here are the best known values. In most cases they have been taken from the Raman spectrum.

The results of the calculations with the three models are presented in appendix 2, B_1, B_2 and B_3). They show that:

Model 1 is not satisfactory; f_1 seems to be rather large, f_3 has a large negative value, which is unlikely for a principal force constant), f_4 is much too large for a bending force constant, and f_8 ($= f_9$) is too small. The frequency agreement (calculated frequencies vs. observed frequencies) is not optimum either.

Model 2 gives a very good solution; all force constants have good values and the frequencies are in good agreement.

Model 3 does not give such a good description, but is fairly satisfactory; f_3 is negative, but is so small that it might have been found to be zero or positive upon a slight change in the observed frequencies within their limits of accuracy. However, the frequency agreement is rather poorer than in the case of model 2.

On these grounds we can reject model 1, implying that the peak at 397 cm^{-1} belongs to species E'. This is in agreement with the conclusions drawn from

the out-of-plane vibrations (sec. 3.4.4) since the peak at 397 cm^{-1} (and 375 cm^{-1}) could not possibly belong to species A''_2 or E''.

Summarising, there is a preference for model 2, as regards both the frequency agreement and the values of the force constants. The two infrared peaks at 1250 cm^{-1} for the crystal could then originate from species A'_2 (not active in the case of the 'free' ion, but infrared-active in A_{2u} for the crystal).

3.4.6. *Application of the isotope product rule*

The results of the previous section can be checked with the isotope product rule (Teller and Redlich). This rule can be applied to each symmetry block, and reads:

$$\frac{\nu_1\ \nu_2 \ldots \nu_n}{\nu_1'\ \nu_2' \ldots \nu_n'} = \sqrt{\frac{|G|}{|G'|}}$$

(see, for example, Woodward [3-2]), page 207 ff), where ν_1 to ν_n are the frequencies of the vibrations of the species in question and $|G|$ is the determinant of the appertaining G block *). The prime refers to the modified isotope composition.

We now define

$$P_o = \frac{\nu_1\ \nu_2 \ldots \nu_n}{\nu_1'\ \nu_2' \ldots \nu_n'}$$

and

$$P_c = \sqrt{\frac{|G|}{|G'|}},$$

which enables us to compare the observed and calculated values per block **). The P values for block A'_1 are as follows:

$$P_o = \frac{1573 \times 769 \times 624}{1605 \times 769 \times 631} = 0.969; \quad P_c = 0.962.$$

The frequencies contain the same minor errors with respect to composition as earlier mentioned (3.4.5). P_o and P_c would have agreed better if the highest frequency of composition i had not been taken equal to 1573 cm^{-1} but somewhat lower, as it should be for a composition with 20% ^{10}B (instead of 33% ^{10}B). For species E' we have for the three models, respectively:

*) This value is equal to $\lambda_1\lambda_2 \ldots \lambda_n$, where the λ_t's are the non-zero roots of $|G - \lambda E| = 0$, G being the block in question of the block-diagonalised G matrix G_s.

**) The observed frequencies always refer to the isotope composition i' (19% ^{10}B and 81% ^{11}B) and i (93% ^{10}B and 7% ^{11}B); the G block of composition i is based on 100% ^{10}B.

composition:	model 1		model 2		model 3	
	i′	i	i′	i	i′	i
frequencies (cm^{-1})	1450	1480	1460	1480	1450	1480
	1390	1440	1390	1440	1252	1270
	1252	1270	969	973	969	973
	969	973	473	476	473	476
	473	476	397	397	397	397
P_o	0.923		0.936		0.956	
P_c	0.935		0.935		0.935	

There is clearly a preference for model 2, in accordance with the result of the previous section.

3.4.7. *Potential energy distribution and the displacements of the atoms during the normal vibrations*

Computer program VSEC yields, for given force constants, a large number of data. Among these data are the frequencies, the potential energy distribution and the (relative) displacements of the atoms during the normal vibrations (in cartesian coordinates).

The potential energy distribution of the $B_3O_6^{3-}$ ion over the force constants per normal vibration is given in appendix 3 (based on the frequencies and force constants of model 2). It is evident from this energy distribution that the normal vibration with frequency 1610 cm^{-1} is virtually exclusively determined by f_2 ($= f_R$), i.e. by the extra-annular B–O stretching (99.56%) *). Likewise, the normal vibration with frequency 767 cm^{-1} is largely determined by f_1 ($= f_r$), the intra-annular B–O stretching (92.91%). The largest contribution to the normal vibration with frequency 625 cm^{-1} is given by f_4 ($= f_\beta$), the intra-annular B–O–B bending (78.94%).

The relative amplitudes of the atoms are also given in appendix 3. For each normal vibration the program calculates the amplitudes (multiplied by a specific vibration-dependent scale factor). The potential energy V of the harmonic oscillator is given by

$$V = (v + \tfrac{1}{2})\, h\nu',$$

where v is the vibrational quantum number and ν' the frequency of the oscillator in s^{-1}. Using eq. (3.7) for the potential energy we can now calculate the amplitudes of the atoms expressed in internal coordinates. The relative cartesian displacements can then be obtained from these internal coordinate amplitudes by using the B matrix. For the special case of $v = 1$, the amplitudes for the vibrations in the species A'_1 are calculated. These can be found in the following table:

*) It should be noted that negative contributions are also possible (the sum of negative and positive contributions is 100%).

	1610 cm^{-1}	767 cm^{-1}	625 cm^{-1}
$V = \frac{1}{2} hc\nu \times 10^{20}$ J	4.7928	2.2823	1.8621
$\frac{1}{2} f_2 \Delta R^2 \times 10^{20}$ J	4.7717	0.1148	0.3948
$3 f_1 \Delta r^2 \times 10^{20}$ J	0.5358	2.1205	0.0084
$\frac{1}{2} f_4 (r\Delta\beta)^2 \times 10^{20}$ J	0.8339	0.1693	1.4700
$\Delta R \times 10^2$ Å	5.71	8.85	1.64
$\Delta r \times 10^2$ Å	1.75	3.48	2.19
$r\Delta\beta \times 10^2$ Å	7.52	3.38	9.97
amplitude extra-annular oxygen $\times 10^2$ Å	1.92	1.80	4.30
amplitude intra-annular oxygen $\times 10^2$ Å	0.65	4.45	2.77
amplitude boron $\times 10^2$ Å	3.77	2.69	2.73

(f_1 = 5.823 mdyn/A, f_2 = 9.77 mdyn/A, and f_4 = 0.997 mdyn/A)

The values of the amplitudes of the various atoms are also calculated, and listed in the table above. The vibrations are now fully determined. With these data we can usefully turn our attention to the vitreous borates.

3.5. Calculations on $Na_3B_3O_6$

The calculations on the crystal do not differ in essence from those on the $B_3O_6^{3-}$ ion. The dimension of the problem, however, is very much increased: the number of internal coordinates in one primitive cell is 108. This number is given by the internal coordinates of the two $B_3O_6^{3-}$ ions (2×33) and the Na–O stretchings (42). Some comments are called for at this point:

(1) The number of internal coordinates per ring is now 33 instead of 30. The reason is that we have proceeded in this calculation from torsions instead of 'out-of-plane wag' to define the out-of-plane movement of the extra-annular O.

(2) Only the Na–O stretchings have been taken into account. This bonding is ionic and we assume that only the Na–O attraction plays a role.

(3) In order to avoid making the problem still more complicated, we have not considered the rotation of the two rings relative to one another (libration). This would require the definition of a separate internal coordinate.

Appendix 4 gives the projection of the hexagonal cell on the x–y plane, with the numbers chosen for the atoms. The primitive cell is formed by rings C and F, and six sodium atoms. These atoms are numbered from 1 to 24. The definitions of the 108 internal coordinates are also given in appendix 4.

With these data the G matrix can be calculated using the method already described for diamond.

As for $B_3O_6^{3-}$, the U matrix can be determined using the Nielsen and Berryman method. The resulting U matrix will not be given here, because of its length.

After setting up the U matrix, program GMOPSECONDVERSION can be run. This delivers the block-diagonalised G matrix and, in addition, the

Sun–Parr–Crawford G and U matrices. Since the SPC U matrix contains 6500 non-zero elements (corresponding to 19500 numbers), it will not be given here. The block-diagonalised G matrix and the SPC G matrix are listed in appendix 4.

The latter is the matrix obtained after reduction using the program *GZ* CONVERSION, that is to say after removal of zero coordinates, inactive species, and one of each pair of degenerate blocks and after renumbering the matrix. The resulting matrix is 'only' of order 35. Now that the block-diagonalised G matrix is known, we can find the determinants of the resultant blocks and again apply the isotope product rule. The calculated values $P_c = (|G|/|G'|)^{\frac{1}{2}}$ are compared with the values for $B_3O_6^{3-}$; G relates to the isotope composition 100% ^{11}B, and G' to composition 100% ^{10}B.

$Na_2O.B_2O_3$		$B_3O_6^{3-}$	
block	P_c	block	P_c
A_{1g}	0.954	A'_1	0.954
A_{1u}	0.954	A''_1	no active vibrations
A_{2g}	0.916	A'_2	0.960
A_{2u}	0.916	A''_2	0.965
E_g	0.867	E'	0.920
E_u	0.874	E''	0.960

It can be seen from the above table that the lattice vibration of symmetry species A_{1g} (besides the three internal vibrations, which also occur in the ion, there is only one lattice vibration in A_{1g}) very probably has no isotope splitting, since the P_c values of A_{1g} and A'_1 are identical. Moreover, this is an indication that taking the $B_3O_6^{3-}$ ring for the crystal is a reasonable approximation in the case of the total symmetrical species. In the same way we can approximate to the glass by considering separate $B_3O_6^{3-}$ rings. The fact that the P_c values of the other species do not show a more direct agreement is due to the more complicated relationship between these species. Thus, for example, all vibrations of E' and E'' correlate with those of E_g and E_u (see the correlation table in table 2-VI). Therefore, the P_c values of E' and E'' must be multiplied in order that they can be compared with the P_c value of E_g or E_u. The difference then remaining will probably be attributable to the lattice vibrations, which may also show an isotope shift. However, such a shift must necessarily be small, since $B_3O_6^{3-}$ moves as a rigid entity in the lattice vibrations and the mass ratio $^{10}B_3O_6$ to $^{11}B_3O_6$ is only 126 to 129. The equation now yields:

$$P_c(E') \times P_c(E'') = 0.883; \quad P_c(E_g) = 0.867$$
$$P_c(A'_2) \times P_c(A''_2) = 0.926; \quad P_c(A_{2u}) = 0.916.$$

By analogy with the method of calculation used for $B_3O_6^{3-}$ we can now set out to find the Z matrix. We have chosen the same force constants, with the

exception of those that relate to the out-of-plane movement of the extra-annular oxygen atoms (see comment no. 1 at the beginning of this sec). Moreover, force constants have to be added that determine the attraction between sodium and oxygen. For this purpose we have introduced only two different force constants, namely one for the attraction between Na^+ and an extra-annular oxygen atom and one for the attraction between Na^+ and an intra-annular oxygen atom. The Na–O bonds are assumed to be completely ionic, so that the attraction may be considered to be inversely proportional to the square of the distance. Since there are three different distances between Na^+ and extra-annular O, this saves two unknown f constants. The definition of the force constants is given in appendix 4. The resultant Z-matrix is now easily drawn up. Unfortunately the SPC Z matrix obtained with program *GZ* CONVERSION contains too many elements (more than 4000) to be reproduced.

After the SPC G and Z matrix have been established, it is the turn of program FLEPO to start calculating a set of force constants from the observed frequencies. This calculation has been carried out on the basis of the force constants already obtained for the $B_3O_6^{3-}$ ion. It was found that eigenvalues pertaining to a given symmetry species were shifted to the block of another species. This was due to an error in the subroutine which calculates these eigenvalues. Time was too short to overcome this imperfection.

The results after the first perturbations, apart from the block division, are particularly encouraging. It is found, for example, that the frequencies of the gerade and ungerade vibrations (vibrations of the rings in phase or in anti-phase) show very little difference, i.e. the calculated differences are often smaller than the observed differences. Furthermore the frequency values found for the crystal are in good agreement with those found for the 'free' ion.

REFERENCES

3–1) E. B. Wilson, J. C. Decius and P. C. Cross, Molecular vibrations, McGraw-Hill Book Company, New York, 1955.
3–2) L. A. Woodward, Introduction to the theory of molecular vibrations and vibrational spectroscopy. Oxford University Press, London, 1972.
3–3) J. H. Schachtschneider, Techn. Rep. No. 231-64 (Vol. I and II), Shell Development Company, Emeryville, California, 1966.
3–4) W. T. King, Characteristic group vibrations, Ph.D. Thesis, University of Minnesota, 1956. Diss. Abstr. **18**, 2172, 1958.
W. T. King, I. M. Mills and B. L. Crawford, J. chem. Phys. **27**, 455, 1957.
3–5) T. Shimanouchi and M. Tsuboi, J. chem. Phys. **35**, 1957, 1961.
3–6) L. H. Jones, Inorganic vibrational spectroscopy, vol. 1, Marcel Dekker, Inc., New York, 1971.
3–7) C. E. Sun, R. G. Parr and L. Crawford, J. chem. Phys. **17**, 840, 1949.
3–8) D. L. Vogel, Internal report, Eindhoven University of Technology, 1974.
3–9) B. Noble, Applied linear algebra, Prentice-Hall, Inc., Englewood Cliffs, N.J., 1969.
3–10) J. F. Cornwell, Group theory and electronic energy bands in solids, Appendix 1, North-Holland Publishing Company, 1969.
3–11) C. J. Bradley and A. P. Cracknell, The mathematical theory of symmetry in solids: Representation theory for point groups and space groups, Clarendon, London, 1972.
3–12) J. R. Nielsen and L. H. Berryman, J. chem. Phys. **17**, 659, 1949.

[3-13]) A. N. Pandey and D. K. Sharma, Spectrosc. Lett. **6**, 491, 1973.
[3-14]) K. Ramaswamy and P. Muthusubramanian, Indian J. Phys. **45**, 477, 1971.
[3-15]) R. Fletcher and M. J. D. Powell, Comput. J. **6**, 163, 1963.
[3-16]) M. Wells, Commun. ACM **8**, 169, 1965.
[3-17]) R. Fletcher, Commun. ACM **9**, 686, 1966.
[3-18]) T. G. M. H. Dikhoff, Struktuuronderzoek van wolframaat en molybdaat glazen met behulp van IR- en Ramanspectroscopie, Report Eindhoven University of Technology, 1975.
[3-19]) A. Nussbaum, Amer. J. Phys. **36**, 529, 1968.

4. RAMAN SPECTRA OF SOME BORATE GLASSES

4.1. Introduction

Using the data obtained from the calculations on the metaborate ring we shall construct in this chapter a (limited) model for the structure of the alkali borate glasses. Many attempts have been made to determine the structure of the borate glasses. Krogh-Moe [4-1]) has given a review of the attempts made to throw light on the structure of B_2O_3 glass. Extending ideas put forward by Goubeau and Keller [4-3]), Krogh-Moe [4-4]) concluded that this glass consists of a random three-dimensional network with a large fraction of boroxol rings.

Mozzi and Warren [4-2]) confirm his conclusion on the grounds of X-ray measurements (fluorescence excitation).

Kristiansen and Krogh-Moe [4-5]) and Nagarajan [4-6]) have carried out a normal coordinate analysis on the boroxol ring. We shall consider these calculations more closely since they form the basis for the conclusions on the occurrence of the boroxol ring in glass.

In glasses with less than 20 mole% alkali oxide the excess of oxygen is used only for the formation of BO_4 tetrahedra. This has been concluded from NMR and other measurements (Bray and O'Keefe [4-7]), Beekenkamp [4-26])) and partly explains the so-called boron oxide anomaly. With the aid of the infrared spectra Krogh-Moe [4-4]) determined the distribution of the BO_4 tetrahedra over the structural units and found indications for the formation of large and typical borate groups. As will appear later in this chapter, the Raman spectra can supplement these data.

Also considered in this chapter is the influence of temperature on the structure of two borate glasses. Finally an interpretation is given of a peak which is always present near the excitation line.

4.2. Vibration spectra of glasses

Several research workers, including Gaskell [4-8]), Shuker and Gammon [4-9]), Bell et al.[4-10,11,12]) and Lazarev [4-13]), have tried to give a more fundamental description of the vibration spectra of glasses. The most recent and, in the present author's opinion, the best description has been given by Brawer [4-14]). The starting premises and conclusions of his article will be briefly recapitulated here.

Brawer considers an oxidic glass network built up from certain structural groups. Each structural group consists of several atoms, and together these groups form the glass network. Brawer compares these structural groups with the unit cells in a crystal. The equations of motion for a structural group include the disorder. Disorder means here the deviation from a strict translational repetition of the groups, which would convert the glass into the crystalline state. The result of solving these equations depends on the coupling of the

modes between the structural groups. For two cases he works out in more detail the Raman intensity and the width of the peaks, firstly for the case where the interaction between the structural groups is negligible (molecular structure) and secondly for the case where this interaction is significant. The conclusions drawn by Brawer are the following:

(1) The spectra of glass and crystal (with the same composition) show considerable agreement if certain conditions are satisfied. The main conditions are that the same groups should occur both in the glass and in the crystal and that there should be very little coupling between the structural groups. *This coupling must be considered for each vibrational mode.* The agreement remains even when the degree of disorder increases. The width of the peak increases with increasing disorder.

(2) The disorder in the glass can enhance the polarisability. For this reason certain modes that were not or hardly visible in the crystal spectrum can become visible in the corresponding glass spectrum.

(3) In the case of strong coupling, calculation shows that the width of the modes generally increases considerably.

Without going any further into the calculations given by Brawer, we shall use his conclusions to interpret our glass spectra.

The calculations carried out by Brawer on the metasilicate glass would also be particularly useful for the borate glasses. However, a good set of force constants is needed in order to carry out calculations on different borates. If we were to disregard virtually all force constants, as Brawer does, we might also be able in the short term to perform calculations on the borates. The resultant model would be a rough approximation, which is easier to set up for the silicates than for the borates, in view of the changing coordination number of the B atoms.

4.3. Alkali borate glasses

The Raman spectra of B_2O_3 and of the alkali borate glasses are not new. As long ago as 1936, Kujumzelis [4–15]) described a spectrum of B_2O_3. The advent of laser Raman spectroscopy, however, led various research workers to embark upon a more systematic study of glasses. Bobovich [4–16]) has studied a number of sodium borate glasses. The slit width he used was too large, and therefore he did not discover the existence side by side of the peaks at 806 cm^{-1} and 770 cm^{-1}. White et al.[4–17]) have determined the spectra of a number of alkali borate glasses, but they have not yet published their data.

Recently Krishnan [4–18]) redetermined the Raman spectrum of B_2O_3 and found a number of new strong peaks at 2000 cm^{-1}. We have not been able to observe these peaks. However, he used very old samples and probably observed vibrations due to water and carbon dioxide bound to the glass.

The most recent data have been reported by Konijnendijk [4–19]). He used

the borate spectra for interpreting those of borosilicate glasses. We have determined a number of data from the glass spectra that have not been described by the above-mentioned authors. These are the intensity ratio of the two large Raman peaks at 806 cm^{-1} and 770 cm^{-1}, the half-width of the 806 cm^{-1} peak and the frequency of the peak near the excitation line as a function of composition.

Glass spectra were recorded for alkali contents equal to 0, 5, 10, 15, 16, 17, 20, 25, 30, 35 and 40 mole%. Only those for 15% and 16% are shown (figs 4.5 and 4.6). These spectra show the rapid growth of the peak at 770 cm^{-1} with an increase of alkali content. The data from the spectra of all compositions have been collected in figs 4.1, 4.2, 4.3 and 4.4.

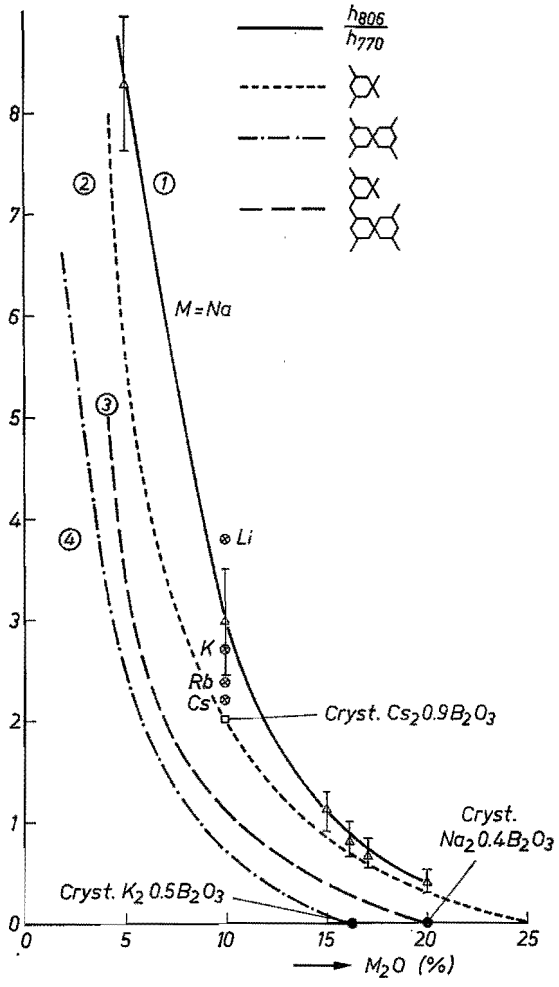

Fig. 4.1. Ringstructures in alkali borates.
Curve 1: the ratio of the peak heights of the peaks at 806 cm^{-1} and 770 cm^{-1} for sodium borate glasses. The ratio of the peak heights of the peaks at 806 cm^{-1} and 770 cm^{-1} is also given for some other alkali borate glasses of the composition 10% M_2O . 90% B_2O_3.
Curve 2: the calculated ratio of the maximum number of boroxol rings to the number of triborate rings (all BO_4 units are situated *in* the rings).
Curve 3: the calculated ratio of the maximum number of boroxol rings to twice the number of pentaborates groups.
Curve 4: the calculated ratio of the maximum number of boroxol rings to three times the number of tetraborate groups.

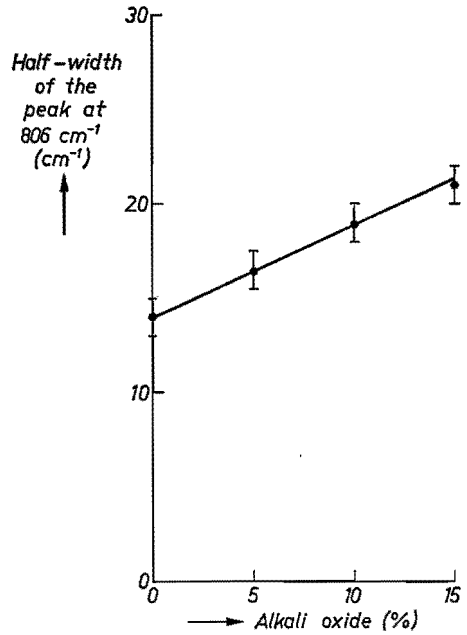

Fig. 4.2. Half-width of the peak at 806 cm^{-1} as a function of alkali-oxide content.

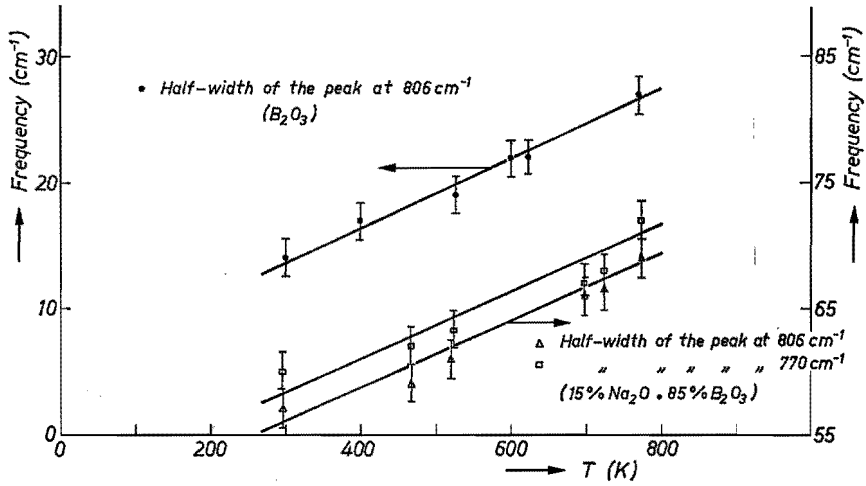

Fig. 4.3. Half-width as function of temperature for 100% B_2O_3 and 15% Na_2O . 85% B_2O_3 glasses.

Looking at the spectra of the borate glasses we note immediately that the strongest peaks lie at 806 cm^{-1} and 770 cm^{-1}. Kristiansen and Krogh-Moe [4–5]) assigned the 806 cm^{-1} peak to a deformation vibration of the boroxol ring. This assignment does not entirely agree with our interpretation of the spectra. We shall go into this question here in rather more detail.

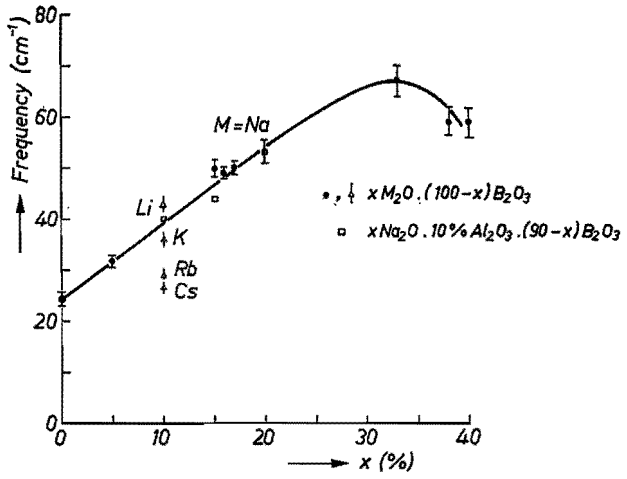

Fig. 4.4. Frequency of the peak near the excitation line as a function of alkali content, and Al_2O_3 content.

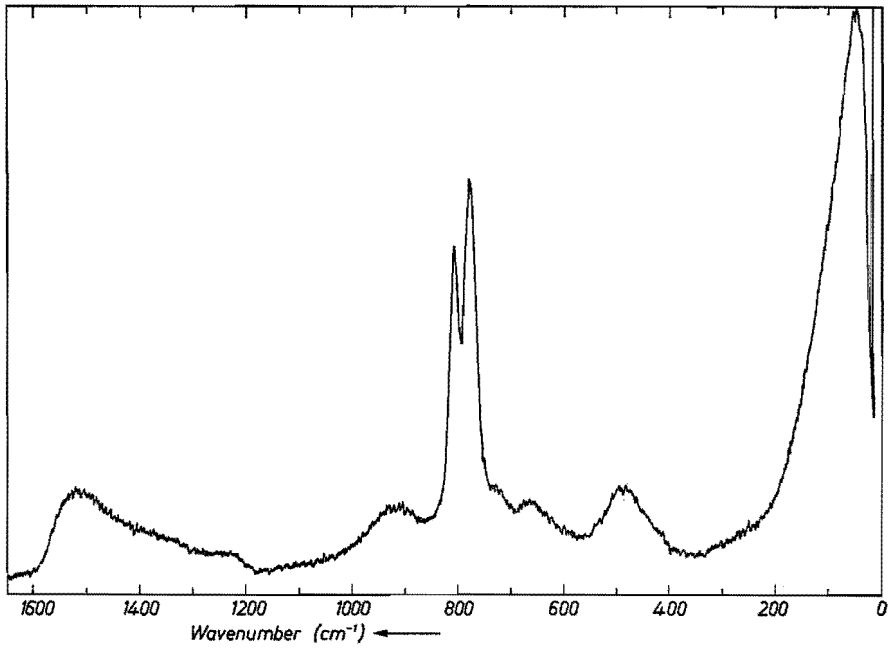

Fig. 4.5. Raman spectrum of vitreous 15% Na_2O . 85% B_2O_3.

As already discussed in chapter 1, a distinction must be made between the boroxol ring and the metaborate ring. The distances in both rings (B–O) are different, and so too is the bonding state. This leads to different force constants in the ring and thus to different ring frequencies. Kristiansen and Krogh-Moe [4–5]) did not have Raman spectra at their disposal. Their assignment of

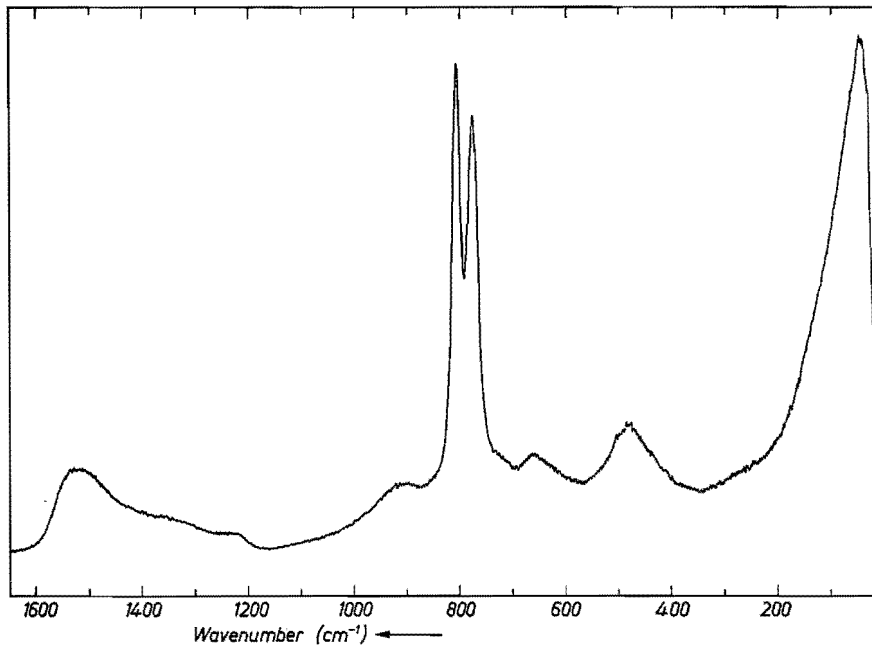

Fig. 4.6. Raman spectrum of vitreous 16% Na_2O . 84% B_2O_3.

the Raman active A'_1 species of the metaborate ring was taken from Hisatsune and Suarez [4–20]). These authors assigned the A'_1 species vibrations to a number of weak infrared bands. Of course this led to mistakes in the calculations of Kristiansen and Krogh-Moe, as is shown in table 4-I.

TABLE 4-I

Comparison of observed and calculated frequencies

Kristiansen and Krogh-Moe		this work	
observed frequency	calculated frequency	observed frequency	calculated frequency
1167 cm^{-1}	1243 cm^{-1}	1573 cm^{-1}	1569 cm^{-1}
823 cm^{-1}	817 cm^{-1}	769 cm^{-1}	767 cm^{-1}
616 cm^{-1}	619 cm^{-1}	624 cm^{-1}	624 cm^{-1}

With the incorrect frequencies Krogh-Moe finds too low a value for the extra-annular B–O stretching force constant:

	d_{B-O}	Krogh-Moe	this work
f_2 (extra-annular B–O stretching)	1.28 Å	5.8 mdyn/Å	9.8 mdyn/Å
f_1 (intra-annular B–O stretching)	1.43 Å	6.4 mdyn/Å	5.8 mdyn/Å

It is evident that the shortest B–O distance must also yield the largest bonding force constant (see e.g. Coulson and Dingle [4–21]), and for this reason too the values of Krogh-Moe cannot be correct.

In spite of these objections we can, however, endorse the conclusion of Kristiansen and Krogh-Moe that the 770 cm^{-1} peak (in their calculations 823 cm^{-1}) will not be much influenced by the mass of the extra-annular atoms. This may be explained as being due to the not very significant amplitude of the extra-annular oxygen atom (see the table in sec. 3.4.7), in consequence of which this atom has little influence on the vibration. This, then, is a vibration that has little coupling with the environment. According to Brawer, the spectra of crystal and glass show considerable agreement as far as such vibrations are concerned. The conclusion is that the peak at 770 cm^{-1} (for crystalline $Na_3B_3O_6$: 769 cm^{-1}) in the glasses with high alkali content (40%) may be attributed to the 'ring breathing' of the metaborate ring. The other peaks from these glasses are much less intensive (except for the peak near the excitation line) and we have not attempted to assign these.

Many authors assume that the boroxol ring is present in B_2O_3 glass (Mozzi and Warren [4–2]), Goubeau and Keller [4–3]), and Krogh-Moe [4–4])). If we also assume that this boroxol ring is in fact present in the glass, it is obvious to assign the breathing of this ring to the peak at 806 cm^{-1}. The difference in value between 806 cm^{-1} and 770 cm^{-1} might be explained as follows.

As appears from the potential energy distribution (sec. 3.4.7), the vibration of the metaborate ring at 770 cm^{-1} is mainly determined by the intra-annular force constant f_1. The magnitude of this force constant depends mainly on the bonding state between the boron atom and the oxygen atom in the ring.

In view of the bonding distance of 1.43 Å, this bond is weak compared with that in the boroxol ring (1.37 Å). We can explain this change in bond strength as being due to the different character of the bonding in the metaborate ring and that in the boroxol ring. In the metaborate ring the bonding between boron and extra-annular oxygen is very strong (9.8 mdyne/Å), and it is very probable that in addition to the σ bond it will also have the character of a π bond. This is confirmed by Coulson and Dingle [4–21]). *Inside* the metaborate ring the π bond character will be much less, the p_z orbital of the sp_2 hybrid boron atom being already 'filled'. Inside the boroxol ring, on the other hand, the bonding will much rather have the character of a π bond. The p_z orbital of the boron atom not yet being filled, this may be done equally by the extra-annular and the intra-annular oxygen atoms. The intra-annular B–O distance is therefore shorter and the bond consequently stronger.

The boroxol ring and the metaborate ring have the same symmetry, and in the boroxol ring there must, therefore, be a vibration corresponding to the vibration at 770 cm^{-1} of the metaborate ring. Since the comparable force constant B–O (intra-annular) of the boroxol ring must be greater than that in

the metaborate ring, the frequency of this ring vibration must also be higher. It is evident that the peak at 806 cm^{-1} satisfies this condition. Moreover, it appears from the glass spectra that the peak at 806 cm^{-1} is strongly polarised and must therefore be due to a symmetric vibration; the ring vibration sought for belongs to the *A* species (and is therefore symmetric). By assuming that the π bond character of the bonding determines the frequency 806 cm^{-1} or 770 cm^{-1} we can also see clearly why $Na_2O.B_2O_3$ and $K_2O.B_2O_3$ have the same ring frequency 770 cm^{-1}. The B–O distance in the ring is different: 1.43 Å ($Na_2O.B_2O_3$) and 1.39 Å ($K_2O.B_2O_3$), but the bonding state is identical. In both cases there is no π-bond in the ring. The potential energy as a function of the distance B–O has the same shape for both rings. Only the equilibrium distance is moved over a short distance. However, the second derivative with respect to the distance (i.e. the force constants) will be the same for both functions.

The foregoing theory concerning the existence of two comparable ring vibrations also makes it possible to explain the 770 cm^{-1} peak in the vitreous alkali borates. This peak is already observable at very small concentrations of alkali oxide (5%). From the crystal structures of the alkali borates with a low alkali content it appears that the BO_4 units formed are taken up in the rings. The boron atom in the BO_4 unit has an sp_3 hybridisation and therefore no p_z orbital. Consequently, there can be no question of a π bond with the oxygen atoms in the ring. The 'resonance structure' found in the boroxol ring cannot therefore possibly be maintained, and the bonding state in the ring corresponds much rather to that in the metaborate ring. The appertaining force constant and the frequency of the vibration will then also correspond to those of the metaborate ring.

With these data we can frame the following hypothesis:

(1) The 806 cm^{-1} peak originates from the breathing vibration of the boroxol ring.

(2) The 770 cm^{-1} peak is due to ring breathing,where the π-bond character in the ring is disturbed. This may apply both to rings with one and two BO_4 groups and to rings with one or two non-bridging oxygen atoms.

We can now use this hypothesis to interpret the spectra of the alkali borates.

The structural units that occur in the crystalline alkali borates have already been dealt with in chapter 1. Crystals containing less than 25% alkali oxide only have structural groups with BO_4 and BO_3 units; there are no non-bridging oxygen atoms. Together with data obtained on the vitreous alkali borates (NMR, viscosity, etc.) this is sufficient to allow the assumption that below the 20% alkali oxide content the number of non-bridging oxygen atoms in glasses is negligible and only BO_3 (*a*) and BO_4 (*c*) units occur. A BO_4 unit can be incorporated in a structural group in various ways. The manner of incorporation determines the maximum number of boroxol groups that will be present in the glass, if all BO_3 units that are not bound to BO_4 units in structural

groups have been taken up in boroxol groups. If, for example, all BO_4 units are incorporated in pentaborate groups (a_4c) then the maximum number of boroxol groups that can be formed is (expressed as a fraction of the total amount of material in moles)

$$\frac{2-12x}{3},$$

where x is the mole fraction of alkali-oxide (composition $x\ M_2O.(1-x)\ B_2O_3$). For the triborate group (a_2c) this maximum number is

$$\frac{2-8x}{3},$$

and for the tetraborate group (a_6c_2)

$$\frac{2-10x}{3}.$$

In the cases of crystalline $K_2O.5B_2O_3$ and $Na_2O.4B_2O_3$ we see that the number of boroxol groups is zero, since these borates are built up respectively from pentaborate groups and tetraborate groups. In the case of $Cs_2O.9B_2O_3$ a number of boroxol groups is left, but in this crystal triborate groups are formed in addition to the boroxol groups (2 boroxol and 1 triborate).

The three crystalline alkali borates mentioned, of which the $K_2O.5B_2O_3$ has three modifications, are the only alkaliborates with an alkali oxide content $\leqslant 20$ mole% and a known crystal structure. In glasses it is precisely the region up to 20% alkali-oxide that is interesting, because in this region the peak at 806 cm^{-1} decreases in intensity with rising alkali content in favour of the peak at 770 cm^{-1}. In terms of the hypothesis on the origin of the peaks this means qualitatively that the number of boroxol rings decreases and rings with BO_4 units are formed.

We can work this out in somewhat more quantitative terms if we assume that the intensity of the peaks is proportional to the number of vibrating rings. The intensity can be approximated by the product of the halfwidth and the height of the appertaining peak. The half-width, however, cannot be accurately determined. We shall, therefore, take the ratio of the peak heights and assume that the width of the peaks increases to the same extent with increasing alkali content (within the accuracy of the measurement this was in fact the case). The ratio of the peak intensities does not equal a priori the ratio of the number of boroxol rings to the numbers of rings with a BO_4 unit. For of course the contribution of the various kinds of rings to the intensity might differ or, in other words, the rings might possess a different oscillator strength. However, since the vibrations with which we are concerned here are largely analogous, we may assume that each ring will have roughly the same oscillator strength.

(If the oscillator strengths were not identical, the ratio of the heights would have to be multiplied by a constant factor.)

We can now plot the peak heights versus the alkali-oxide percentage, as shown in fig. 4.1. The ratio of the maximum number of boroxol rings to the number of triborate rings versus the alkali oxide content is also plotted in this figure. The measured ratio h_{806}/h_{770} equals 2 for the glass composition 10% Cs_2O.90% B_2O_3. From the crystal structure of $Cs_2O.9B_2O_3$ it appears that the ratio of the number of boroxolrings to the number of triborate rings is also equal to 2. Supposing the latter to be the case for the vitreous state as well this agreement implies that the oscillator strengths of boroxol ring and triborate ring are indeed equal. We see, however, in fig. 4.1 that the experimental curve of the sodium borate glasses is clearly above the calculated curves for triborate, tetraborate and pentaborate groups. This means that the number of boroxol rings is greater than the calculated maximum number. Hence, it is clear that the glass structure must also contain structural groups with a higher content of BO_4 units, e.g. diborate groups (a_2c_2), di-triborate groups (ac_2), di-pentaborate groups (a_3c_2) or groups which are interconnected by a BO_4 (c) unit. For the smaller ions this effect is even stronger, as can be seen from fig. 4.1 for the alkali content 10%. This effect may be due to the higher field strength with decreasing (alkali) ionic radius and the tendency of small alkali ions to form low coordination numbers (see for instance Gossink [4–22]). These small alkali ions will result in shorter distances to their charge compensating anions, i.e. $BO_4(c)$ units and hence give rise to the formation of a_2c_2, ac_2, a_3c_2 groups or c-units. This gives rise to an increase in the maximum number of boroxol groups and also diminishes the mean size of the groups.

Half-width of the 806 cm^{-1} peak

From the spectra of the alkali-borate glasses it is also possible to determine the half-width of the 806 cm^{-1} peak. This peak lends itself particularly well to such a measurement up to about 20% alkali oxide. A typical result is presented in fig. 4.2, where the peak width (within the experimental accuracy) is seen to be independent of the type of alkali ion. If we assume with Brawer that the disorder increases with peak width, then the B_2O_3 glass would seem to have the most ordered state. This might partly explain the strong glassforming tendency of B_2O_3.

Temperature dependence

Another phenomenon we have investigated is the influence of temperature on the spectra of B_2O_3 glass and glass of the composition 15% Na_2O.85% B_2O_3. We found that the only change that occurs in B_2O_3 is a considerable broadening of the 806 cm^{-1} peak. Fig. 4.3 gives the half-width as a function of absolute temperature. The other peaks are too broad for an accurate study, but they

too are undoubtedly broadened. Hence, with increasing temperature no other structural groups are formed. Only the disorder increases.

We established that the form of the spectra does not even change, above the transformation range of the glass. Even at the moment when the sample started dripping no change was found! The conclusion, therefore, is that the melt and the glass contain the same structural groups, viz. boroxol rings.

Nor is there any significant change in the spectra up to 500 °C for the composition 15% Na_2O.85% B_2O_3. For this composition the transformation temperature lies at about 350 °C, and the viscosity at 500 °C is still 10^8 poise (see Visser [4–24]). The ratio of the peak heights (h_{806}/h_{770}) underwent no measurable change either.

It is remarkable that the broadening of the 806 cm^{-1} peak at 500 °C for B_2O_3 glass (relative to the width at 20 °C) is just as great as the broadening of the double peak (peaks at 770 and 806 cm^{-1} are overlapping) found for the composition 15% Na_2O.85% B_2O_3, being in both cases 13 cm^{-1}.

The low frequency peak

In all spectra of the borate glasses one particularly strong peak is found, namely a peak near the excitation line. Fig. 4.4 gives the frequency of this peak as a function of composition. Up to about 30% Na_2O the frequency rises linearly. In the two compositions that have a very high alkali content (at the edge of the glass-forming region) a deviation is found; the frequency decreases slightly and, moreover, the peak becomes very broad. This effect may be due to a phase separation through partial crystallisation (this means that the alkali oxide content of the remaining glass is lowered). In the composition with 40% Na_2O it is clear from the sharp peak at 630 cm^{-1} that partial crystallisation must have taken place.

The origin of the low frequency peak is unknown. Stolen [4–25] has stated that this peak in B_2O_3 glass must originate from a band of modes. The temperature dependence he finds is that of a harmonic oscillator. Vibrations with such a low frequency may be due to a translation or to a libration of part of the network. The vibrations of these movements depend both on the mass (moment of inertia) and on a force constant or constants. Let us (with Stolen) assume for simplicity that the frequency is proportional to $(k/m)^{\frac{1}{2}}$, where k is the force constant and m the mass of the vibrating fragment of the network. The force constant k will probably change only very gradually with the composition, since it is mainly determined by the bonding forces between boron and oxygen atoms. When alkali oxide is added, more and more boron atoms change to a four-membered surrounding. The associated force constants are slightly smaller, but the number of bonds increases, so that the overall effect is small. If the alkali-oxide percentage increases still further, non-bridging oxygen atoms will start to appear, and these are bound to the rest of the glass in an entirely different way. In that

case the force constant may show a very marked decrease, and this may perhaps explain the decrease in the frequency at high alkali contents (fig. 4.4).

At the lower alkali oxide percentages ($\leqslant 30\%$) the frequency will depend mainly on the mass of the vibrating fragment. It can be seen from fig. 4.4 that the frequency decreases with decreasing alkali oxide percentage, and this could then mean that the mass of the fragment rises considerably. Assuming that a glass with 50% alkali oxide consists of $B_3O_6^{3-}$ groups (b_3) with mass 130, and taking as the frequency of vibration in question a value of 100 cm^{-1} at this composition (obtained by extrapolation in fig. 4.4), we obtain a mass of approximately 3000 for the fragments in vitreous B_2O_3 (frequency 24 cm^{-1}). This will imply more then 200 atoms. If we add 10% Al_2O_3 to the glass (samples indicated with a square in the figure) we know that the aluminium atom will partly take the place of the four-membered boron atoms (Konijnendijk [4–19]). The size of the fragments should not then undergo any significant increase, and the measured frequencies in fig. 4.4 indeed agree with this.

Changing the alkali ion, however, does have an effect. From the foregoing we know that the small alkali ions cause a decrease of the mean size of the structural groups, and this is what we see happening here (fig. 4.4). The glasses with the smaller alkali ions have a higher frequency at the same alkali oxide content and therefore the mass of the fragment must be smaller.

REFERENCES

[4–1] J. Krogh-Moe, J. non-cryst. Solids **1**, 269, 1969.
[4–2] R. L. Mozzi and B. E. Warren, J. appl. Cryst. **2**, 164, 1969.
[4–3] J. Goubeau and H. Keller, Z. anorg. allg. Chem. **272**, 303, 1953.
[4–4] J. Krogh-Moe, Phys. Chem. Glasses **6**, 46, 1965.
[4–5] L. A. Kristiansen and J. Krogh-Moe, Phys. Chem. Glasses **2**, 96, 1968.
[4–6] G. Nagarajan, Bull. soc. chim. Belg. **71**, 431, 1962.
[4–7] P. J. Bray and J. G. O'Keefe, Phys. Chem. Glasses **4**, 37, 1963.
[4–8] P. H. Gaskell, Trans. Faraday Soc. **62**, 1493, 1966.
[4–9] R. Shuker and R. W. Gammon, Phys. Rev. Lett. **25**, 222, 1970.
[4–10] R. J. Bell, N. F. Bird and P. Dean, J. Phys. **C1**, 299, 1968.
[4–11] R. J. Bell, P. Dean and D. C. Hibben-Butler, J. Phys. **C3**, 2111, 1970.
[4–12] R. J. Bell, P. Dean and D. C. Hibben-Butler, J. Phys. **C4**, 1214, 1971.
[4–13] A. N. Lazarev, Vibrational spectra and structure of silicates, Consultants Bureau, New York - London, 1972.
[4–14] S. Brawer, Phys. Rev. **B11**, 3173, 1975.
[4–15] J. Kujumzelis, Z. Phys. **100**, 221, 1936.
[4–16] Ya. S. Bobovich, Op. Spectry **15**, 412, 1963 (Eng.).
[4–17] W. B. White, G. J. MacCarthy and J. McKay, Amer. ceram. Soc. Bull. **50**, 411, 1971.
[4–18] R. S. Krishnan, Ind. J. pure appl. Phys. **9**, 916, 1971.
[4–19] W. L. Konijnendijk, Philips Res. Repts Suppl. 1975, no. 1.
[4–20] I. C. Hisatsune and N. H. Suarez, Inorg. Chem. **3**, 168, 1964.
[4–21] C. A. Coulson and T. W. Dingle, Acta cryst. **B24**, 153, 1968.
[4–22] R. G. Gossink, Philips Res. Repts **3**, 1971.
[4–23] A. E. R. Westman in J. D. Mackenzie (ed.), Modern aspects of the vitreous state vol. 1, Butterworths, London, 1960, pp. 63-92.
[4–24] Th. J. M. Visser, Rheological properties of alkali borate glasses, Thesis Eindhoven University of Technology, 1971.
[4–25] R. H. Stolen, Phys. Chem. Glasses **11**, 83, 1970.

APPENDIX 1

Numerical data for $B_3O_6^{3-}$

For symmetrical matrices M only the elements M_{ij} are given for which holds $i \geqslant j$, Only non-zero elements are given.

B matrix (139 non-zero elements)

The row number is equal to the number of the corresponding internal coordinate. The column number is equal to: (3× atom number − 3) + i, where i = 1, 2, 3 for x-, y- and z-coordinate, respectively.

row no.	column no.										
1	1	−1.000000	1	4	1.000000	2	4	−0.582123	2	7	0.582123
2	5	−0.813101	2	8	0.813101	3	7	0.500001	3	10	−0.500001
3	8	−0.866025	3	11	0.866025	4	10	0.995227	4	13	−0.995227
4	11	−0.097582	4	14	0.097582	5	13	0.499998	5	16	−0.499998
5	14	0.866026	5	17	−0.866026	6	16	−0.413105	6	1	0.413105
6	17	0.910684	6	2	−0.910684	7	1	0.541708	7	19	−0.541708
7	2	0.840567	7	20	−0.840567	8	7	−0.998806	8	22	0.998806
8	8	0.048849	8	23	−0.048849	9	13	0.457099	9	25	−0.457099
9	14	−0.889416	9	26	0.889416	10	16	−0.910684	10	1	0.910684
10	17	−0.413105	10	5	−0.999999	10	2	1.413104	11	4	0.813101
11	10	0.866025	11	7	−1.679126	11	5	−0.582123	11	11	0.500001
11	8	0.082122	12	10	0.097582	12	16	−0.866026	12	13	0.768444
12	11	0.995228	12	17	0.499998	12	14	−1.495226	13	7	0.813101
13	4	−0.813101	13	2	−1.000000	13	8	−0.582123	13	5	1.582123
14	7	0.866025	14	13	0.097582	14	10	−0.963607	14	8	0.500001
14	14	0.995228	14	11	−1.495228	15	13	−0.866025	15	1	−0.910684
15	16	1.776710	15	14	0.499998	15	2	−0.413105	15	17	−0.086893
16	16	0.860696	16	19	0.889385	16	1	−1.750081	16	17	0.390429
16	20	−0.573169	16	2	0.182740	17	19	−0.889386	17	1	0.889396
17	20	0.573170	17	5	0.945109	17	2	−1.518279	18	4	−0.768469
18	22	0.051686	18	7	0.716783	18	5	0.550169	18	23	1.056816
18	8	−1.606985	19	22	−0.051686	19	10	−0.818488	19	7	0.871074
19	23	−1.056816	19	11	−0.472555	19	8	1.529371	20	10	−0.092226
20	25	−0.941073	20	13	1.033298	20	11	−0.940598	20	26	−0.483647
20	14	1.424245	21	25	0.941073	21	16	0.818489	21	13	−1.759562
21	26	0.483647	21	17	−0.472553	21	14	−0.011094	22	21	1.000000
22	6	0.824458	22	18	0.824459	22	3	−2.648917	23	24	1.000000
23	12	0.824457	23	6	0.824457	23	9	−2.648915	24	27	1.000000
24	18	0.824457	24	12	0.824456	24	15	−2.648913	25	3	−1.229860
25	6	2.399408	25	12	1.098076	25	9	−2.267624	26	6	−1.098076
26	9	2.267625	26	15	1.229860	26	12	−2.399409	27	9	−1.229860
27	12	2.399409	27	18	1.098076	27	15	−2.267624	28	12	−1.098075
28	15	2.267624	28	3	1.229862	28	18	−2.399412	29	15	−1.229861
29	18	2.399416	29	6	1.098076	29	3	−2.267631	30	18	−1.098078
30	3	2.267626	30	9	1.229858	20	6	−2.399407			

G matrix (177 non-zero elements)

The masses of the boron and oxygen atoms are: B = 10.811 and O = 15.999 (natural abundance). Row and column numbers are the numbers of the corresponding internal coordinates.

row no.	column no.											
1	1	0.155001	1	2	−0.036384	1	6	−0.038212	1	7	−0.050107
1	10	−0.084237	1	11	0.050821	1	13	−0.050821	1	15	0.084237
1	16	0.161880	1	17	−0.082267	1	18	−0.048031	2	2	0.155001
2	3	−0.038211	2	8	−0.050107	2	10	0.050821	2	11	−0.084237
2	13	−0.050821	2	14	0.084237	2	17	−0.048031	2	18	−0.082267
2	19	0.161880	3	3	0.155001	3	4	−0.036384	3	8	−0.050107
3	11	−0.084237	3	12	0.050821	3	13	0.084237	3	14	−0.050821
3	18	0.161880	3	19	−0.082267	3	20	−0.048031	4	4	0.155001
4	5	−0.038211	4	9	−0.050107	4	11	0.050821	4	12	−0.084237
4	14	−0.050821	4	15	0.084237	4	19	−0.048031	4	20	−0.082267
4	21	0.161880	5	5	0.155001	5	6	−0.036384	5	9	−0.050107
5	10	0.050821	5	12	−0.084237	5	14	0.084237	5	15	−0.050821
5	16	−0.048031	5	20	0.161880	5	21	−0.082267	6	6	0.155001
6	7	−0.050107	6	10	−0.084237	6	12	0.050821	6	13	0.084237
6	15	−0.050821	6	16	−0.082267	6	17	0.161880	6	21	−0.048031
7	7	0.155001	7	10	0.155502	7	13	−0.077751	7	15	−0.077751
7	16	−0.073483	7	17	−0.073483	8	8	0.155001	8	11	0.155502
8	13	−0.077751	8	14	−0.077751	8	18	−0.073483	8	19	−0.073483
9	9	0.155001	9	12	0.155502	9	14	−0.077751	9	15	−0.077751
9	20	−0.073483	9	21	−0.073483	10	10	0.386424	10	11	0.036384
10	12	0.036384	10	13	−0.229596	10	15	−0.229597	10	16	−0.182607
10	17	−0.182606	10	18	−0.034387	10	21	−0.034387	11	11	0.386424
11	12	0.036384	11	13	−0.229596	11	14	−0.229596	11	17	−0.034387
11	18	−0.182607	11	19	−0.182607	11	20	−0.034387	12	12	0.386424
12	14	−0.229596	12	15	−0.229596	12	16	−0.034387	12	19	−0.034387
12	20	−0.182606	12	21	−0.182607	13	13	0.382770	13	14	0.038211
13	15	0.038212	13	16	−0.016903	13	17	0.233897	13	18	0.233897
13	19	−0.016903	14	14	0.382770	14	15	0.038211	14	18	−0.016903
14	19	0.233897	14	20	0.233897	14	21	−0.016903	15	15	0.382770
15	16	0.233897	15	17	−0.016903	15	20	−0.016903	15	21	0.233897
16	16	0.412194	16	17	−0.239611	16	21	0.032499	17	17	0.412194
17	18	0.032499	18	18	0.412194	18	19	−0.239611	19	19	0.412194
19	20	0.032499	20	20	0.412194	20	21	−0.239611	21	21	0.412194
22	22	0.796511	22	23	0.042485	22	24	0.042485	22	25	0.424984
22	26	−0.056584	22	27	0.056585	22	28	−0.424985	22	29	0.735844
22	30	−0.735842	23	23	0.796510	23	24	0.042485	23	25	0.735841
23	26	−0.735841	23	27	0.424983	23	28	−0.056584	23	29	0.056584
23	30	−0.424983	24	24	0.796509	24	25	0.056584	24	26	−0.424983
24	27	0.735841	24	28	−0.735841	24	29	0.424984	24	30	−0.056584
25	25	0.050746	25	26	−0.804992	25	27	0.422642	25	28	−0.215273
25	29	0.422643	25	30	−0.875766	26	26	1.050747	26	27	−0.875766
26	28	0.422642	26	29	−0.215273	26	30	0.422642	27	27	1.050746
27	28	−0.804992	27	29	0.422643	27	30	−0.215272	28	28	1.050748
28	29	−0.875769	28	30	0.422643	29	29	1.050752	29	30	−0.804994
30	30	1.050746									

Block-diagonalised G matrix (based on the U matrix of table 2-VII)

symmetry block A'_1

row no.	column no.										
1	1	0.155001	1	2	−0.070862	1	3	0.155502	1	4	0.155502
1	5	−0.103921	2	2	0.080405	2	3	−0.047257	2	4	−0.047257
2	5	0.031582	3	3	0.459193	3	4	0.459193	3	5	−0.306875
4	4	0.459193	4	5	−0.306875	5	5	0.205082			

Row and column numbers refer to the first five symmetry coordinates.

symmetry block A'_2

row no.	column no.							
1	1	0.229596	1	2	0.196115	2	2	0.619305

Symmetry coordinates 6 and 7 (row and column nos. 1 and 2)

symmetry block A''_2

row no.	column no.							
1	1	0.881479	1	2	1.721677	2	2	3.792064

Symmetry coordinates 9 and 10 (row and column nos. 1 and 2)

symmetry block E'

row no.	column no.										
1	1	0.155001	1	2	−0.035431	1	3	−0.061368	1	4	0.155502
1	5	−0.077751	1	6	−0.051960	1	7	−0.089998	2	2	0.137722
2	3	−0.033092	2	4	−0.023629	2	5	−0.131436	2	6	−0.211238
2	7	0.140192	3	3	0.172279	3	4	−0.165411	3	5	0.103169
3	6	0.140192	3	7	0.046705	4	4	0.350040	4	5	−0.229596
4	6	−0.153438	4	7	−0.181531	5	5	0.344558	5	6	0.342733
5	7	−0.020702	6	6	0.564499	6	7	−0.207509	7	7	0.259889

Row (column) numbers 1 to 7 correspond to the symmetry coordinates 11 to 17.

and

row no.	column no.										
1	1	0.155001	1	2	−0.035431	1	3	−0.061368	1	4	0.155502
1	5	−0.077751	1	6	−0.051960	1	7	−0.089998	2	2	0.137772
2	3	−0.033092	2	4	−0.023629	2	5	−0.131436	2	6	−0.211238
2	7	0.140192	3	3	0.172279	3	4	−0.165411	3	5	0.103169
3	6	0.140192	3	7	0.046704	4	4	0.350040	4	5	−0.229596
4	6	−0.153438	4	7	−0.181531	5	5	0.344558	5	6	0.342732
5	7	−0.020702	6	6	0.564499	6	7	−0.207509	7	7	0.259889

The row (column) numbers 1 to 7 correspond to the symmetry coordinates 18 to 24.

symmetry block E''

row no.	column no.										
1	1	0.754025	1	2	0.380721	1	3	0.740804	2	2	0.262470
2	3	0.510712	3	3	0.993739						

The row (column) numbers 1 to 3 correspond to the symmetry coordinates 25 to 27.

and

row no.	column no.										
1	1	0.754026	1	2	0.380722	1	3	0.740806	2	2	0.262471
2	3	0.510713	3	3	0.993740						

The row (column) numbers 1 to 3 correspond to the symmetry coordinates 28 to 30.

Z matrix

The first two elements correspond with the row and the column numbers of the F matrix element F_{ij}, respectively. The third element is the number of the force constant (table 3-III). The last element corresponds with the coefficient of that force constant F_{ij}

1	1	1	1	1	2	9	1	1	6	8	1	1	7	10	1
1	10	11	1	1	11	12	1	1	13	13	1	1	15	14	1
1	16	16	1	1	17	15	1	1	18	17	1	2	2	1	1
2	3	8	1	2	8	10	1	2	10	12	1	2	11	11	1
2	13	13	1	2	14	14	1	2	17	17	1	2	18	15	1
2	19	16	1	3	3	1	1	3	4	9	1	3	8	10	1
3	11	11	1	3	12	12	1	3	13	14	1	3	14	13	1
3	18	16	1	3	19	15	1	3	20	17	1	4	4	1	1
4	5	8	1	4	9	10	1	4	11	12	1	4	12	11	1
4	14	13	1	4	15	14	1	4	19	17	1	4	20	15	1
4	21	16	1	5	5	1	1	5	6	9	1	5	9	10	1
5	10	12	1	5	12	11	1	5	14	14	1	5	15	13	1
5	16	17	1	5	20	16	1	5	21	15	1	6	6	1	1
6	7	10	1	6	10	11	1	6	12	12	1	6	13	14	1
6	15	13	1	6	16	15	1	6	17	16	1	6	21	17	1
7	7	2	1	7	10	18	1	7	13	19	1	7	15	19	1
7	16	20	1	7	17	20	1	8	8	2	1	8	11	18	1
8	13	19	1	8	14	19	1	8	18	20	1	8	19	20	1
9	9	2	1	9	12	18	1	9	14	19	1	9	15	19	1
9	20	20	1	9	21	20	1	10	10	3	1	10	11	21	1
10	12	21	1	10	13	22	1	10	15	22	1	10	16	23	1
10	17	23	1	10	18	24	1	10	21	24	1	11	11	3	1
11	12	21	1	11	13	22	1	11	14	22	1	11	17	24	1
11	18	23	1	11	19	23	1	11	20	24	1	12	12	3	1
12	14	22	1	12	15	22	1	12	16	24	1	12	19	24	1
12	20	23	1	12	21	23	1	13	13	4	1	13	14	25	1
13	15	25	1	13	16	27	1	13	17	26	1	13	18	26	1
13	19	27	1	14	14	4	1	14	15	25	1	14	18	27	1
14	19	26	1	14	20	26	1	14	21	27	1	15	15	4	1
15	16	26	1	15	17	27	1	15	20	27	1	15	21	26	1
16	16	5	1	16	17	28	1	16	21	29	1	17	17	5	1
17	18	29	1	18	18	5	1	18	19	28	1	19	19	5	1
19	20	29	1	20	20	5	1	20	21	28	1	21	21	5	1
22	22	7	1	22	23	34	1	22	24	34	1	22	25	35	1
22	26	37	1	22	27	37	1	22	28	35	1	22	29	36	1
22	30	36	1	23	23	7	1	23	24	34	1	23	25	36	1
23	26	36	1	23	27	35	1	23	28	37	1	23	29	37	1
23	30	35	1	24	24	7	1	24	25	37	1	24	26	35	1
24	27	36	1	24	28	36	1	24	29	35	1	24	30	37	1
25	25	6	1	25	26	31	1	25	27	32	1	25	28	33	1
25	29	32	1	25	30	30	1	26	26	6	1	26	27	30	1
26	28	32	1	26	29	33	1	26	30	32	1	27	27	6	1
27	28	31	1	27	29	32	1	27	30	33	1	28	28	6	1
28	29	30	1	28	30	32	1	29	29	6	1	29	30	31	1
30	30	6	1												

Sun–Parr–Crawford U matrix

row no.	column no.										
1	10	−0.408248	1	11	−0.408248	1	12	−0.408248	1	13	−0.408248
1	14	−0.408248	1	15	−0.408248	2	10	0.174425	2	11	0.174425
2	12	0.174425	2	13	−0.174425	2	14	−0.174425	2	15	−0.174425
2	16	0.369111	2	17	0.369111	2	18	0.369111	2	19	0.369111
2	20	0.369111	2	21	0.369111	3	7	0.577350	3	8	0.577350
3	9	0.577350	4	1	0.408248	4	2	0.408248	4	3	0.408248
4	4	0.408248	4	5	0.408248	4	6	0.408248	5	10	0.369111
5	11	0.369111	5	12	0.369111	5	13	−0.369111	5	14	−0.369111
5	15	−0.369111	5	16	−0.174425	5	17	−0.174425	5	18	−0.174425
5	19	−0.174425	5	20	−0.174425	5	21	−0.174425			
6	1	0.408248	6	2	−0.408248	6	3	0.408248	6	4	−0.408248
6	5	0.408248	6	6	−0.408248	7	16	0.408248	7	17	−0.408248
7	18	0.408248	7	19	−0.408248	7	20	0.408248	7	21	−0.408248
8	25	0.408248	8	26	0.402848	8	27	0.408248	8	28	0.408248
8	29	0.408248	8	30	0.408248						
9	22	0.577350	9	23	0.577350	9	24	0.577350	10	25	0.408248
10	26	−0.488248	10	27	0.408248	10	28	−0.408248	10	29	0.408248
10	30	−0.408248									
11	1	0.343296	11	2	0.019951	11	3	−0.363247	11	4	−0.363247
11	5	0.019951	11	6	0.343296	11	10	0.419442	11	11	−0.209721
11	12	−0.209721	11	13	0.198202	11	14	−0.396405	11	15	0.198202
12	1	−0.102242	12	2	−0.005942	12	3	0.108184	12	4	0.108184
12	5	−0.005942	12	6	−0.102242	12	10	0.348448	12	11	−0.174224
12	12	−0.174224	12	13	−0.059030	12	14	0.118059	12	15	−0.059030
12	16	0.500861	12	17	0.500861	12	18	−0.250430	12	19	−0.250430
12	20	−0.250430	12	21	−0.250430	13	7	0.816497	13	8	−0.408248
13	9	−0.408248	14	1	0.070959	14	2	0.364565	14	3	−0.534424
14	4	−0.435524	14	5	0.364565	14	6	0.070959	14	10	−0.263280
14	11	0.131640	14	12	0.131640	14	13	−0.179973	14	14	0.359946
14	15	−0.179973	14	16	0.124414	14	17	0.124414	14	18	−0.062207
14	19	−0.062207	14	20	−0.062207	14	21	−0.062207	15	1	0.447205
15	2	−0.447205	15	5	−0.447205	15	6	0.447205	15	10	−0.200545
15	11	0.100272	15	12	0.100272	15	13	−0.137089	15	14	0.274178
15	15	−0.137089	15	16	0.094768	15	17	0.094768	15	18	−0.047384
15	19	−0.047384	15	20	−0.047384	15	21	−0.047384	16	10	0.509691
16	11	−0.254846	16	12	−0.254846	16	13	−0.269656	16	14	0.539312
16	15	−0.269656	16	16	−0.240857	16	17	−0.240857	16	18	0.120428
16	19	0.120428	16	20	0.120428	16	21	0.120428	17	18	0.500000
17	19	−0.500000	17	20	−0.500000	17	21	0.500000			
18	1	−0.221239	18	2	−0.407923	18	3	−0.186684	18	4	0.186684
18	5	0.407923	18	6	0.221239	18	11	−0.363247	18	12	0.363247
18	13	−0.343296	18	15	0.343296	19	1	0.065891	19	2	0.121490
19	3	0.055599	19	4	−0.055599	19	5	−0.121490	19	6	−0.065891
19	11	−0.301764	19	12	0.301764	19	13	0.102242	19	15	−0.102242
19	18	−0.433758	19	19	−0.433758	19	20	0.433758	19	21	0.433758
20	8	−0.707107	20	9	0.707107	21	1	−0.461932	21	2	−0.292418
21	3	0.169514	21	4	−0.169514	21	5	0.292418	21	6	0.461932
21	11	0.228007	21	12	−0.228007	21	13	0.311722	21	15	−0.311722
21	18	−0.107746	21	19	−0.107746	21	20	0.107746	21	21	0.107746
22	1	0.258194	22	2	−0.258194	22	3	−0.156388	22	4	0.516388
22	5	0.258194	22	6	−0.258194	22	11	0.173677	22	12	−0.173677
22	13	0.237445	22	15	−0.237445	22	18	−0.082072	22	19	−0.082072
22	20	0.082072	22	21	0.082072	23	11	−0.441405	23	12	0.441405
23	13	0.467058	23	15	−0.467058	23	18	0.208588	23	19	0.208588
23	20	−0.208588	23	21	−0.208588	24	16	0.577350	24	17	−0.577350
24	18	−0.288675	24	19	0.288875	24	20	−0.288675	24	21	0.288675
25	25	−0.028204	25	26	0.513505	25	27	0.513505	25	28	−0.028204

Sun–Parr–Crawford U matrix, continued

row no	column no										
25	29	−0.485301	25	30	−0.485301	26	23	0.707107	26	24	−0.707107
27	25	0.576661	27	26	−0.263905	27	27	−0.263905	27	28	0.576661
27	29	−0.312756	27	30	−0.312756						
28	25	0.576661	28	26	0.263906	28	27	−0.263906	28	28	−0.576661
28	29	−0.312755	28	30	0.312755	29	22	0.816497	29	23	−0.408248
29	24	−0.408248	30	25	0.028203	30	26	0.513505	30	27	−0.513505
30	28	−0.028203	30	29	0.485301	30	30	−0.485301			

Sun–Parr–Crawford G matrix

Only blocks containing optically active modes are given: A'_1, A''_2, E' and E''. One of each pair of degenerated blocks is only retained, the other one being identical with the first.

row no.	column no.										
1	1	0.155001	1	2	−0.070862	1	3	0.243231	2	2	0.080406
2	3	−0.073918	3	3	1.123468	4	4	0.881480	4	5	1.721677
5	5	3.792065	6	6	0.155001	6	7	−0.046969	6	8	−0.084031
6	9	0.191780	7	7	0.242025	7	8	0.030402	7	9	0.086802
7	10	−0.335433	8	8	0.209236	8	9	−0.214702	8	10	−0.000478
9	9	0.709673	9	10	−0.240921	10	10	0.668055	11	11	0.754024
11	12	0.832911	12	12	1.256209						

Row (and column) numbers 1 to 3 belong to A'_1.
Row (and column) numbers 4 to 5 belong to A''_2.
Row (and column) numbers 6 to 10 belong to E'.
Row (and column) numbers 11 and 12 belong to E''.

Sun–Parr–Crawford Z matrix

The meaning of the four numbers is identical to that for the Z matrix. The block division is identical to that for the SPC-G matrix.

2	2	1 1.000000	7	7	1 0.655247	7	8	1-0.262604	8	8	1 0.799969
1	1	2 1.000000	6	6	2 1.000000	3	3	3 0.408728	7	7	3 0.103974
7	8	3 0.079199	7	9	3-0.201287	8	8	3 0.060327	8	9	3-0.153324
9	9	3 0.389678	3	3	4 0.408728	7	7	4 0.194342	7	8	4 0.148034
7	9	4 0.291185	8	8	4 0.112760	8	9	4 0.221801	9	9	4 0.436286
3	3	5 0.182544	7	7	5 0.046436	7	8	5 0.035371	7	9	5-0.089898
8	8	5 0.028943	8	9	5-0.068477	9	9	5 0.174036	10	10	5 1.000000
5	5	6 1.000000	12	12	6 1.000000	4	4	7 1.000000	11	11	7 1.000000
2	2	8 1.000000	7	7	8-0.625036	7	8	8 0.453003	8	8	8 0.399985
2	2	9 1.000000	7	7	9 0.482839	7	8	9 0.262604	8	8	9-0.799969
1	2	10 1.414214	6	7	10 0.173813	6	8	10 1.095424	2	3	11 0.904133
7	7	11-0.112092	7	8	11-0.395912	7	9	11 0.108502	8	8	11-0.538108
8	9	11 0.683810	2	3	12 0.904133	7	7	12-0.575896	7	8	12 0.133886
7	9	12 0.557447	8	8	12 0.538108	8	9	12-0.683810	2	3	13-0.904133
7	7	13-0.940590	7	8	13-0.358233	7	9	13-0.704650	2	3	14-0.904133
7	7	14 0.787342	7	8	14-0.183042	7	9	14 0.589843	8	8	14-0.735683
8	9	14-0.723549	2	3	15-0.427252	7	7	15 0.052970	7	8	15 0.187090
7	9	15-0.051273	7	10	15 0.800089	8	8	15 0.254284	8	9	15-0.323137
8	10	15-0.447205	2	3	16-0.427252	7	7	16 0.052970	7	8	16 0.187090
7	9	16-0.051273	7	10	16-0.800089	8	8	16 0.254284	8	9	16-0.323137
8	10	16 0.447205	2	3	17-0.427252	7	7	17 0.272142	7	8	17-0.063268
7	9	17-0.263424	7	10	17 0.506483	8	8	17-0.254284	8	9	17 0.323137
8	10	17 0.447205	1	3	18 0.639318	6	7	18-0.322451	6	8	18-0.245616
6	9	18 0.624242	1	3	19-1.278637	6	7	19-0.440842	6	8	19-0.335798
6	9	19-0.660520	1	3	20-0.604225	6	7	20 0.304751	6	8	20 0.232133
6	9	20-0.589976	3	3	21 0.817456	7	7	21-0.103974	7	8	21-0.079199
7	9	21 0.201287	8	8	21-0.060327	8	9	21 0.153324	9	9	21-0.389678
3	3	22-1.634912	7	7	22 0.284300	7	8	22 0.216556	7	9	22-0.062207
8	8	22 0.164955	8	9	22-0.047385	9	9	22-0.824648	3	3	23-0.772585
7	7	23-0.196534	7	8	23-0.149703	7	9	23 0.380476	8	8	23-0.114031
8	9	23 0.289815	9	9	23-0.736575	3	3	24-0.772585	7	7	24 0.098267
7	8	24 0.074852	7	9	24-0.190238	7	10	24-0.394920	8	8	24 0.057016
8	9	24-0.144907	8	10	24-0.300817	9	9	24.0.368288	9	10	24 0.764537
3	3	25 0.817456	7	7	25-0.194342	7	8	25-0.148034	7	9	25-0.291185
8	8	25-0.112760	8	9	25-0.221801	9	9	25-0.436286	3	3	26 0.772585
7	7	26-0.134347	7	8	26-0.102334	7	9	26 0.029396	7	10	26-0.539919
8	8	26-0.077950	8	9	26 0.022392	8	10	26-0.411267	9	9	26 0.389691
9	10	26-0.808968	3	3	27 0.772585	7	7	27-0.134347	7	8	27-0.102334
7	9	27 0.029396	7	10	27 0.539919	8	8	27-0.077950	8	9	27 0.022392
8	10	27 0.411267	9	9	27 0.389691	9	10	27 0.808968	3	3	28 0.182544
7	7	28 0.046436	7	8	28 0.035371	7	9	28-0.089898	8	8	28 0.026943
8	9	28-0.068477	9	9	28 0.174036	10	10	28-1.000000	3	3	29 0.182544
7	7	29-0.023218	7	8	29-0.017686	7	9	29 0.044949	7	10	29 0.186621
8	8	29-0.013471	8	9	29 0.034238	8	10	29 0.142152	9	9	29-0.087018
9	10	29-0.361285	10	10	29 0.500000	5	5	30-1.000000	12	12	30-0.582125
5	5	31-1.000000	12	12	31-0.413102	5	5	32 2.000000	12	12	32-1.000000
5	5	33-1.000000	12	12	33 0.995227	4	4	34 2.000000	11	11	34-1.000000

APPENDIX 2

Results of program FLEPO

A. Calculations with two A'_1 blocks together, one of the samples enriched with $^{10}B(93\,\%)$ and one of the samples with natural abundance of the two isotopes $^{11}B(81\,\%)$.

A.1. $F_6 = 0$ and kept constant.

Data: Variable force constants nos. 1, 2, 3, 4 and 5
Constant force constant no. 6
Number of iterations: 50
Initial values (mdyn/Å):

$F_1 = f_2 = 9.5$

$F_2 = f_1 + f_8 + f_9 = 8.5$

$F_3 = 0.41 f_3 + 0.41 f_4 + 0.18 f_5 = 0.34$

$F_4 = 1.41 f_{10} = 2.1$

$F_5 = -0.43 f_{15} = 0.22$ *)

$F_6 = 0$

Results:

FORCE CONSTANTS AFTER 50 PERTURBATIONS:

1 9.652738 2 7.254965 3 0.389279 4 3.641003 5 −0.170012

	OBS. FREQ. (CM−1)	CALC. FREQ. (CM−1)	DIFFERENCE (CM−1)	% ERROR	WEIGHT
1	1604.7	1612.0	−7.3	−0.455	0.2517
2	769.4	771.2	−1.8	−0.232	1.0951
3	630.6	629.1	1.5	0.244	1.6302
4	1573.0	1569.6	3.4	0.218	0.2620
5	769.0	765.8	3.2	0.413	1.0962
6	624.0	626.1	−2.1	−0.338	1.6648

AVERAGE ERROR = 3.22 CM−1, OR 0.317%
SUMDD = 0.000077

These results are used as initial values for the calculations in *A.2* and *A.3*.

A.2. Problem no. *A.1*, continued.
Another 50 perturbations.
Results:

*) When the initial values were established the negative sign was forgotten. This was automatically corrected by the program.

FORCE CONSTANTS AFTER 46 PERTURBATIONS *):

1 9.992551 2 7.006609 3 0.387263 4 3.726446 5 −0.043835

	OSB. FREQ. (CM−1)	CALC. FREQ. (CM−1)	DIFFERENCE (CM−1)	% ERROR	WEIGHT
1	1604.7	1609.5	−4.8	−0.297	0.2517
2	769.4	771.9	−2.5	−0.320	1.0951
3	630.6	628.3	2.3	0.369	1.6302
4	1573.0	1569.0	4.0	0.252	0.2620
5	769.0	767.6	1.4	0.183	1.0962
6	624.0	623.7	0.3	0.052	1.6648

AVERAGE ERROR = 2.54 CM−1, OR 0.246%.
SUMDD = 0.000047

A.3. All force constants taken to be variable.

Data: Variable force constants (F) nos. 1, 2, 3, 4, 5 and 6
Number of iterations: 50
Initial values: see the results of *A.1.*

Results:

FORCE CONSTANTS AFTER 40 PERTURBATIONS *):

1 9.773469 2 7.010711 3 0.398321 4 3.729067 5 −0.041481
6 0.043119

	OBS. FREQ. (CM−1)	CALC. FREQ. (CM−1)	DIFFERENCE (CM−1)	% ERROR	WEIGHT
1	1604.7	1609.3	−4.6	−0.286	0.2517
2	769.4	771.6	−2.2	−0.286	1.0951
3	630.6	628.4	2.2	0.342	1.6302
4	1573.0	1568.6	4.4	0.283	0.2620
5	769.0	767.1	1.9	0.242	1.0962
6	624.0	624.1	−0.1	−0.022	1.6648

AVERAGE ERROR = 2.57 CM−1, OR 0.243%.
SUMDD = 0.000048

A.4. All force constants variable. Initial values all zero.

Data: Variable force constants (F) nos. 1, 2, 3, 4, 5 and 6
Number of iterations: 100
Initial values: $F_1 = F_2 = F_3 = F_4 = F_5 = F_6 = 0$.

Results:

*) This perturbation had the lowest average error.

FORCE CONSTANTS AFTER 50 PERTURBATIONS:

1 6.410791 2 5.242864 3 1.871938 4 3.018461 5 −0.048075
6 −2.162397

	OBS. FREQ. (CM−1)	CALC. FREQ. (CM−1)	DIFFERENCE (CM−1)	% ERROR	WEIGHT
1	1604.7	1598.7	6.0	0.373	0.2517
2	769.4	773.5	−4.1	−0.536	1.0951
3	630.6	634.6	−4.0	−0.640	1.6302
4	1573.0	1580.3	−7.3	−0.467	0.2620
5	769.0	766.9	2.1	0.267	1.0962
6	624.0	623.2	0.8	0.132	1.6648

AVERAGE ERROR = 4.06 CM−1, OR 0.402%.
SUMDD = 0.000115.

B. Calculations based on the blocks A'_1 and E' together

The calculations are based on the hypothetic sample 100% ^{10}B. Three models are tested. The number of perturbations is 50 in each case. The initial values of the force constants and the choice in taking them constant or variable are the same for the three calculations.

Data: Variable force constants (f's) nos. 1, 3, 4, 5, 8 (9), 11 (13), 15, 22, 23 (26) and 28.
Constant force constants (f's) nos. 2, 10, 16, 17, 18, 19, 20, 21, 24, 25, 27, 29.
Initial values (mdyn/Å):

f_1	5.5	f_2	9.77	f_3	0.4	f_4	0.4	f_5	0.4
f_8	0.75	f_9	0.75	f_{10}	2.64	f_{11}	1.0	f_{12}	0
f_{13}	1.0	f_{14}	0	f_{15}	0.10	f_{16}	0	f_{17}	0
f_{18}	0	f_{19}	0	f_{20}	−0.07	f_{21}	0	f_{22}	0.12
f_{23}	0	f_{24}	0	f_{25}	0	f_{26}	0	f_{27}	0
f_{28}	0	f_{29}	0						

B.1. Model 1

Force constants after 50 perturbations (mdyn/Å):

f_1	7.15	f_2	9.77	f_3	−1.80	f_4	5.26	f_5	0.21
f_8	0.036	f_9	0.036	f_{10}	2.64	f_{11}	0.51	f_{12}	0
f_{13}	0.51	f_{14}	0	f_{15}	0.87	f_{16}	0	f_{17}	0
f_{18}	0	f_{19}	0	f_{20}	−0.07	f_{21}	0	f_{22}	0.46
f_{23}	−1.50	f_{24}	0	f_{25}	0	f_{26}	−1.50	f_{27}	0
f_{28}	−1.78	f_{29}	0						

	OBS. FREQ. (CM−1)	CALC. FREQ. (CM−1)	DIFFERENCE (CM−1)	% ERROR	WEIGHT
1	1604.7	1654.9	−50.2	−3.126	0.5197
2	769.4	759.3	10.1	1.311	1.6955
3	630.6	595.8	34.8	5.514	2.5240
4	1480.0	1588.9	−108.9	−7.361	0.1527
5	1440.0	1469.6	−29.6	−2.053	0.1613
6	1275.0	1230.0	45.0	3.531	0.4116
7	973.2	949.2	24.0	2.464	1.0597
8	476.2	389.7	86.5	18.160	1.4754

AVERAGE ERROR = 48.63 CM−1, OR 5.440%
SUMDD = 0.018348.

B.2. Model 2

Force constants after 49 perturbations (mdyn/Å):

f_1	5.82	f_2	9.77	f_3	0.072	f_4	0.99	f_5	0.44
f_8	0.60	f_9	0.60	f_{10}	2.64	f_{11}	0.45	f_{12}	0
f_{13}	0.45	f_{14}	0	f_{15}	0.17	f_{16}	0	f_{17}	0
f_{18}	0	f_{19}	0	f_{20}	−0.07	f_{21}	0	f_{22}	0.038
f_{23}	−0.079	f_{24}	0	f_{25}	0	f_{26}	−0.079	f_{27}	0
f_{28}	−0.34	f_{29}	0						

	OBS. FREQ. (CM−1)	CALC. FREQ. (CM−1)	DIFFERENCE (CM−1)	% ERROR	WEIGHT
1	1604.7	1610.3	−5.6	−0.350	0.4095
2	769.4	766.8	2.6	0.336	1.3361
3	630.6	624.7	5.9	0.930	1.9889
4	1480.0	1504.4	−24.4	−1.646	0.1204
5	1440.0	1444.1	−4.1	−0.287	0.1271
6	973.2	971.5	1.7	0.179	0.5567
7	476.2	479.5	−3.3	−0.692	3.4878
8	397.4	392.6	4.8	1.207	1.6694

AVERAGE ERROR = 6.55 CM−1, OR 0.703%.
SUMDD = 0.000340.

B.3. Model 3

Force constants after 50 perturbations (mdyn/Å):

f_1	5.41	f_2	9.77	f_3	−0.05	f_4	0.86	f_5	0.36
f_8	0.83	f_9	0.83	f_{10}	2.64	f_{11}	0.37	f_{12}	0
f_{13}	0.37	f_{14}	0	f_{15}	0.28	f_{16}	0	f_{17}	0
f_{18}	0	f_{19}	0	f_{20}	−0.07	f_{21}	0	f_{22}	−0.033
f_{23}	−0.18	f_{24}	0	f_{25}	0	f_{26}	−0.18	f_{27}	0
f_{28}	−0.36	f_{29}	0						

	OBS. FREQ. (CM−1)	CALC. FREQ. (CM−1)	DIFFERENCE (CM−1)	% ERROR	WEIGHT
1	1604.7	1616.0	−11.3	−0.707	0.3820
2	769.4	764.5	4.9	0.642	1.2462
3	630.6	622.1	8.5	1.342	1.8551
4	1480.0	1508.9	−28.9	−1.954	0.1123
5	1275.0	1279.0	−4.0	−0.313	0.1513
6	973.2	968.5	4.7	0.481	0.5193
7	476.2	476.0	0.2	0.037	3.2532
8	397.4	381.9	15.5	3.904	1.5571

AVERAGE ERROR = 9.76 CM−1, OR 1.173%.
SUMDD = 0.000664.

APPENDIX 3

A. Potential energy distribution

The potential energy distribution over the force constants is given for every normal vibration belonging to symmetry species A'_1 and E'. In eq. (3.7) sec. 3.2 for the potential energy $V = \frac{1}{2} f_1 r_1^2 + \ldots$. 29 force constants occur. The contribution (in fractions) of every force constant is given, their algebraic sum being equal to 1. The fractions in the first row refer to force constants f_1 to f_9, those in the second row to f_{10} to f_{18}, those in the third row to f_{19} to f_{27}, and those in the last row to f_{28} and f_{29}.

POTENTIAL ENERGY DISTRIBUTION

FREQUENCY = 1610.3 CM−1

0.1118	0.9956	0.0127	0.1745	0.0350	0.0000	0.0000	0.0115	0.0115
−0.3302	−0.0737	0.0000	0.0737	0.0000	0.0134	0.0000	0.0000	0.0000
0.0000	0.0178	0.0000	−0.0269	0.0264	0.0000	0.0000	−0.0264	0.0000
−0.0266	0.0000							

FREQUENCY = 766.8 CM−1

0.9291	0.0503	0.0054	0.0742	0.0149	0.0000	0.0000	0.0953	0.0953
−0.2140	0.1387	0.0000	−0.1387	0.0000	−0.0252	0.0000	0.0000	0.0000
0.0000	−0.0026	0.0000	−0.0114	0.0112	0.0000	0.0000	−0.0112	0.0000
−0.0113	0.0000							

FREQUENCY = 624.7 CM−1

0.0045	0.2120	0.0575	0.7894	0.1585	0.0000	0.0000	0.0005	0.0005
0.0306	−0.0315	0.0000	0.0315	0.0000	0.0057	0.0000	0.0000	0.0000
0.0000	−0.0174	0.0000	−0.1216	0.1193	0.0000	0.0000	−0.1193	0.0000
−0.1203	0.0000							

FREQUENCY = 1504.4 CM−1

0.0830	1.0735	0.0062	0.0195	0.0201	0.0000	0.0000	0.0003	0.0072
−0.2127	−0.0320	0.0000	0.0204	0.0000	0.0035	0.0000	0.0000	0.0000
0.0000	0.0129	0.0000	−0.0031	0.0129	0.0000	0.0000	−0.0009	0.0000
−0.0107	0.0000							

FREQUENCY = 1444.1 CM−

0.8161	0.0456	0.0024	0.1758	0.2105	0.0000	0.0000	−0.0806	0.2070
−0.0261	−0.0117	0.0000	−0.1579	0.0000	−0.0844	0.0000	0.0000	0.0000
0.0000	0.0016	0.0000	−0.0058	0.0049	0.0000	0.0000	−0.0610	0.0000
0.1499	0.0000							

FREQUENCY = 971.5 CM−1

1.3355	0.1620	0.0144	0.0019	0.0885	0.0000	0.0000	0.1296	−0.1031
−0.4543	−0.2672	0.0000	−0.0083	0.0000	0.0575	0.0000	0.0000	0.0000
0.0000	0.0076	0.0000	0.0015	0.0298	0.0000	0.0000	−0.0014	0.0000
0.0071	0.0000							

FREQUENCY = 479.5 CM−1

0.0063	0.0718	0.0469	0.7968	0.1539	0.0000	0.0000	0.0006	−0.0002
−0.0209	0.0334	0.0000	−0.0231	0.0000	−0.0057	0.0000	0.0000	0.0000
0.0000	−0.0092	0.0000	−0.0552	0.0973	0.0000	0.0000	−0.0133	0.0000
−0.0796	0.0000							

FREQUENCY = 392.6 CM−1

0.3884	0.0002	0.0126	0.0083	0.3368	0.0000	0.0000	−0.0124	0.0390
−0.0056	−0.0801	0.0000	0.0298	0.0000	0.0739	0.0000	0.0000	0.0000
0.0000	0.0003	0.0000	−0.0020	0.0260	0.0000	0.0000	−0.0174	0.0000
0.2031	0.0000							

B. *Amplitudes* of the atoms during the normal vibrations (in cartesian coordinates). Symmetry species A'_1 and E'. The amplitudes with respect to their equilibrium state are multiplied with a scale factor, which has been given for the A'_1 species.

EQUILIBRIUM CARTESIAN COORDINATES

ATOM	MASS	X	Y	Z
1	10.013	0.0000	0.0000	0.0000
2	15.999	1.4330	0.0000	0.0000
3	10.013	2.2672	1.1652	0.0000
4	15.999	1.5507	2.4062	0.0000
5	10.013	0.1245	2.5460	0.0000
6	15.999	−0.5920	1.3050	0.0000
7	15.999	−0.6934	−1.0759	0.0000
8	15.999	3.5457	1.1026	0.0000
9	15.999	−0.4606	3.6845	0.0000

A'_1

CARTESIAN COORDINATES FOR ATOMS DISPLACED BY FREQUENCY =1610.3 CM−1. SCALE=8

ATOM	MASS	X	Y	Z
1	10.013	0.1636	0.2538	0.0000
2	15.999	1.4568	−0.0463	0.0000
3	10.013	1.9656	1.1799	0.0000
4	15.999	1.5789	2.4499	0.0000
5	10.013	0.2625	2.2775	0.0000
6	15.999	−0.6439	1.3075	0.0000
7	15.999	−0.7766	−1.2050	0.0000
8	15.999	3.6990	1.0951	0.0000
9	15.999	−0.5308	3.8211	0.0000

CARTESIAN COORDINATES FOR ATOMS DISPLACED BY FREQUENCY =624.7 CM−1. SCALE=5.2

ATOM	MASS	X	Y	Z
1	10.013	0.0769	0.1193	0.0000
2	15.999	1.4990	−0.1283	0.0000
3	10.013	2.1255	1.1721	0.0000
4	15.999	1.6288	2.5275	0.0000
5	10.013	0.1894	2.4198	0.0000
6	15.999	−0.7361	1.3121	0.0000
7	15.999	−0.5724	−0.8881	0.0000
8	15.999	3.3225	1.1136	0.0000
9	15.999	−0.3584	3.4858	0.0000

CARTESIAN COORDINATES FOR ATOMS DISPLACED BY FREQUENCY =766.8 CM−1. SCALE=5.5

ATOM	MASS	X	Y	Z
1	10.013	−0.0801	−0.1243	0.0000
2	15.999	1.5448	−0.2175	0.0000
3	10.013	2.4149	1.1579	0.0000
4	15.999	1.6832	2.6118	0.0000
5	10.013	0.0569	2.6776	0.0000
6	15.999	−0.8363	1.3170	0.0000
7	15.999	−0.7471	−1.1593	0.0000
8	15.999	3.6447	1.0978	0.0000
9	15.999	−0.5059	3.7727	0.0000

CARTESIAN COORDINATES FOR ATOMS DISPLACED BY FREQUENCY =971.5 CM−1.

ATOM	MASS	X	Y	Z
1	10.013	0.1202	0.1866	0.0000
2	15.999	1.1466	−0.0854	0.0000
3	10.013	2.3760	1.1188	0.0000
4	15.999	1.6102	2.4985	0.0000
5	10.013	0.0373	2.6260	0.0000
6	15.999	−0.5515	1.0089	0.0000
7	15.999	−0.6581	−1.0211	0.0000
8	15.999	3.5805	1.1486	0.0000
9	15.999	−0.4331	3.7352	0.0000

E'

CARTESIAN COORDINATES FOR ATOMS DISPLACED BY FREQUENCY =1504.4 CM−1.

ATOM	MASS	X	Y	Z
1	10.013	0.1978	0.3070	0.0000
2	15.999	1.5163	0.0298	0.0000
3	10.013	2.4458	1.0796	0.0000
4	15.999	1.5382	2.3868	0.0000
5	10.013	−0.0272	2.6733	0.0000
6	15.999	−0.5992	1.3932	0.0000
7	15.999	−0.8341	−1.2942	0.0000
8	15.999	3.4163	1.1162	0.0000
9	15.999	−0.3948	3.5723	0.0000

CARTESIAN COORDINATES FOR ATOMS DISPLACED BY FREQUENCY =479.5 CM−1.

ATOM	MASS	X	Y	Z
1	10.013	−0.0716	−0.1111	0.0000
2	15.999	1.3475	0.1317	0.0000
3	10.013	2.2069	1.2853	0.0000
4	15.999	1.7119	2.6688	0.0000
5	10.013	0.2588	2.5408	0.0000
6	15.999	−0.4367	1.2816	0.0000
7	15.999	−0.7929	−1.2308	0.0000
8	15.999	3.4492	1.0098	0.0000
9	15.999	−0.5052	8.5583	0.0000

E' (continued)

CARTESIAN COORDINATES FOR ATOMS DISPLACED BY FREQUENCY =1444.1 CM−1.

ATOM	MASS	*X*	*Y*	*Z*
1	10.013	0.0426	0.0661	0.0000
2	15.999	1.4102	−0.0981	0.0000
3	10.013	2.3256	1.5546	0.0000
4	15.999	1.4675	2.2771	0.0000
5	10.013	0.4550	2.7601	0.0000
6	15.999	−0.6719	1.2437	0.0000
7	15.999	−0.7178	−1.1138	0.0000
8	15.999	3.5207	1.0531	0.0000
9	15.999	−0.4954	3.6413	0.0000

CARTESIAN COORDINATES FOR ATOMS DISPLACED BY FREQUENCY =392.6 CM−1.

ATOM	MASS	*X*	*Y*	*Z*
1	10.013	−0.0912	−0.1415	0.0000
2	15.999	1.3945	−0.0387	0.0000
3	10.013	2.1848	1.2031	0.0000
4	15.999	1.5125	2.3779	0.0000
5	10.013	0.1931	2.4866	0.0000
6	15.999	−0.6113	1.2540	0.0000
7	15.999	−0.7832	−1.2153	0.0000
8	15.999	3.4772	1.4010	0.0000
9	15.999	−0.1606	3.7554	0.0000

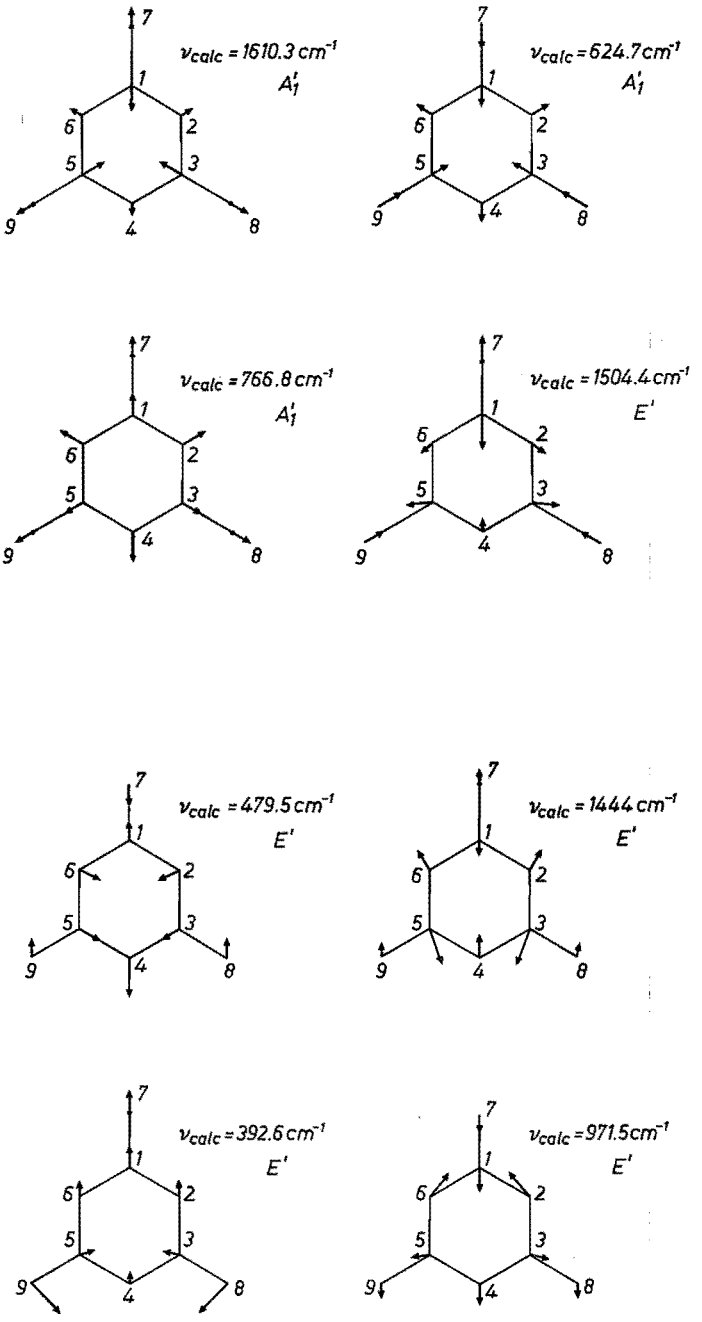

The amplitudes of the atoms during the normal vibrations. The drawings of the vibrations are made with help from the amplitudes in cartesian coordinates. For every vibration a scale factor is used.

APPENDIX 4

Crystalline $Na_3B_3O_6$

Projection of the hexagonal cell on the x–y plane and the definitions of the internal coordinates in the primitive cell.

For rings A, $z = c/6$, for rings B, $z = 2c/6$, etc. Ring C (atom numbers 1 to 9) and ring F (atom numbers 13 to 21) and the sodium atoms nos. 10, 11, 12, 22, 23 and 24 all belong to one primitive cell. Atom nos. 25 and higher are included to define all internal coordinates, which are necessary in the calculation.

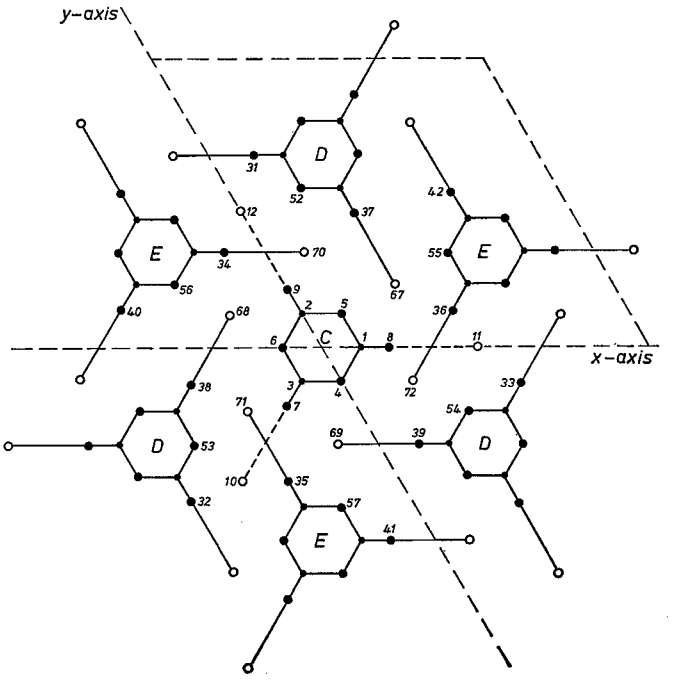

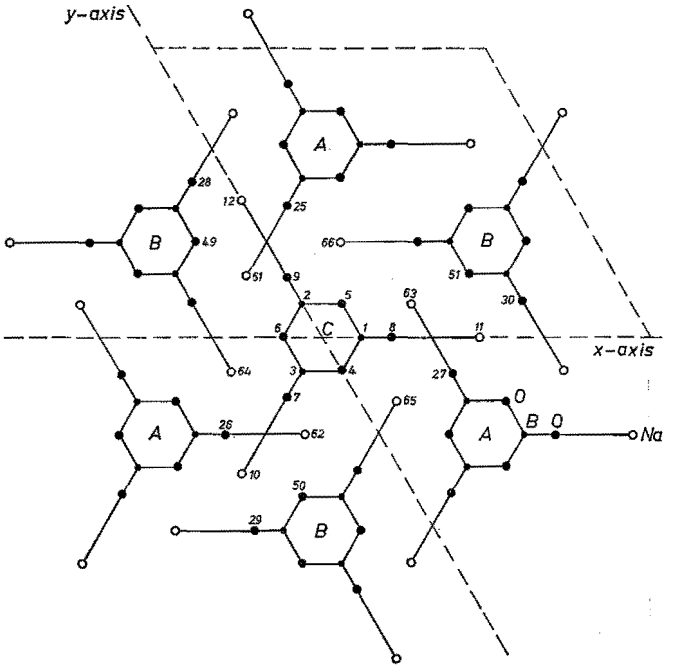
y-axis
x-axis
A
B
C
Na
O
28
12
25
49
51
9
66
63
30
2
5
6
1
8
11
64
3
4
27
7
65
26
62
10
50
29

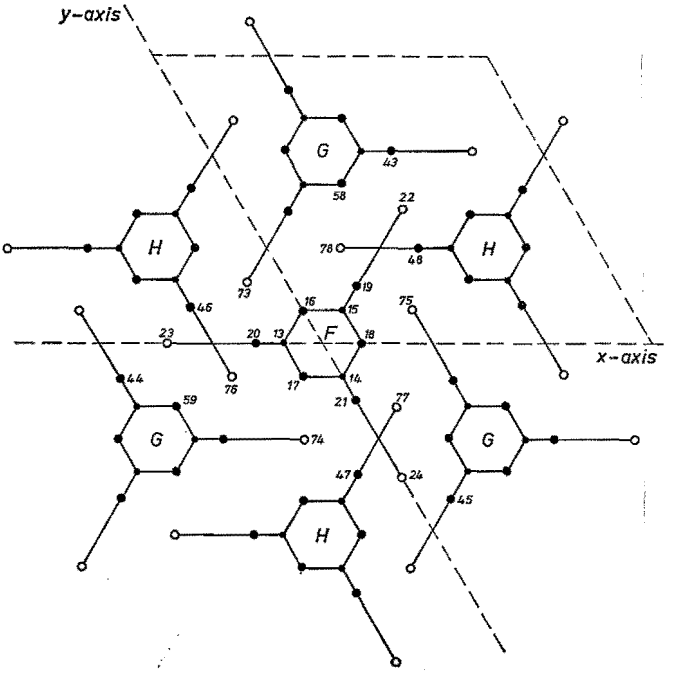
y-axis
x-axis
G
H
F
43
58
22
78
48
73
19
16
15
75
46
23
20
13
18
44
76
17
14
59
21
77
74
47
24
45

Definitions of the internal coordinates in the primitive cell of $Na_3B_3O_6$

Internal coordinates are numbered from 1 to 108.
Code defines the type of coordinate in question:
1 = stretching
2 = bending
4 = torsion.
The atoms are numbered as shown in the projection (see also Schachtschneider [3-3]).
The bending is multiplied by $(r_{ij} \cdot r_{jk})^{\frac{1}{2}}$ to get the dimension of length. The torsion is multiplied by $(r_{ij} \cdot r_{kl})^{\frac{1}{2}}$ for the same reason.

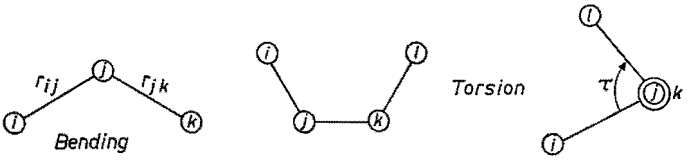

NO.	CODE	I	J	K	L	NO.	CODE	I	J	K	L	NO.	CODE	I	J	K	L
1	1	1	5	0	0	37	1	10	29	0	0	73	2	4	1	8	0
2	1	2	5	0	0	38	1	11	30	0	0	74	2	5	1	8	0
3	1	2	6	0	0	39	1	12	28	0	0	75	2	5	2	9	0
4	1	3	6	0	0	40	1	10	32	0	0	76	2	6	2	9	0
5	1	3	4	0	0	41	1	11	33	0	0	77	2	6	3	7	0
6	1	1	4	0	0	42	1	12	31	0	0	78	2	4	3	7	0
7	1	13	17	0	0	43	1	22	42	0	0	79	2	16	13	20	0
8	1	14	17	0	0	44	1	23	40	0	0	80	2	17	13	20	0
9	1	14	18	0	0	45	1	24	41	0	0	81	2	17	14	21	0
10	1	15	18	0	0	46	1	22	43	0	0	82	2	18	14	21	0
11	1	15	16	0	0	47	1	23	44	0	0	83	2	18	15	19	0
12	1	13	16	0	0	48	1	24	45	0	0	84	2	16	15	19	0
13	1	1	8	0	0	49	1	10	50	0	0	85	4	1	5	2	6
14	1	2	9	0	0	50	1	11	51	0	0	86	4	6	2	6	3
15	1	3	7	0	0	51	1	12	49	0	0	87	4	2	6	3	4
16	1	13	20	0	0	52	1	10	53	0	0	88	4	6	3	4	1
17	1	14	21	0	0	53	1	11	54	0	0	89	4	3	4	1	5
18	1	15	19	0	0	54	1	12	52	0	0	90	4	4	1	5	2
19	1	10	7	0	0	55	1	22	55	0	0	91	4	13	17	14	18
20	1	11	8	0	0	56	1	23	56	0	0	92	4	17	14	18	15
21	1	12	9	0	0	57	1	24	57	0	0	93	4	14	18	15	16
22	1	22	19	0	0	58	1	22	58	0	0	94	4	18	15	16	13
23	1	23	20	0	0	59	1	23	59	0	0	95	4	15	16	13	17
24	1	24	21	0	0	60	1	24	60	0	0	96	4	18	13	17	14
25	1	10	26	0	0	61	2	4	1	5	0	97	4	8	1	5	2
26	1	11	27	0	0	62	2	5	2	6	0	98	4	9	2	5	1
27	1	12	25	0	0	63	2	6	3	4	0	99	4	9	2	6	3
28	1	10	35	0	0	64	2	16	13	17	0	100	4	7	3	6	2
29	1	11	36	0	0	65	2	17	14	18	0	101	4	7	3	4	1
30	1	12	34	0	0	66	2	18	15	16	0	102	4	8	1	4	3
31	1	22	37	0	0	67	2	3	4	1	0	103	4	20	13	17	14
32	1	23	38	0	0	68	2	1	5	2	0	104	4	21	14	17	13
33	1	24	39	0	0	69	2	2	6	3	0	105	4	21	14	18	15
34	1	22	48	0	0	70	2	15	16	13	0	106	4	19	15	18	14
35	1	23	46	0	0	71	2	13	17	14	0	107	4	19	15	16	13
36	1	24	47	0	0	72	2	14	18	15	0	108	4	20	13	16	15

X matrix of $Na_3B_3O_6$

The *X* matrix contains the cartesian coordinates for each of the 60 atoms, which are needed for the definition of the internal coordinates in the primitive cell. The cartesian coordinates have been obtained from the atomic positions given by Marezio et al.[2-3]). Every *X* element is preceeded by a row and column number. The row number refers to the direction of the cartesian coordinate ($x \equiv 1$, $y \equiv 2$, $z \equiv 3$), and the column number to the atom number. The *X* element itself is the value of the appertaining cartesian coordinate (in Å) of the atom in question.

1	1	1.471500	2	1	0.000000	3	1	1.609800	1	2	−0.735750
2	2	1.274360	3	2	1.609800	1	3	−0.735750	2	3	−1.274360
3	3	1.609800	1	4	0.695350	2	4	−1.205250	3	4	1.609800
1	5	0.695850	2	5	1.205250	3	5	1.609800	1	6	−1.391700
2	6	0.000000	3	6	1.609800	1	7	−1.375550	2	7	−2.382520
3	7	1.609800	1	8	2.751100	2	8	0.000000	3	8	1.609800
1	9	−1.375550	2	9	2.382520	3	9	1.609800	1	10	−2.606200
2	10	−4.514070	3	10	1.609800	1	11	5.212400	2	11	0.000000
3	11	1.609800	1	12	−2.606200	2	12	4.514070	3	12	1.609800
1	13	−1.471500	2	13	0.000000	3	13	4.829200	1	14	0.735750
2	14	−1.274360	3	14	4.829200	1	15	0.735750	2	15	1.274360
3	15	4.829200	1	16	−0.695850	2	16	1.205250	3	16	4.829200
1	17	−0.695850	2	17	−1.205250	3	17	4.829200	1	18	1.391700
2	18	0.000000	3	18	4.829200	1	19	1.375550	2	19	2.382520
3	19	4.829200	1	20	−2.751100	2	20	0.000000	3	20	4.829200
1	21	1.375550	2	21	−2.382520	3	21	4.829200	1	22	2.606200
2	22	4.514070	3	22	4.829200	1	23	−5.212400	2	23	0.000000
3	23	4.829200	1	24	2.606200	2	24	−4.514070	3	24	4.829200
1	25	−1.375550	2	25	4.502380	3	25	−0.536600	1	26	−3.211400
2	26	−3.442450	3	26	−0.536600	1	27	4.586950	2	27	−1.059930
3	27	−0.536600	1	28	−4.586950	2	28	5.824970	3	28	0.536600
1	29	−2.751100	2	29	−6.884900	3	29	0.536600	1	30	7.338050
2	30	1.059930	3	30	0.536600	1	31	−2.751100	2	31	6.884900
3	31	2.682900	1	32	−4.586950	2	32	−5.824970	3	32	2.682900
1	33	7.338050	2	33	−1.059930	3	33	2.682900	1	34	−3.211400
2	34	3.442450	3	34	3.756100	1	35	−1.375550	2	35	−4.502380
3	35	3.756100	1	36	4.586950	2	36	1.059930	3	36	3.756100
1	37	1.375550	2	37	4.502380	3	37	2.682900	1	38	−4.586950
2	38	−1.059930	3	38	2.682900	1	39	3.211400	2	39	−3.442450
3	39	2.682900	1	40	−7.338050	2	40	1.059930	3	40	3.756100
2	42	5.824970	3	42	3.756100	1	43	2.751100	2	43	6.884900
1	41	2.751100	2	41	−6.884900	3	41	3.756100	1	42	4.586950
3	43	5.902400	1	44	−7.338050	2	44	−1.059930	3	44	5.902400
1	45	4.586950	2	45	−5.824970	3	45	5.902400	1	46	−4.586950
2	46	1.059930	3	46	6.975600	1	47	1.375550	2	47	−4.502380
3	47	6.975600	1	48	3.211400	2	48	3.442450	3	48	6.975600
1	49	−4.571000	2	49	3.442450	3	49	0.536600	1	50	−0.695850
2	50	−5.679650	3	50	0.536600	1	51	5.266700	2	51	2.237290
3	51	0.536600	1	52	−0.695900	2	52	5.679740	3	52	2.682900
1	53	−4.570800	2	53	−3.442450	3	53	2.682900	1	54	5.266700
2	54	−2.237290	3	54	2.682900	1	55	4.570900	2	55	3.442450
3	55	3.756100	1	56	−5.266700	2	56	2.237290	3	56	3.756100
1	57	0.695750	2	57	−5.679650	3	57	3.756100	1	58	0.695800
2	58	5.679740	3	58	5.902400	1	59	−5.266650	2	59	−2.237200
3	59	5.902400	1	60	4.570900	2	60	−3.442460	3	60	5.902400

Equivalent positions

In the table below the atoms of the primitive cell are given in the first column (nos. 1 to 24). Behind these atom numbers the numbers of the equivalent atoms in neighbouring cells are given, as far as these atoms are necessary for the definition of the internal coordinates. (see sec 3.3.1).

1					9	27	35	42	44	17	51	52			
2					10					18	49	53			
3					11					19	28	33	38	47	
4	56	58			12					20	29	31	39	48	
5	57	59			13					21	30	32	37	46	
6	55	60			14					22					
7	25	36	40	45	15					23					
8	26	34	41	43	16	50	54			24					

Block-diagonalised G matrix of $Na_3B_3O_6$ *(natural abundance:* 81% ^{11}B, 19% ^{10}B)

A_{1g}

1	1	0.080363	1	2	−0.070793	1	6	−0.045287	1	7	−0.047124
1	8	0.047124	1	9	0.031485	2	2	0.155001	2	3	−0.062502
2	4	−0.021621	2	5	0.004914	2	7	0.155565	2	8	−0.155565
2	9	−0.103937	3	3	0.106000	3	4	0.037172	3	5	−0.055082
3	6	−0.001346	4	4	0.013039	4	5	−0.019635	4	6	−0.000461
5	5	0.058247	5	6	0.001552	6	6	0.078372	6	7	−0.124425
6	8	0.124425	6	9	0.083131	7	7	0.459277	7	8	−0.459277
7	9	−0.306854	8	8	0.459277	8	9	0.306854	9	9	0.205017

A_{2g}

1	1	0.229638	1	4	−0.047989	1	5	0.196127	2	2	0.198961
2	3	0.020517	2	4	−0.000963	2	5	0.057302	2	7	−0.136483
3	3	0.153753	3	4	0.047377	3	5	0.120339	3	7	0.064777
4	4	0.133628	4	5	0.023340	4	6	0.188993	4	7	−0.066351
5	5	0.619209	6	6	3.796186	6	7	−0.516521	7	7	0.386562

A_{1u}

1	1	0.080363	1	2	−0.070793	1	6	0.045287	1	2	−0.047124
1	8	0.047124	1	9	0.031465	2	2	0.155001	2	3	−0.062502
2	4	−0.021621	2	5	−0.004914	2	7	0.155565	2	8	−0.155565
2	9	−0.103937	3	3	0.106000	3	4	0.037172	3	5	−0.045254
3	6	−0.001346	4	4	0.013039	4	5	−0.016235	4	6	−0.000481
5	5	0.058247	5	6	0.001552	6	6	0.078372	6	7	0.124425
6	8	−0.124425	6	9	−0.083131	7	7	0.459277	7	8	−0.459277
7	9	−0.306854	8	8	0.459277	9	9	0.306854	9	9	0.205017

A_{2u}

1	1	0.229638	1	4	0.047989	1	5	0.196127	2	2	0.198961
2	3	0.011318	2	4	−0.000963	2	5	0.057302	2	7	−0.136483
3	3	0.153753	3	4	0.047377	3	5	−0.120339	3	7	−0.064777
4	4	0.133628	4	5	−0.023340	4	6	−0.188993	4	7	0.066351
5	5	0.619209	6	6	3.796186	6	7	−0.516521	7	7	0.386562

E_g (one of the two equal E_g-blocks)

1	1	0.137840	1	2	−0.033184	1	3	−0.035396	1	9	−0.045287
1	11	−0.023562	1	12	−0.131467	1	13	−0.211318	1	14	0.140182
2	2	0.172161	2	3	−0.061309	2	14	0.047989	2	1	−0.165408
2	12	0.103109	2	11	0.140182	2	14	0.046676	3	3	0.155001
3	4	0.062502	3	5	−0.010811	3	6	−0.018725	3	7	0.002457
3	8	0.004256	3	11	0.155566	3	2	−0.077783	3	13	−0.051969
3	14	−0.090012	4	4	0.106000	4	5	−0.018580	1	6	−0.005258
4	7	0.027541	4	8	−0.039191	4	9	0.000673	4	10	−0.001165
5	5	0.152480	5	6	−0.014796	5	7	0.010479	5	8	0.011931
5	9	−0.000843	5	10	−0.000209	5	13	0.042976	5	14	−0.024812
5	17	0.102362	5	10	−0.059099	6	6	0.059519	6	7	0.011931
6	8	−0.009597	6	9	−0.000209	6	10	−0.000601	6	13	−0.024812
6	14	0.014325	6	17	−0.059099	6	18	0.034121	7	7	0.129876
7	8	−0.066233	7	9	0.035921	7	10	0.019843	7	13	0.090255
7	14	−0.052109	7	17	−0.048583	7	18	0.028049	8	8	0.082124
8	9	0.019843	8	10	0.013008	8	13	−0.052109	8	14	0.030085
8	17	0.028049	8	18	−0.016194	9	9	0.143556	9	10	0.037634
9	11	−0.062212	9	12	0.124425	9	13	0.083131	10	10	0.068444
10	11	−0.030253	10	14	0.023340	10	15	−0.060815	10	16	−0.094497
10	18	0.066351	11	11	0.350318	11	12	−0.229638	11	13	−0.153427
11	14	−0.181684	12	12	0.344323	12	13	0.342435	12	14	−0.020543
13	13	0.564300	13	14	−0.270432	14	14	0.259927	15	15	0.367734
15	16	0.571404	15	17	−0.401155	15	18	−0.169606	16	16	0.887879
16	17	−0.623336	16	18	−0.263543	17	17	0.916703	17	18	−0.091583
18	18	0.237923									

E_u (one of the two equal E_u-blocks)

1	1	0.137840	1	2	−0.033184	1	3	−0.035396	1	9	0.045287
1	11	−0.023562	1	12	−0.131467	1	13	−0.211318	1	14	0.140182
2	2	0.172161	2	3	−0.061308	2	10	−0.047989	2	11	−0.165408
2	12	0.103109	2	13	0.140182	2	14	0.046676	3	3	0.155001
3	4	0.062502	3	5	−0.010811	3	6	−0.018725	3	7	−0.002457
3	8	−0.004258	3	11	0.155566	3	12	−0.077783	3	13	−0.051969
3	14	−0.090012	4	4	0.106000	4	5	−0.018586	4	6	−0.005258
4	7	0.022627	4	8	−0.047702	4	9	0.000673	4	10	−0.001165
5	5	0.152480	5	6	−0.014796	5	7	0.004430	5	8	0.017386
5	9	−0.000843	5	10	−0.000209	5	13	0.042976	5	14	−0.024812
5	17	0.102362	5	18	−0.059099	6	6	0.059519	6	7	0.017386
6	8	−0.009347	6	9	−0.000209	6	10	−0.000601	6	13	−0.024812
6	14	0.014325	6	17	−0.059099	6	18	0.034121	7	7	0.129876
7	8	−0.068233	7	9	0.035921	7	10	0.019843	7	13	−0.090255
7	14	0.052108	7	17	0.048583	7	18	−0.028049	8	8	0.082124
8	9	0.019843	8	10	0.013008	8	13	0.052109	8	14	−0.030085
8	17	−0.028049	8	18	0.016194	9	9	0.143556	9	10	0.037634
9	11	0.062212	9	12	−0.124425	9	13	−0.083131	10	10	0.068444
10	11	0.030253	10	14	−0.023340	10	15	0.060815	10	16	0.094497
10	18	−0.066351	11	11	0.350318	11	12	−0.229638	11	13	−0.153427
11	14	−0.181684	12	12	0.344323	12	13	0.342435	12	14	−0.020543
13	13	0.564300	13	14	−0.207432	14	14	0.259927	15	15	0.367734
15	16	0.571404	15	17	−0.401155	15	18	−0.169606	16	16	0.887879
16	17	−0.623336	16	18	−0.263543	17	17	0.916703	17	18	−0.091583
18	18	0.237932									

Sun–Parr–Crawford G matrix of $Na_3B_3O_6$ *after GZ conversion*

This *G* matrix is made by conversion with the SPC-*U* matrix and removal of the rendundant coordinates. Inactive symmetry species and one of each pair of degenerate blocks are also removed. The matrix has been renumbered. There is one redundancy left in species A_{1g}.

Coordinates 1 to 5 belonging to species A_{1g}
6 to 12 belonging to species A_{2u}
13 to 24 belonging to species E_g
25 to 35 belonging to species E_u

1	1	0.099062	1	2	−0.067549	1	3	−0.013865	1	4	0.064998
1	5	−0.067604	2	2	0.186803	2	3	−0.021478	2	4	−0.049672
2	5	0.269017	3	3	0.161809	3	4	0.005464	3	5	0.135010
4	4	0.044060	4	5	−0.042045	5	5	1.122859	6	6	0.229639
6	9	0.047989	6	10	0.196127	7	7	0.198961	7	8	0.011318
7	9	−0.000963	7	10	0.057301	7	12	−0.136483	8	8	0.153753
8	9	0.047377	8	10	−0.120339	8	12	−0.064777	9	9	0.133628
9	10	−0.023340	9	11	−0.188994	9	12	0.066351	10	10	0.619209
11	11	3.790185	11	12	−0.516522	12	12	0.386563	13	13	0.356035
13	14	0.047225	13	15	−0.018965	13	16	−0.008413	13	17	−0.011378
13	18	0.082723	13	19	−0.204132	13	20	−0.139054	13	21	0.148585
13	22	0.177498	13	23	0.147130	14	14	0.255332	14	15	−0.097738
14	16	0.007407	14	17	0.010571	14	18	−0.009451	14	19	−0.029685
14	20	−0.016681	14	21	0.081467	14	22	−0.140917	14	23	−0.133507
15	15	0.159143	15	16	0.059473	15	17	−0.017145	15	18	−0.007339
15	19	0.001539	15	20	0.003090	15	21	−0.046392	15	22	0.160975
15	23	0.133915	16	16	0.105301	16	17	−0.018171	16	18	−0.004622
16	19	0.036458	16	20	−0.032208	16	21	−0.001091	16	22	−0.011928
16	23	−0.010035	17	17	0.155853	17	18	−0.027105	17	19	0.037789
17	20	0.033890	17	21	−0.023554	17	22	−0.082564	17	23	0.048682
17	24	−0.074542	18	18	0.091822	18	19	−0.055294	18	20	−0.054647
18	21	0.042136	18	22	0.109879	18	23	0.012652	18	24	0.050265
19	19	0.368683	19	20	0.064864	19	21	−0.132343	19	22	−0.132200
19	23	−0.159569	19	24	0.027529	20	20	0.121447	20	21	−0.014349
20	22	−0.089993	20	23	−0.046655	20	24	−0.021452	21	21	0.301272
21	22	−0.050097	21	23	−0.045948	21	24	−0.007181	22	22	0.709072
22	23	0.090229	22	24	−0.172041	23	23	0.692972	23	24	0.198701
24	24	1.819178	25	25	0.401910	25	26	0.058318	25	27	0.061906
25	28	−0.174704	25	29	−0.067912	25	30	0.086495	25	31	0.260981
25	32	−0.162900	25	33	0.041610	26	26	0.258418	26	27	−0.093347
26	28	0.021995	26	29	0.005932	26	30	−0.026606	26	31	0.028459
26	32	0.083912	26	33	−0.188076	26	34	−0.012879	27	27	0.224674
27	28	−0.034626	27	29	−0.039715	27	30	0.026270	27	31	0.066896
27	32	−0.159955	27	33	0.205672	27	34	−0.000150	28	28	0.221684
28	29	0.023671	28	30	−0.064355	28	31	−0.094782	28	32	0.107723
28	33	−0.118769	28	34	0.000123	29	29	0.175935	29	30	−0.043270
29	31	−0.076694	29	32	0.058126	29	33	−0.022687	29	34	0.092845
29	35	−0.076627	30	30	0.093441	30	31	0.092226	30	32	−0.078696
30	33	0.061712	30	34	−0.060418	30	35	0.050224	31	31	0.428359
31	32	−0.200828	31	33	0.063878	31	34	0.035289	31	35	−0.024910
32	32	0.322189	32	33	−0.182797	32	34	−0.015349	32	35	0.019147
33	33	0.579455	33	34	0.008361	33	35	0.001713	34	34	0.610845
34	35	0.262724	35	35	1.819197						

Definitions of the force constants in $Na_3B_3O_6$ (GQVF Field)

The force constants f_1 to f_{33} are identical with those in the $B_3O_6^{3-}$ ring (see table 3-III).

no.		explanation
f_{34}	$f_{\tau\nu}$	two bonds (r) common, the common B atom is central atom in both coordinates.
f_{35}	$f_{\tau\nu}^{I}$	two bonds (r) common, a common B atom of τ and ν is in τ at the end and in ν in the centre.
f_{36}	$f_{\tau\nu}^{II}$	only the central r of ν is common.
f_{37}	$f_{\tau\nu}^{III}$	only the r at the end of ν is common.
f_{38}	$f_{\tau\nu}^{IV}$	the central B atom in ν is common.
f_{39}	$f_{\tau\nu}^{V}$	the B atom at the end of ν is common.
f_{40}	$f_{\nu\nu}$	two bonds (r) common.
f_{41}	$f_{\nu\nu}^{I}$	one R is common.
f_{42}	$f_{\nu\nu}^{II}$	a B atom is common, this atom is in one coordinate in the centre and in the other one at the end.
f_{43}	$f_{\nu\nu}^{III}$	one B atom is common, in both coordinates at the end.
f_{44}	f_{Na}	ionic attraction of sodium and oxygen outside the ring, distance 2.4613 Å.
f_{44a}		dito, distance 2.474 Å.
f_{44b}		dito, distance 2.6065 Å.
f_{45}	f_{Na}	ionic attraction of sodium and oxygen in the ring, at a distance of 2.4819 Å.

The force constants f_{44a} and f_{44b} can be calculated from f_{44} (these force constants are proportional to $1/r^2$):

$$f_{44a} = 0.9896 f_{44} \quad \text{and} \quad f_{44b} = 0.8917 f_{44}.$$

This can be entered in the Z-matrix, hence the force constants f_{44a} and f_{44b} are not explicitly necessary.

τ = torsion, in which only atoms in the ring participate.
ν = torsion, in which also the oxygen atom outside the ring participates. It replaces the out of plane wag.

Summary

Since the appearance of gaslasers Raman spectroscopy has emerged as a new tool in research on the structure of glasses. Knowledge of crystalline compounds is indispensable for such research. This thesis firstly describes an investigation of the vibrational spectra of crystalline sodium metaborate, including a normal coordinate analysis (chapters 2 and 3). With the data of this investigation an interpretation is given of the Raman spectra of some vitreous borates (chapter 4), leading to the conclusion that the vitreous borates contain structural groups similar to the crystalline borates.

The methods used to interpret the vibrational spectra of sodium metaborate included single-crystal recordings, isotope substitution and recording of isomorphous compounds. The results provided an explanation for a large part of the spectrum. For some peaks different possibilities remained, resulting in three different interpretations of the complete spectrum. One of the three interpretations was chosen as preferable for the subsequent calculations.

Chapter 3 describes the methods of calculation. The computer programs reported by Schachtschneider are extended with a program to calculate the kinetic energy of the vibrations (*G* matrix) of crystals, particulars are also given of a method devised by Vogel for removing the redundant coordinates from the calculations. The calculations are mainly made for the 'free' metaborate ion. This seems to be a good approximation for the same ion in the sodium metaborate crystal. The force constants, the potential energy distribution of the normal vibrations and the amplitudes of the atoms during the vibrations are calculated. With the isotope product rule a rough comparison is made between the frequencies of the 'free' metaborate ion and those of the ion in the crystal.

In chapter 4 the strongest peaks of the Raman spectrum of vitreous alkali borates (at 806 cm^{-1} and 770 cm^{-1}) are assigned to the ring breathing of respectively the boroxol group and a group containing a six-membered ring with at least one BO_4 or BO_3^- unit.

An explanation is also suggested for a peak appearing near the excitation line. This peak is possibly due to a translation or libration of large fragments of the network.

The last investigation of this chapter concerns the temperature dependence of the Raman spectra of the vitreous alkali borates. It appeared that, except for an expected line-broadening, nothing happened, not even above the transition temperature. This leads us to the conclusion that the structural groups found must also exist at higher temperatures and even in the melt.

The work described in this thesis was supported in part by the Netherlands Foundation for Chemical Research (SON) with financial aid from the Netherlands Organization for the Advancement of Pure Research (ZWO).

Samenvatting

De Ramanspectroscopie is sedert de beschikbaarheid van gaslasers een nieuw hulpmiddel bij het onderzoek naar de struktuur van glazen. Hiervoor is echter de kennis van de vibratiespektra van kristallijne verbindingen onontbeerlijk.

Dit proefschrift beschrijft in de hoofdstukken 2 en 3 de interpretatie van de vibratiespektra van natriummetaboraat en de daarbij behorende normaalkoördinatenanalyse. Met behulp van de verkregen gegevens, zoals de potentiële energieverdeling van de trillingen van het metaboraat en de berekende krachtskonstanten, zijn in hoofdstuk 4 de vibratiespektra van de alkaliboraat glazen onderzocht. Het bleek hiermee mogelijk de belangrijkste pieken uit deze glasspektra toe te kennen aan ringvibraties van bepaalde struktuureenheden. Met deze overbrenging van gegevens van het kristal via de vibratiespektra en de normaalkoördinatenanalyse naar het glas is er een mogelijkheid ontstaan om een beter inzicht te verkrijgen in de opbouw van de glasstruktuur.

Voor de interpretatie van de vibratiespektra van natriummetaboraat is gebruik gemaakt van éénkristalopnamen, isotoopsubstitutie en isomorfe verbindingen. Hiermee kon een groot deel van het spektrum verklaard worden. Voor een aantal pieken bleven echter verschillende mogelijkheden over. Eén hiervan bleek bij de berekeningen de voorkeur te verdienen. In hoofdstuk 3 is uiteengezet welke berekeningswijze is gevolgd. De hierbij gebruikte computerprogramma's van Schachtschneider zijn aangevuld met een programma om de *G*-matrix van kristallen te berekenen. Voorts is een door Vogel uitgewerkte methode beschreven om de redundante koördinaten uit de berekeningen te verwijderen gebaseerd op een principe van Sun, Parr en Crawford.

De berekeningen zijn voornamelijk uitgevoerd aan het 'vrije' metaboraat ion. Dit blijkt een goede benadering te zijn voor ditzelfde ion in het natriummetaboraat kristal. De krachtskonstanten, de potentiële energieverdeling van de normaalvibraties en de maximale amplitudes van de atomen tijdens die vibraties zijn berekend. Met behulp van de isotopen produktregel is globaal een vergelijking gemaakt tussen de frequenties van het 'vrije' metaboraat ion en de vibraties van dit ion in het kristal.

In het laatste hoofdstuk zijn de sterkste pieken uit de Ramanspektra van de alkaliboraatglazen (bij 806 cm^{-1} en 770 cm^{-1}) toegekend aan een ringbreathing van de z.g. boroxolring en van een zesring met één of meer BO_4 en/of BO_3^- groepen.

Er is een suggestie gegeven voor een steeds voorkomende piek in de glasspektra vlakbij de excitatielijn. Deze piek zou toegeschreven kunnen worden aan een translatie of libratie van grote brokstukken uit het borium–zuurstofnetwerk.

Als laatste is onderzocht wat de temperatuurinvloed op de glasspektra is.

Het blijkt dat er, behalve een verwachte lijnverbreding, zelfs tot boven het transformatietrajekt niets gebeurt. De konklusie is dat de gevonden struktuureenheden ook bij hogere temperaturen blijven bestaan.

Het onderzoek beschreven in dit proefschrift werd mogelijk gemaakt door financiele steun van de Nederlandse Organisatie voor Zuiver-Wetenschappelijk-Onderzoek (ZWO) via de Stichting Scheikundig Onderzoek Nederland (SON).

Levensbericht

30 maart 1948	Geboren te Eindhoven.
1965	Eindexamen HBS-B, Gemeentelijk Lyceum Eindhoven.
1971	Ingenieursexamen Scheikundige Technologie T.H. te Eindhoven.
1971-1975	Medewerker van de Nederlandse Organisatie voor Zuiver-Wetenschappelijk-Onderzoek (Stichting SON) bij de groep silicaatchemie (vakgroep anorganische chemie) T.H. te Eindhoven.
15 februari 1974	Gehuwd met Letty Cras.
1975-heden	Medewerker van het Natuurkundig Laboratorium van de N.V. Philips' Gloeilampenfabrieken te Waalre in de groep Magnetic Devices.

STELLINGEN

bij het proefschrift van

T. W. Bril

14 mei 1976
Eindhoven

I

Het Ramanspectrum van glasachtig B_2O_3, zoals weergegeven door Krishnan, is onjuist.

R. S. Krishnan, Ind. J. pure appl. Phys. **9**, 916, 1971.

II

De toekenning van de vibratiefrequenties en de hierop gebaseerde normaal-coordinatenanalyse van het metaboraat anion door Kristiansen en Krogh-Moe zijn onjuist.

L. A. Kristiansen en J. Krogh-Moe, Phys. Chem. Glasses **2**, 96 1968.
Dit proefschrift paragraaf 4.3

III

De toekenning van de Raman aktieve piek bij 630 cm^{-1} in borosilikaat glazen aan een z.g. deformatie trilling van de metaboraat ring wordt niet bevestigd door Raman experimenten met ^{10}B en ^{11}B gesubstitueerde glazen.

W. L. Konijnendijk, Philips Res. Repts Suppl. 1975, no. 1.

IV

De invloed van een magneetveld in de lengterichting van een dun langgerekt permalloy element — zoals de „bar" in bubble devices — op de domeinstruktuur is door O'Dell onzorgvuldig weergegeven.

T. H. O'Dell, Magnetic bubbles, The Macmillan press Ltd. London, 1974, p. 119.

V

Stoffen als b.v. rhodamine B worden vaak gebruikt als luminescentie standaard vanwege het konstante kwantumrendement. Deze methode lijkt aantrekkelijker dan hij in de praktijk is.

J. W. Eastman, Photochemistry and Photobiology **6**, 55, 1967.

VI

De invloed van polarisatie-effecten op luminescentie-metingen, zoals beschreven door Cehelnik, Mielenz en Velapoldi is vrijwel te verwaarlozen bij metingen aan poedermonsters.

E. D. Cehelnik, K. D. Mielenz en R. A. Velapoldi, J. Res. natl Bur. Stand. **79A**, 1, 1975.

VII

De berekening van Hempstead aan de stationaire temperatuurverdeling in een half-oneindige warmtegeleider bij een periodieke warmtestroom is niet consistent.

R. D. Hempstead, IEEE Trans. on Magnetics **MAG-11**, 1224, 1975.

VIII

De constatering van Visser dat alkaliboraat glazen bij zeer hoge viscositeiten een Bingham gedrag vertonen wordt niet bevestigd door meting van het rheologisch gedrag als functie van de temperatuur.

Th. J. M. Visser, Rheological properties of alkaliborate glasses, proefschrift Technische Hogeschool Eindhoven, 1971.

IX

Bij de vaststelling van de hoogte van de z.g. Kalkarheffing had men vooraf rekening moeten houden met de inkomsten verkregen uit de 16% BTW op deze bijdrage.

Consumentengids, **23**, 501, 1975.

X

Het gewijzigd ontwerp van wet gewetensbezwaren militaire dienst ziet ten onrechte het aantal beschikbare arbeidsplaatsen voor vervangende dienstplicht als limitering voor het aantal erkenningen.

Wijziging van de wet gewetensbezwaren militaire dienst.
Bijlagen tot de Handelingen Tweede Kamer der Staten-Generaal, 1975/1976, 11155, nr. 9.

XI

Het verdient aanbeveling stoplichten zodanig af te stellen dat er voor fietsers een z.g. groene golf ontstaat.